2015

The N-Glycosylation of immunoglobulin G as a novel biomarker of Parkinson's disease

Alyce Christine Russell
Edith Cowan University

2015

The N-Glycosylation of immunoglobulin G as a novel biomarker of Parkinson's disease

Alyce Christine Russell
Edith Cowan University

Edith Cowan University

Copyright Warning

EDITH COWAN UNIVERSITY

School of Medical Sciences

The *N*-Glycosylation of Immunoglobulin G as a Novel Biomarker of Parkinson's Disease

A thesis submitted for the partial fulfilment
of the requirements for the degree of

Master of Science (Human Biology)

by

Alyce Christine Russell, BSc (Biomedical Science)

Prof Wei Wang, MD PhD FFPH
Principal Supervisor
School of Medical Sciences, Edith Cowan University

Dr Meghan Thomas, BSc (Hons) PhD
Co-supervisor
School of Medical Sciences, Edith Cowan University

Page intentionally left blank

The declaration page
is not included in this version of the thesis

Abstract

For neurodegenerative diseases, interventions during the early stages of the disease, before significant neurodegeneration has occurred, are associated with an increased probability of slowing or halting the disease process. In order to intervene early, it is essential that an accurate diagnosis is obtained and that disease progression can be monitored. This is particularly relevant for Parkinson's disease (PD; International Classification of Diseases version 10) because significant neurodegeneration has already occurred by the time the clinical motor symptoms are present. Therefore, the development of translatable, high-throughput biomarkers for large scale population screening is a crucial area of research. Of promise are the emerging "omics" technologies, which enable the detection of preclinical biomolecule fluctuations associated with the development of different diseases.

One such field is glycomics which is the study of the set of sugar structures, hereon in known as glycans, in a given protein, cell or tissue. Notably, the functional diversity of proteins is increased by several magnitudes with the addition of glycans, a process known as glycosylation. The glycosylation of certain proteins, including immunoglobulin G (IgG), has been found to remain fairly stable over short periods of time, with modifications thought to result from changes in the cellular environment or disease presence. Indeed, IgG has the ability to exert both anti-inflammatory and pro-inflammatory effects throughout the body and these properties are controlled by the *N*-glycosylation of the fragment crystallisable (Fc) portion.

To our knowledge, this was the first time that the potential of using IgG glycomic biomarkers to identify people with PD, as well as identify people with PD who are at risk of cognitive decline, was investigated. It was demonstrated that the peripheral IgG glycome in the PD cases was indicative of an increased capacity to biologically age. While advancing age has previously been associated with modifications to the glycosylation of IgG, making them more pro-inflammatory, advancing age was only associated with significant increases in modifications to the peripheral IgG glycome that infer more pro-inflammatory IgG in the PD cases but not the controls. In PD, the severity of the underlying pathology increases as the individual ages and, therefore, is a confounder of the effect of advancing age on pro-inflammation. Consequently, the peripheral IgG in people with PD have a propensity to become more pro-inflammatory at a faster rate as they age, and this may be linked to the severity of pathology during the course of the disease. PD has a heterogeneous presentation of clinical symptoms, and many factors contribute to the development of the disease. While this is true, it was demonstrated that the peripheral IgG glycome does not have utility in identifying risk of cognitive decline, which

would result from progression of PD pathology in the central nervous system (CNS). These results are indicative of the peripheral IgG interacting with PD pathology in the enteric nervous system (ENS) as well as when it propagates from the ENS to the CNS along the vagal nerve. Inflammation may facilitate the neuron-to-neuron propagation of PD inclusions along this pathway and thus be a contributor to PD development during the prodromal phase. Hence, the peripheral IgG glycome may be useful as a novel biomarker of PD presence in the prodromal phase of the disease.

Publications

Review Article Associated with this Thesis:

Russell, A., Drozdova, A., Wang, W., & Thomas, M. (2014). The Impact of Dementia Development Concurrent with Parkinson's Disease: A New Perspective. *CNS & Neurological Disorders – Drug Targets, 13(7), 1160 – 1168.*

Co-authored Research Articles Associated with Biomarkers:

Wang, W., **Russell, A**., Yan, Y., on behalf of Global Health Epidemiology Reference Group (GHERG). (2014). Traditional Chinese medicine and new concepts of predictive, preventive and personalized medicine in diagnosis and treatment of suboptimal health. *The EPMA Journal, 5 (4).* DOI: 10.1186/1878-5085-5-4

Wu, J., Zhang, L., Zhang, J., Dai, Y., Bian, L., Song, M., **Russell, A**., & Wang, W. (2013). The genetic contribution of CIDEA polymorphisms, haplotypes and loci interaction to obesity in a Han Chinese population. *Molecular biology reports, 40*(10), 5691-5699.

Wang, Y., Wu, L., Yu, X., Zhao, F., **Russell, A.,** Song, M., & Wang, W. (2013). The Expected Number of Background Disease Events during Mass Immunization in China. *PloS one, 8*(8), e71818.

Presentations

Conference Oral Presentation Associated with Study 1:

Russell, A., Pucic-Bakovic, M., Black, M., Lauc, G., Thomas, M., Rudan, I., Campbell, H., & Wang, W. (2014). *Profiles of N-glycosylation of immunoglobulin G differ in people with Parkinson's disease.* Paper presented at the 2014 International Symposium on Clinical and Translational Medicine, Chinese Academy of Engineering-National Institute of Sciences (USA) co-organised meeting, Shanghai, China.

Other Oral Presentations Associated with this Thesis:

Russell, A., Thomas, M., & Wang, W. (2014). *My Research Journey @ ECU.* Presentation at Capital Medical University, Beijing, China.

Russell, A., Thomas, M., & Wang, W. (2013). *Utilising N-Linked Glycomics in the Assessment of Suboptimal Health.* Presentation at Capital Medical University, Beijing, China

Russell, A., Thomas, M., & Wang, W. (2013). *Utilising Genomics and Glycomics in the Assessment of Suboptimal Health.* Presentation at Research Week, Edith Cowan University, Perth, Australia.

Page intentionally left blank

Acknowledgements

First and foremost, I would like to thank the participants of the larger cohorts who have contributed their cognitive and medical tests, as well as their blood samples, to further medical research. I would like to give a special thank you to Dr Maja Pucic Bakovic and Lucija Klaric from Genos Ltd for answering all my questions regarding the control cohort and procedures.

To my supervisors, Prof Wei Wang and Dr Meghan Thomas, thank you for all the support, guidance and constructive criticism during my research journey thus far. They have encouraged me to grow immensely over the last two years and I am so very grateful for everything they have both done for me and my research project. Thank you for financially supporting my research, providing expertise and ongoing writing support, pushing my limits and giving me the added research responsibility. I was able to publish my first leading-author paper as well as papers outside my own personal research; present my research at an international conference, of which Dr Robin Warren (2005 Nobel Prize winner) was also a speaker; represent Edith Cowan University in China and at local workshops; and be notified of the Summer School in Statistical Omics that was held in Croatia, of which I attended. Through these activities, I have been able to not only work alongside Wei's and Meghan's national and international research partners, but form my own collaborations.

Alongside my supervisors, I would not have made it through the last two years without the support of my fellow office buddies, family and friends. In particular: the help with proposal, article and thesis editing by Alesya Drozdova, Caitlin Timms, Dr Joanne Tresize, Andy Govus, Dr Kathryn Russell and Monique Garcia; the odd coffee walks with Michelle Tickner, Monique, Dr Darren Webb, Dr Greg Levin, Melissa Stemp, Joanne and Karen Lombardi; statistics debates with Dr Michael Black, Tom Egling, Andy and Greg; wine nights and life debriefs with Megan Williams, Jayne Campbell, Stacey Francis, Carlee Ackland, Rikki Shepherd, Morgan Berg, Emma Shynn, Rachel Fisher, Sam Hewitt, Michelle, Monique, Tina Phan, Melissa, Joanne, Lucy Millar, Dr Sabrina Skorski, and Vanesa Bochkezanian; babysitting during high workload periods by Keith Mackintosh, Katie Goodlich, Emma, Kathryn, Kristy Tait, Mai Tascon, Roxy Angove, Rochelle Fraser, my sister Courtney Russell, my dad (Michael Russell) and my mum (Karen Russell); the precooked dinner nights by Emma, Mai, Nick Taylor and my mum; emotional and financial support from my family; and most of all, everyone's patience during the course of my degree.

Above all, I would like to thank my beautiful daughter Sophie Mackintosh for allowing her mummy to follow her dreams and be as good as she can be. Although she is too young to read this now, I hope one day she understands the reasons for me pursuing such a career and pushing my personal limits. I love you little miss.

Abbreviations

[^{123}I]FP-CIT-SPECT – iodine 123–radiolabeled 2β-carbomethoxy-3β-(4-iodophenyl)-*N*-(3-fluoropropyl) nortropane with single-photon emission computed tomography

2-AB – 2-Aminobenzamide

ACN – Acetonitrile

ADCC – Antibody-dependent cell cytotoxicity

Asn – Asparagine

BBB – Blood brain barrier

BMI – Body mass index

CNS – Central nervous system

CRP – C-reactive protein

CSF – Cerebral spinal fluid

CV – Column volumes

DC-SIGN – Dendritic cell-specific intercellular adhesion molecule-3-grabbing non-integrin

df – Degrees of freedom

DMSO – Dimethyl sulphoxide

ENS – Enteric nervous system

Fc portion – Fragment crystallisable portion

FcR – Fragment crystallising receptor

Glc – Glucose

GlcNAc – *N*-Acetylglucosamine

GP – Glycan peak

HILIC-SPE – Hydrophilic interaction chromatography solid phase extraction

ICD-10 – International Classification of Disease, version 10

ID – Indeterminate

IgG – Immunoglobulin G

IL-6 – Interleukin 6

INF-γ – Interferon gamma

MBL – Mannose-binding lectin

MCI – Mild cognitive impairment

MDS – Movement Disorder Society

MDS-UPDRS – Movement Disorder Society sponsored Unified Parkinson's Disease Rating Scale

MPTP - 1-Methyl-4-phenyl-1,2,3,6-tetrahydropyridine

ParkC – Parkinson's Centre

PCA – Principal components analysis

PD – Parkinson's disease

PIGD – Postural instability and gait dysfunction

Ser – Serine

SN – Substantia nigra

SNP – Single nucleotide polymorphism

SNARE – Soluble *N*-ethylmaleimide-sensitive factor attachment protein receptor

TD – Tremor dominant

Thr – Threonine

TNF-α – Tumour necrosis factor alpha

UKBBC – United Kingdom Brain Bank Criteria

UPDRS – Unified Parkinson's Disease Rating Scale

UPLC – Ultra performance liquid chromatography

Page intentionally left blank

List of Figures

List of Tables

Page intentionally left blank

1.0 Introduction

For neurodegenerative diseases, interventions during the early stages of the disease, before significant neurodegeneration has occurred, are associated with an increased probability of slowing or halting the disease process. In order to intervene early, it is essential that an accurate diagnosis is obtained and that disease progression can be monitored. This is particularly relevant for Parkinson's disease (PD; International Classification of Diseases version 10 code G20) because significant neurodegeneration has already occurred by the time the clinical motor symptoms are present. Therefore, the development of translatable, high-throughput biomarkers for large scale population screening is a crucial area of research. A biomarker is defined as "*a characteristic that is objectively measured and evaluated as an indicator of normal biologic processes, pathogenic processes, or pharmacologic responses to a therapeutic intervention*" (Atkinson et al., 2001). Of promise are the emerging "omics" technologies which enable the detection of preclinical biomolecule fluctuations associated with the development of different diseases, and include such research fields as genomics, proteomics, metabolomics and glycomics.

Glycomics is the study of the set of sugar structures, hereafter referred to as glycans, in a given protein, cell or tissue. Notably, there are over 82,000 proteins in the Protein Data Bank (RCSB Protein Data Bank, 2013) and the functional diversity of proteins are increased by several magnitudes with post-translational modifications, including the addition of glycans (Lu et al., 2011). These modifications are part of the biosynthesis of many proteins (Varki et al., 2009), and are not template driven (Lu et al., 2011; Varki et al., 2009). Of the many types of post-translational modifications, glycosylation is amongst the most common and complex (Khoury et al., 2011; Lu et al., 2011; Saldova et al., 2012; Tharmalingam et al., 2013), and is the process of attaching a glycan to a protein or lipid to form a glycoprotein or glycolipid, respectively (Varki et al., 2009). Glycans are more information-dense than other macromolecules (DeMarco & Woods, 2008; Nelson et al., 2008). Moreover, multiple glycan structures can attach to a protein at a given time (Lu et al., 2011), and the number of ways a glycan can be modified makes them highly diverse (Varki et al., 2009).

The glycosylation of certain proteins, including immunoglobulin G (IgG), has been found to remain fairly stable over short periods of time, such as a year (Horvat et al., 2011; Knezevic et al., 2009; Lu et al., 2011), with modifications thought to result from changes in the cellular environment or disease presence (Knezevic et al., 2009; Lauc & Zoldo, 2010; Lu et al., 2011; Pucic et al., 2010; Zhang et al., 2012). The purpose of this thesis was to analyse the peripheral

IgG glycome and determine its utility in identifying people with PD, through a case-control epidemiological approach, as well as identifying risk of cognitive impairment. However, to fully realise the potential of peripheral IgG *N*-glycans as a biomarker, a sound understanding of PD development, presentation and progression is necessary.

1.1 Parkinson's Disease (PD)

PD is a complex chronic disease that is degenerative in nature, incurable and associated, although not caused by, advancing age. It is the second most common neurodegenerative disease in Australia, exceeded only by Alzheimer's disease, with an estimated 1 in every 350 individuals in the general population living with PD (Deloitte Access Economics, 2011). In 2011, the total cost of PD to Australia was $775.4 million which mainly reflects individually incurred costs over the course of the disease; the cost per person with PD approximately $12,000 per year and a median of 12.2 years lived post-diagnosis (Deloitte Access Economics, 2011).

James Parkinson first recorded PD in his 1817 publication "*An Essay on the Shaking Palsy*" and described Shaking Palsy (*Paralysis Agitans*) as:

> Involuntary tremulous motion, with lessened muscular power, in parts not in action and even when supported; with a propensity to bend the trunk forward, and to pass from a walking to a running pace: the senses and intellects being uninjured. (Parkinson, 1817, p. 1)

PD is still characterised by the classical motor symptoms of resting tremor, rigidity, bradykinesia, postural instability, and impaired coordination. However, unlike James Parkinson's 1817 description of PD, it is now recognised that non-motor symptoms also play a vital role in the consequences of the disease. These include psychoses, autonomic failure, digestive dysfunction, sleep abnormalities, fatigue, apathy, non-smoking related cancers, cognitive impairment and dementia (Russell et al., 2014). In particular, enteric nervous system (ENS) and olfactory dysfunction precede the clinical presentation of PD by years in many cases (Derkinderen et al., 2011; Kuo et al., 2010; Lebouvier et al., 2010), and cognitive impairment develops in about 80% of PD cases during the course of the disease (Aarsland et al., 2003; Hely et al., 2008).

PD can be inherited or idiopathic. Although more than 85% of PD cases are of idiopathic origins (Lesage & Brice, 2009; Meissner et al., 2011), having a sibling with PD infers a risk of developing the disease that is two to seven times greater than in the general population (Marder et al., 2003; Sveinbjörnsdóttir et al., 2000). Moreover, PD has 18 known gene loci associated with an increased risk of the disorder (Thenganatt & Jankovic, 2014). While risk does not necessarily equate to PD development, people who have genetic mutations associated with increased risk are thought to be more vulnerable to environmental insults (Meissner et al., 2011). PD is therefore a model disorder for studying how genes and the environment can interact and negatively impact an individual. While a gene-environment interaction is hypothesised, it is still unknown what causes idiopathic PD. Indeed, determining the mechanisms by which pathogenesis is initiated is a requisite to identifying valid biological markers of PD.

Like most chronic diseases, there is a prodromal phase whereby individuals with PD pathology have no or mild clinical symptoms that are not currently characterised as being associated with PD (Braak et al., 2003; Del Tredici & Braak, 2012). It is during this phase that the key PD-associated inclusions, alpha-synuclein immunoreactive Lewy bodies and Lewy neurites, begin developing in vulnerable nervous tissues. These become more severe and progress to other vulnerable projection neurons, particularly dopaminergic neurons (Del Tredici & Braak, 2012). An individual will be diagnosed as having clinical PD when a suboptimal pathological level is breached (Wang et al., 2014). Braak and colleagues (2003) have demonstrated this to be the point where a substantial amount of dopaminergic neurons within the substantia nigra (SN) pars compacta have been lost to apoptosis, with surviving dopaminergic neurons containing the aforementioned alpha-synuclein immunoreactive inclusions. Progression of pathology continues through the basal forebrain and mesocortex to the neocortical regions of the brain with concomitant cognitive decline (Braak et al., 2003).

Given the extensive neurodegeneration present at the time of diagnosis, the translation of neuroprotective and disease-modifying interventions often fails (Meissner et al., 2011). Much research in the realm of chronic disorders, including PD, is now focused on defining clinically translatable biomarkers that can be used to identify individuals within the suboptimal, prodromal phase of a disease.

1.1.1 Prodromal Phase

While familial forms of PD have been identified, there is little agreement on the cause of idiopathic PD. Two pathways to degeneration of the SN, however, are hypothesised;

anterograde degeneration from the olfactory bulb towards the temporal lobe, and retrograde degeneration originating in the ENS and travelling via the afferent parasympathetic vagal nerve fibres to the dorsal motor nucleus of the vagus (Hawkes et al., 2007). Importantly, these are the only nervous tissues in the body that are exposed to environmental substances and as such, are vulnerable to insult.

Olfactory dysfunction is one of the most common observations in people with PD. Notably many individuals have the perception that their sense of smell is lost many years, sometimes decades, before they are diagnosed with PD (Derkinderen et al., 2011). Post mortem PD studies have solidified these claims by identifying alpha-synuclein immunoreactive inclusions in the olfactory bulb that advance to other olfactory structures (Braak et al., 2003). A prerequisite of the involvement of olfactory dysfunction in the progression of PD pathology to non-olfactory cortical regions is subcortical involvement from Lewy aggregates that have progressed from the lower medulla oblongata to the basal forebrain (Braak et al., 2003). However, the appearance of these inclusions appears to be subsequent to the development of Lewy pathology in the periphery.

Other symptoms known to develop preclinical to or early in PD include dysphagia, nausea, gastroparesis, reduced bowel movement frequency and dyschesia (Derkinderen et al., 2011; Kuo et al., 2010; Lebouvier et al., 2010), all of which are involved in the ENS. Notably, ENS dysfunction occurs in newly diagnosed people with PD, therefore it is unlikely to be caused by medications (Kuo et al., 2010). In rodent models, it has been reported to occur prior to dysfunction in the autonomic innervation of the heart or olfaction, and prior to pathological changes in the medulla oblongata (Kuo et al., 2010). The ENS, the gastrointestinal tracts own intrinsic nervous system, is comprised of an extensive integrative network of neurons organised into two plexuses; the myenteric plexus and the submucosal plexus (Cersosimo & Benarroch, 2008; Furness, 2012). Intestinal motility and secretion are controlled by the ENS through local enteric reflexes and reflexes that pass through sympathetic ganglions, largely independent of extrinsic innervation by the central nervous system (CNS) (Cersosimo & Benarroch, 2008; Furness, 2012). There are, however, multiple reflexes that pass through the CNS and return to the gastrointestinal tract (Cersosimo & Benarroch, 2008; Furness, 2012). Dopaminergic neurons are present as a small population of the intrinsic innervation of both plexuses of the ENS, and changes in dopaminergic function are associated with marked changes to colonic motility (Cersosimo & Benarroch, 2008; Derkinderen et al., 2011; Kuo et al., 2010). Braak and colleagues (2006) demonstrated the presence of alpha-synuclein immunoreactive Lewy neurites in the axons of the submucosal and myenteric plexus neurons

during the very early stages of idiopathic PD. Moreover, Kuo and colleagues (2010) found ENS dysfunction in mice to be directly linked to mutant alpha-synuclein expression and aggregation rather than abnormal CNS innervation of the gut, suggesting that ENS dysfunction is the result of an intrinsic rather than an extrinsic defect. Indeed, it is evident that the primary pathological features of PD occur in both the CNS and the ENS, and the damage to the ENS most likely precedes damage in the CNS, however the initiator of the neurodegenerative process is still unknown.

One school of thought is that genetically vulnerable people are being exposed to an environmental toxin or pathogens that then damage vulnerable nervous tissues, i.e. the olfactory bulb and the ENS, initiating the neurodegenerative process (Jang et al., 2009; Pan-Montojo et al., 2010; Taylor et al., 2013). Animal models of PD support the notion of an interplay between genetic mutations and the environment (Jang et al., 2009; Taylor et al., 2013). Indeed, environmental toxins including pesticides such as rotenone and paraquat are commonly used to induce PD-like progression of pathology in rodent models.

Rotenone is an organic pesticide that directly inhibits mitochondrial complex I in mice, disrupting the electron transport chain and inducing the loss of SN dopaminergic neurons (Tanner et al., 2011). This is significant as mitochondrial dysfunction is implicated in the pathogenesis of PD. Systemic administration of rotenone fails to induce the pathological features of PD (Pan-Montojo et al., 2010); however, intragastric administration has been used with promising results. Ingested rotenone mimics the characteristic staging pattern of PD pathology found in humans, with changes progressing from the ENS to the CNS (Pan-Montojo et al., 2010; Tanner et al., 2011). Pan-Montojo and colleagues (2010) found intracellular accumulation of alpha-synuclein within the neurons of the ENS, dorsal motor nucleus of the vagus, intermediolateral nucleus in the spinal cord and the SN following chronic intragastric exposure to rotenone.

Paraquat is another environmental toxin and commonly used herbicide which is utilised to influence PD-like progression of pathology in animal models. It has been reported that PD is 2.5 times more likely to develop in people who have ever been exposed to rotenone when compared to paraquat (Tanner et al., 2011). Nevertheless, paraquat produces cellular changes associated with PD, including increased production of free radicals leading to oxidative stress, selective SN injury and aggregation of misfolded insoluble alpha-synuclein (Henchcliffe & Beal, 2008; Tanner et al., 2011). Moreover, paraquat exposure causes an earlier age of clinical PD onset in rodent models when compared to mitochondrial complex I inhibitors, such as

rotenone. This is important as oxidative stress is a presumed pathophysiological characteristic of familial PD (Tanner et al., 2011). Unfortunately paraquat is still one of the most widely used pesticides worldwide, therefore making it a potential public health concern (Tanner et al., 2011).

Although the degenerative pathway may begin in both the olfactory bulb and the ENS, it appears that it is the Lewy inclusions originating in the ENS that propagate along the afferent parasympathetic vagal nerve to the dorsal motor nucleus of the vagus that precedes the neurodegeneration of the SN pars compacta (Braak, de Vos, et al., 2006; Braak et al., 2003). Indeed, deposition of Lewy pathology in surviving projection neurons extending from the dorsal motor nucleus of the vagus, through to the medulla oblongata and eventually to the SN, may be a direct route of neuronal insult (Braak et al., 2003). While more work remains to be done in characterising the prodromal phase, understanding the underlying mechanisms of this phase will be critical for the development of sensitive and valid biomarkers of PD.

1.1.2 Clinical Phase

1.1.2.1 Motor Characteristics

The United Kingdom Brain Bank Criteria (UKBBC) are used worldwide for clinically diagnosing PD (Hughes et al., 1992). The criteria rely upon a patient having at least bradykinesia, plus one of the other motor symptoms of PD (e.g. resting tremor, rigidity, postural instability), as well as the absence of a number of exclusion criteria. PD is highly heterogeneous, which may complicate clinical diagnosis. As such, research regarding the clinical heterogeneity of PD has used large data sets with a focus on clustering clinical features rather than utilising individual case reports. Jankovic and colleagues (1990) released one of the earliest classifications of PD subtypes using the United PD Rating Scale (UPDRS) subscales II and III. They successfully subtyped PD into two clinical groups, tremor dominant and non-tremor dominant or postural instability and gait dysfunction (PIGD) subtypes, with an 'indeterminate' subtype of those that cannot be classified into either group. Subsequently, an additional two PD subtypes were proposed based on the age of diagnosis and progression rate of the disease; young-onset PD and rapid disease progression PD (Lewis et al., 2005; Selikhova et al., 2009; Thenganatt & Jankovic, 2014). Interestingly, people with rapid disease progression PD tend to have a worse prognosis than young-onset PD; a slower progressing syndrome that is most often tremor dominant and less likely to lead to cognitive decline.

In 2008, the Movement Disorder Society (MDS) released an updated version of the UPDRS, namely the MDS-sponsored UPDRS revision (MDS-UPDRS; Goetz et al., 2008). The objective was to make the MDS-UPDRS more comprehensive with several new items added to assess the non-motor aspects of PD, and place a greater emphasis on distinguishing between milder symptoms (Goetz et al., 2008). The MDS-UPDRS is the current gold standard for determining the clinical subtype of a person with PD using the equations described by Stebbins et al. (2013). These equations are summarised in the Methods (see **Section 2.3.3.1**).

Delineating the natural history of a PD subtype is of interest as patients respond differently to certain medications depending on their motor and cognitive symptoms (Eggers et al., 2011; Eggers et al., 2012), and these differences may also be detected as different levels of certain biomarkers. Studies utilising iodine 123–radiolabeled 2β-carbomethoxy-3β-(4-iodophenyl)-*N*-(3-fluoropropyl) nortropane with single-photon emission computed tomography ([^{123}I]FP-CIT-SPECT) have demonstrated its usefulness for imaging the extent and pattern of dopamine transporter loss in the striatum between tremor dominant and non-tremor dominant PD subtypes (Eggers et al., 2011; Eggers et al., 2012). Indeed, not only do PD patients with a tremor dominant subtype show a distinct loss of dopamine uptake in the caudate nucleus and the lateral putamen, but their non-tremor dominant counterparts demonstrate a distinct loss in dopaminergic projections to the dorsal putamen (Eggers et al., 2011; Eggers et al., 2012). Furthermore, compared to tremor dominant PD the progression of dopaminergic loss in people with a non-tremor dominant subtype is more severe in the bilateral putamen and this progression correlates with a worsening of phenotype (Eggers et al., 2011; Eggers et al., 2012). Therefore, these subtypes have different aetiopathological pathways of PD development and progression.

Pathologically, alpha-synuclein immunoreactive Lewy bodies and Lewy neurites from the medulla oblongata have increased by this stage in severity and propagated to other vulnerable long and slender projection neurons, particularly dopaminergic neurons in the SN (Braak et al., 2003; Del Tredici & Braak, 2012). The aggregation of alpha-synuclein disrupts the intracellular activity of these dopaminergic neurons, eventually causing them to degenerate and release neuromelanin into the surrounding tissue (Collins et al., 2012; Perry et al., 2010). The SN dopaminergic neurons are involved in the extrapyramidal system that controls muscle tone, balance, subconscious regulation of movement, and reflex activity. Hence, the degeneration of such neurons leads to the presentation of the classical motor symptoms that define PD.

1.1.2.2 Cognitive Impairment and Dementia Development

The occurrence of dementia is increasingly being recognised as a complication of PD (Litvan et al., 2012; Marras et al., 2013; Svenningsson et al., 2012), particularly in the later stages of the disease. It is associated with faster disease progression and an increased mortality rate compared to healthy-aged controls, people with PD or people with Alzheimer's disease (de Lau et al., 2005; Dewey & Saz, 2001; Emre et al., 2007; Irwin et al., 2012; Reid et al., 1996). The prevalence of dementia in PD ranges from 19.7 to 35.3% (Aarsland et al., 2003; Baldivia et al., 2011; de Lau et al., 2005; Hobson & Meara, 2004; Hoegh et al., 2013; Levy et al., 2002; Rana et al., 2012; Riedel et al., 2008); however, 78.2 to 83% of people with PD will develop dementia during the course of the disease (Aarsland et al., 2003; Hely et al., 2008). People with PD have a 2.6 to 5.9-fold increased risk of developing dementia (Aarsland et al., 2003; de Lau et al., 2005; Hobson & Meara, 2004; Williams-Gray et al., 2013) and a 1.29 to 1.83-fold increased risk of mortality compared to the general population (de Lau et al., 2005; Hughes et al., 2004; Williams-Gray et al., 2013). Furthermore, people with PD dementia have a 1.9 to 2.5-fold increased risk of mortality compared to the general population (Hely et al., 2008; Hughes et al., 2004), higher than that of PD alone.

The subsequent development of dementia in many cases is associated with the clinical motor subtype in PD. Alves and colleagues (2006) found that the development of dementia almost exclusively occurred in those with a PIGD subtype. Importantly, the transition from a tremor dominant to a PIGD, non-tremor dominant clinical subtype was unidirectional, irreversible and predicted subsequent dementia (Alves et al., 2006). Non-dopaminergic deficits are thought to cause PIGD in PD because people with this motor subtype respond poorly to dopaminergic therapy (Muller et al., 2013). An increase in neocortical amyloid-beta plaques, pathology normally associated with Alzheimer's disease, is presumed to be the mechanism of cognitive dysfunction in people with a PIGD subtype (Muller et al., 2013; Sellal, 2006). Furthermore, elderly people with PIGD unrelated to PD show an increased incidence of cognitive impairment (Yarnall et al., 2013). Alves and colleagues (2006), at the four year follow-up of their population-based PD cohort, reported that 42 of 128 patients (32.8%) had developed dementia and 41 of these (97.6%) had the PIGD-dominant PD subtype. At eight years, 48 out of 84 patients (57%) had developed dementia, all of whom had the PIGD-dominant PD subtype (Alves et al., 2006). Consequently, determining the clinical subtype of a patient with PD is important for prognosis of the disorder, and may be predictive of the development of cognitive impairment and dementia.

The presence of mild cognitive impairment (MCI) is often detected at diagnosis and may be a possible indication of the future development of dementia (Leroi et al., 2012; Litvan et al., 2012; Svenningsson et al., 2012). A recent multicentre analysis (n=1346; Aarsland et al., 2010) found that MCI was prevalent in 25.8% of people with newly diagnosed PD, non-amnestic MCI the most common at baseline, a finding corroborated by other studies (Litvan et al., 2012; Nie et al., 2012; Reid et al., 1996). Importantly, non-amnestic dementia development is most likely caused by the progression of PD pathology whereas amnestic dementia is most likely caused by Alzheimer's disease-type pathology (Reid et al., 1996). Cognitive dysfunction, therefore, is not exclusively a complication of the later stages of PD as MCI can begin to have an impact on quality of life much sooner than anticipated. Furthermore, impairment of semantic fluency, categorical memory, during the clinical phase of PD is a predictor of cognitive impairment (Hu et al., 2014; Pereira et al., 2014; Williams-Gray et al., 2009). Categorical memory deficits are linked to temporal lobe dysfunction, which may be caused by differential progression of PD (Ibarretxe-Bilbao et al., 2011). The animal naming task is one tool used to assess semantic fluency in PD, with a low score indicating impairment and risk of cognitive impairment (summarised in the Methods, **Section 2.3.3.2**).

Pathologically, the development of PD dementia is associated with the propagation of alpha-synuclein immunoreactive Lewy inclusions from the mesocortex to the neocortex, particularly the premotor areas, primary motor field, and sensory association areas (Braak et al., 2003). Upon macroscopic inspection, the SN pars compacta has lost its black colour by this point due to extensive degeneration of dopaminergic neurons and the release of neuromelanin into the surrounding extracellular tissue during the process (Braak et al., 2003). There is also a reduction in the number of neurons containing Lewy pathology due to the extensive neuronal loss (Braak et al., 2003). Knowledge of the differential development of idiopathic PD will expand understanding of why the disease is so heterogeneous and why dementia develops in most but not all people with PD, as well as allow for the development of biomarkers that can diagnose and monitor the progression of the disease. The development of valid biomarkers will be a product of deciphering the interaction of genetic and environmental factors, and how an individual is predisposed to the development of PD.

1.2 Inflammation in PD

A degree of inflammation is associated with PD, both in the CNS and in the periphery. Inflammation, caused by mitochondrial dysfunction and oxidative stress, is associated with the propagation of alpha-synuclein pathology. This multistep process begins with the misfolding of endogenous alpha-synuclein protein that subsequently aggregates into higher order oligomers

and disrupts normal cellular function (Angot et al., 2012). Both *in vitro* and *in vivo* studies support neuron-to-neuron transmission of alpha-synuclein oligomers through healthy cells endocytosing previously exocytosed protein aggregates of affected cells (Desplats et al., 2009; Lee, 2013; Olanow & Brundin, 2013; Volpicelli-Daley et al., 2011). Further evidence for this propagation is provided by post-mortem studies of PD patients who had striatal human foetal cell transplants 11 to 16 years prior to death (Kordower et al., 2008; Li et al., 2008; Li et al., 2010). Li and colleagues (2010) reported that 2 to 5% of 12 to 16 year old grafted dopaminergic neurons contained alpha-synuclein immunoreactive Lewy bodies. Undoubtedly, Lewy pathology is evident in the host striatum surrounding transplanted human foetal cells (Kordower et al., 2008; Li et al., 2008; Li et al., 2010) and thus further supports the hypothesis that PD pathology propagates from neuron-to-neuron. Interestingly, it has been demonstrated that a higher degree of microglial activation, and hence increased neuroinflammation, occurs in these grafts compared with host striatum or SN (Hirsch & Hunot, 2009; Kordower et al., 2008).

1.2.1 Neuroinflammation

Neuroinflammation is a key contributor to the neurodegenerative processes in PD and Alzheimer's disease, as well as multiple sclerosis (Gyoneva et al., 2014). In PD, neuroinflammation may facilitate the neuron-to-neuron spread of Lewy inclusions (Tomé et al., 2013). Factors influencing the development of inflammation include alpha-synuclein protein aggregation, mitochondrial dysfunction and increased levels of oxidative species (Hirsch & Hunot, 2009; Kordower et al., 2008; Taylor et al., 2013). In the CNS, these cause the activation of resident microglia and astrocytes, increased levels of inflammatory mediators such as cytokines and chemokines, and an infiltration of CD4+ and CD8+ T-cell lymphocytes into nervous tissue in an attempt to resolve the conspirator of the inflammation (Collins et al., 2012; Hirsch & Hunot, 2009; Perry et al., 2010). The normal function of these glial cells, especially the microglia, is to maintain an inflammatory homeostasis within the CNS (Gyoneva et al., 2014). However, persistent inflammatory stimuli can lead to the overproduction of pro-inflammatory factors potentiating neuronal damage through the generation of reactive oxygen species, particularly superoxide and hydrogen peroxide (Keane et al., 2011; Taylor et al., 2013).

Mitochondrial dysfunction and oxidative stress exist in unison, further promoting the detriment of the other. In brief, mitochondrial outer membrane permeabilisation occurs in response to intracellular stress eventually leading to over generation of reactive oxygen

species and the release of cytochrome c, and other apoptotic-initiating proteins normally contained within the mitochondria, into the cytoplasm which then form a multiprotein complex that triggers the caspase-9 to caspase-3 proteolytic cascade (Galluzzi et al., 2011). Furthermore, dopamine metabolises into hydrogen peroxide and decreased activity of mitochondrial complex I sub units overwhelms cells with superoxide (Hauser & Hastings, 2013), thus increasing the likelihood of accumulation of reactive oxygen species and intracellular stress within dopaminergic neurons. Indeed, decreased activity of the mitochondrial complex I sub units is observed in the SN and frontal cortex of people with PD (Hauser & Hastings, 2013; Henchcliffe & Beal, 2008). Therefore, dopaminergic neurons, as well as other long and slender projections neurons (Del Tredici & Braak, 2012), are particularly vulnerable to oxidative damage and apoptosis.

Oxidative stress is a cytotoxic condition that occurs when there is an overproduction or accumulation of reactive oxygen species within the cell thereby causing reduced electron transfer rates through mitochondrial complex I subunits (Hauser & Hastings, 2013; Henchcliffe & Beal, 2008; Taylor et al., 2013). Oxidative damage to endogenous alpha-synuclein within dopaminergic neurons can result in protein aggregation, an effect that might partially explain the cellular toxicity of the protein (Henchcliffe & Beal, 2008). Moreover, intracellular accumulation of alpha-synuclein protein promotes oxidative damage as well as encouraging the mitochondria to release cytochrome c into the cytoplasm (Henchcliffe & Beal, 2008).

Endogenous alpha-synuclein is thought to function as a chaperone molecule in neurons with the primary role of maintaining the proteins that constitute soluble *N*-ethylmaleimide-sensitive factor attachment protein receptor (SNARE)-complexes (Volpicelli-Daley et al., 2011). SNARE complexes are involved in the exocytosis of neurotransmitters at the presynaptic terminal, and repeated release of neurotransmitters requires cycles of SNARE-complex assembly and disassembly (Burré et al., 2010). However, mice that overexpress alpha-synuclein have swollen and morphologically abnormal mitochondria, whereas knockout mice models demonstrate increased resistance to 1-methyl-4-phenyl-1,2,3,6-tetrahydropyridine (MPTP), a neurotoxin with similar mode of action as rotenone, through modulation of mitochondrial complex I activity (Henchcliffe & Beal, 2008). Therefore, alpha-synuclein may somehow be involved in chaperoning these environmental toxins to the mitochondria or other parts of the cell that then promote intracellular stress.

When stressed dopaminergic neurons release neuromelanin into the surrounding tissue, it disrupts homeostasis and causes the activation of microglia (Collins et al., 2012; Perry et al.,

2010) and other inflammatory mechanisms. Once activated, the microglia retract their processes that normally penetrate the surrounding three-dimensional space in a 'resting' state, and move in an amoeboid-like fashion to areas of insult, with persistent neuroinflammation causing the microglia to become phagocytic (Gyoneva et al., 2014; Kettenmann et al., 2011; Tansey & Goldberg, 2010). Interestingly, activated microglial cells are one of the biggest producers of reactive oxygen species in the CNS and thus promote further oxidative stress and neuronal damage when chronic stimuli are present (Kettenmann et al., 2011; Taylor et al., 2013). Furthermore, microglia are rarely replaced, have a long lifespan, and as such, are involved in many age-related neurodegenerative diseases (Gyoneva et al., 2014; Tansey & Goldberg, 2010). The release of neuromelanin also stimulates the pro-inflammatory cytokines, such as tumour-necrosis-factor alpha (TNF-α) and interleukin 6 (IL-6), that perpetuate chronic neuroinflammation.

1.2.2 Systemic Inflammation

Although neuroinflammation was originally thought to be isolated from the periphery, it is now known that a bi-directional interaction occurs between the CNS and peripheral immune systems. Microglia are suggested to engage peripheral immune cells to act on the brain resulting in an interplay between their phenotypes (Sanchez-Guajardo et al., 2013). Takeda and colleagues (2014) summarised these interaction pathways as the vagal nerve (the route that alpha-synuclein propagates from the ENS to the CNS), the circumventricular organs which lack a proper blood-brain-barrier (BBB), such as the neurohypophysis and pineal gland, and direct infiltration of monocytes and inflammatory lipid mediators, such as prostaglandins, through the BBB. Mice models of neuroinflammation demonstrate these interactions by exhibiting activated microglia that respond more slowly to tissue damage compared with healthy mice following systemically administered lipopolysaccharide (Gyoneva et al., 2014). Importantly, the BBB in Alzheimer's disease brains is increasingly permeable to peripheral immune cells due to protein aggregation within the CNS (Takeda et al., 2014). Therefore the study of systemic inflammation in Alzheimer's disease and PD may provide important information about the neurodegenerative process.

Systemic inflammation is evident due to increased levels of pro-inflammatory cytokines, particularly IL-6 and TNF-α, and may contribute to the progression of PD (Collins et al., 2012; Perry et al., 2010; Reale et al., 2009; Sanchez-Guajardo et al., 2013). However, these profile alterations appear to be associated with the non-motor symptoms of PD and other diseases

with neuroinflammatory processes. Increased TNF-α is associated with cognitive decline in PD and Alzheimer's disease (Holmes et al., 2009; Menza et al., 2010; Reale et al., 2009). Additionally, plasma levels of both soluble TNF-α receptors (sTNFR1 and sTNFR2) are increased in PD patients (Rocha et al., 2014), and certain single nucleotide polymorphisms (SNPs) in the TNF promoter are associated with PD (Sanchez-Guajardo et al., 2013). Increased levels of IL-6 are also associated with poorer performance in cognitive tasks in multiple sclerosis patients (Patanella et al., 2010) and an increased risk of all-cause dementia (Koyama et al., 2012). Increased levels of interferon gamma (INF-γ) (Reale et al., 2009) and C-reactive protein (CRP) (Koyama et al., 2012) are implicated in PD and all-cause dementia, respectively. Indeed, increased levels of systemic pro-inflammatory cytokines are correlated with chronic neurodegeneration. Thus, it is reasonable to consider that profiling of blood plasma cytokines and other inflammatory markers could provide a valid and non-invasive means of assessing neuroinflammation in relation to PD.

Cytokines are communicative biomolecules that influence other inflammatory mediators and immunoglobulin-producing B-cell lymphocytes in the body. The immunoglobulins are a group of glycoproteins involved in adaptive immunity that account for approximately 20% of all plasma proteins, among which IgG is the most abundant. Lewy bodies and about a third of dopaminergic neurons within the SN show strong immunolabelling for IgG (Sanchez-Guajardo et al., 2013). In fact the proportion of immunolabelled neurons within PD patient's brains has been demonstrated to be positively associated with the number of activated microglia and negatively associated with the number of dopaminergic neurons in the SN (Sanchez-Guajardo et al., 2013). Thus, surface coating of IgG may be indicative of degradation early in the disease process (Sanchez-Guajardo et al., 2013). Additionally, immunoglobulins against alpha-synuclein are not only found in the cerebral spinal fluid (CSF) of familial PD patients, but also in their blood plasma (Sanchez-Guajardo et al., 2013), supporting the hypothesis of a bi-directional interaction between the CNS and the periphery.

IgG is involved in the innate and adaptive immune systems, has the ability to exert both anti- and pro-inflammatory responses throughout the body, and to infiltrate the CNS. IgG consist of two light and two heavy polypeptide chains which are joined by covalent bonds to form a "Y" shaped structure (see **Fig. 1**). There are four classes of IgG within humans and each differs in their heavy chains, and therefore the fragment crystallising (Fc) portion (Anthony et al., 2012). The *N*-glycans of the Fc portion control the inflammatory properties of IgG. The attached *N*-glycans are structurally important; IgG lacking Fc *N*-glycans have a closed conformation which

may hinder Fcγ-receptor (Fcγ-R) binding (Krapp et al., 2003). The monosaccharides that form the attached *N*-glycans alter IgG effector function by changing the conformation of the Fc fragment and the affinity for a number of receptors, such as the affinity of IgG-Fc for Fcγ-RIIIa and the classical complement component C1q (Krapp et al., 2003; Nimmerjahn et al., 2007; Shade & Anthony, 2013). Although originally thought of as being a result of enzymatic competition due to studies *in vitro*, the biosynthesis of the attached *N*-glycans is a predesigned outcome fitted to the needs of the producing B-cell lymphocyte (Pucic et al., 2011) under the influence of its cellular environment, including numerous cytokines and other modulating factors (Wang et al., 2011). This makes the study of these glycan moieties biologically important in terms of the contribution of IgG to inflammation in the pathogenesis of PD.

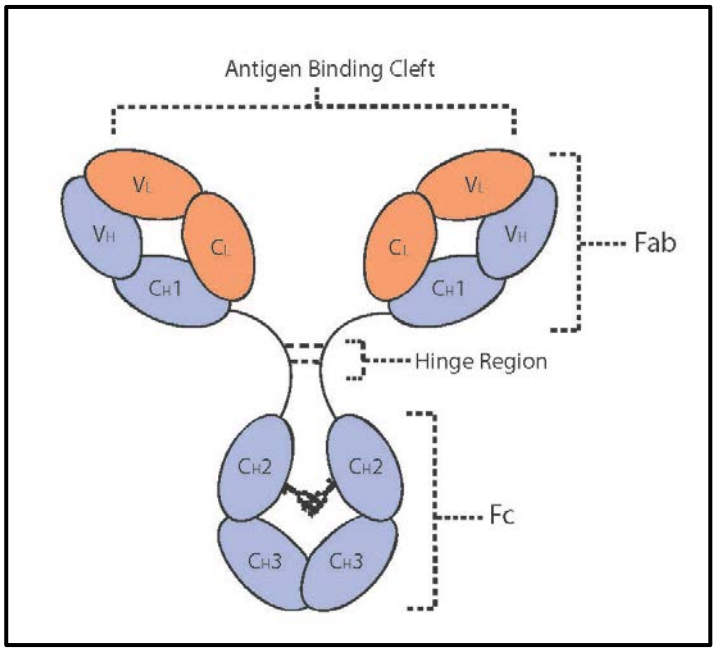

Figure 1: Structure of the IgG glycoprotein. The purple domains represent the heavy chains ('$_H$') and the orange domains represent the light chains ('$_L$'). Further, the IgG glycoprotein has two portions that infer different properties; the fragment antigen-binding (Fab) and fragment crystallising (Fc) portions. The Fab and Fc portions are connected by a hinge region containing disulphide bonds. The Fab portion contains the antigen binding cleft and with its variable regions (V_L and V_H) is responsible for recognising and attaching to specific antigens. The Fc portion contains the glycans within the C_H2 domains of both heavy chains, and is responsible for effector functions by binding to Fc receptors (FcR's) on natural killer and other inflammatory cells. Changes to the attached glycan moieties can significantly alter effector function of the IgG glycoprotein.

1.2.3 *N*-glycans of IgG

Of the many types of post-translational modification, *N*-glycosylation is the most abundant (Horvat et al., 2011; Lu et al., 2011; Robinson et al., 2012; Zhang et al., 2012). Many plasma proteins are modified by covalently-bound glycans that are biologically important for normal physiological processes, including; the folding (Robinson et al., 2012) and function of proteins (Yamaguchi et al., 2012; Zhang et al., 2012), cell-to-cell adhesion and communication (Horvat et al., 2011; Lauc & Zoldo, 2010; Lu et al., 2011; Nelson et al., 2008), self-recognition in immune response (DeMarco & Woods, 2008; Lauc & Zoldo, 2010; Nelson et al., 2008), lectin binding (Blow, 2009; Lauc & Zoldo, 2010; Nelson et al., 2008), and resistance to proteolysis (Yamaguchi et al., 2012; Zhang et al., 2012). Moreover, *N*-glycans are essential for life as life cannot sustain past the embryonic stage if absent, and congenital disorders of glycosylation exist (Knezevic et al., 2009; Pucic et al., 2010). An altered glycan can change the structure and function of the whole glycoprotein, and it is believed that this may account for much of the phenotypic variation in humans (Horvat et al., 2011; Knezevic et al., 2009). There are three major structural types of *N*-glycans; high mannose, complex, and hybrid (**Fig. 2**). Although all types can occur, the vast majority of IgG-Fc *N*-glycans are of the complex type (Krištić et al., 2014; Pucic et al., 2011).

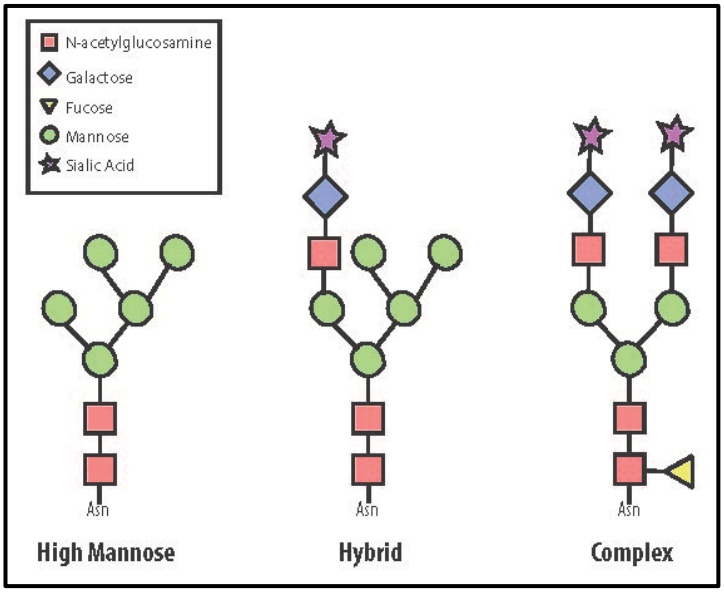

Figure 2: Three major structural types of *N*-glycans.

N-glycans are biosynthesised sequentially (see **Fig. 3**) on dolichol pyrophosphate donor molecules using a combination of hundreds of genes that code for glycosyltransferases, glycosidases and sugar nucleotides (Horvat et al., 2011; Knezevic et al., 2009). They then covalently bind to the nitrogen of asparagine (Asn) residues on the terminus of the polypeptide at the recognition sequence Asn-X-Ser/Thr, whereby X is any amino acid except proline and ends with serine (Ser) or threonine (Thr) (Horvat et al., 2011; Knezevic et al., 2009; Robinson et al., 2012; Zhang et al., 2012). *N*-glycan biosynthesis occurs in a step-wise fashion, commencing on the membrane of the endoplasmic reticulum (see **Fig. 3, step 1**). Here, two *N*-acetylglucosamine (GlcNAc) and five mannose sugar nucleotides are assembled onto the dolichol pyrophosphate donor molecule on the cytoplasmic side of the endoplasmic reticulum membrane, and subsequently the whole structure flips so that it is on the luminal side of the membrane (see **Fig. 3, step 2**; Taylor & Drickamer, 2011). A further four mannose and three glucose (Glc) sugar nucleotides are added before the dolichol-bound precursor glycan is transferred to an Asn recognition sequence by oligosaccharyltransferase (see **Fig. 3, step 5**; Taylor & Drickamer, 2011). The polypeptide is then folded into its respective protein and, following removal of the three Glc via two trimming steps, the glycoprotein is transferred to the *cis* portion of the Golgi apparatus for further processing (see **Fig. 3, step 6-7**; Nelson et al., 2008; Taylor & Drickamer, 2011; Varki et al., 2009). Different glycosidases and glycotransferases remove and add, respectively, different sugar nucleotides throughout the processing steps in the Golgi apparatus, from the *cis* Golgi to the *trans* Golgi (see **Fig. 3, step 8**). Subsequently, the final IgG is secreted or delivered to the plasma membrane of the B-cell lymphocyte (see **Fig. 3, step 9**).

IgG, transferrin and fibrinogen are the most prevalent glycoproteins in the plasma proteome. IgG has been studied extensively as its glycan moieties are known to have a downstream influence on effector functions; that is, whether it is anti-inflammatory or pro-inflammatory. Effector function of an IgG is controlled by the attachment of an *N*-glycan to the Fc portion at Asn-297 on both heavy chains in the C_H2 domain (see **Fig. 1**). The majority of these *N*-glycans are complex biantennary structures (see **Fig. 2**), however a high degree of heterogeneity exists due to the presence or absence of sugar nucleotides (Pucic et al., 2010; Zhang et al., 2012). In total, over 30 IgG glycoforms have been identified (Arnold et al., 2007; Shade & Anthony, 2013) and the two glycan moieties that attach to a single IgG in the Fc portion may vary leading to greater variability in effector function (Nimmerjahn et al., 2007). The most prevalent IgG glycoforms are pictured in **Appendix 1**. As previously mentioned, the biosynthesis of the attached *N*-glycans is a predesigned outcome fitted to the needs of the producing B-cell

lymphocyte. Indeed, even alterations to the IgG-Fc *N*-glycan moieties that appear structurally minute can significantly change the affinity of IgG to different receptors (see **Fig. 4**).

Changes in IgG glycosylation are associated with a number of chronic diseases, including: rheumatoid arthritis (Gindzienska-Sieskiewicz et al., 2007; Malhotra et al., 1995; Troelsen et al., 2012), metabolic syndrome (Lauc et al., 2013; Lu et al., 2011), inflammatory bowel disease (Lauc et al., 2013; Nakajima et al., 2011), systemic lupus erythematosus (Lauc et al., 2013), haematological cancers (Lauc et al., 2013), thyroid cancer (Chen et al., 2012), gastric cancer (Kodar et al., 2012), lung cancer (Chen et al., 2013), ovarian cancer (Saldova et al., 2007), multiple sclerosis (Lauc et al., 2013), and more recently Alzheimer's disease and progressive MCI (Lundström et al., 2014). The most studied glycosylation trait in IgG is the lack of terminal galactose and sialic acid residues; i.e. agalactosylated IgG-Fc glycoforms. Agalactosylated IgG has been linked to an array of chronic diseases, such as rheumatoid arthritis and systemic lupus erythematosus. In fact, a marked increase in agalactosylated IgG in rheumatoid arthritis patients was one of the first glycan biomarker discoveries (Arnold et al., 2007). Following this discovery, Malhotra et al. (1995) demonstrated that amassed agalactosylated IgG had a high affinity to the lectin mannose-binding protein (MBL). An increase in agalactosylated IgG is also associated with advancing age (Pucic et al., 2011; Ruhaak et al., 2010).

The addition of *N*-acetylneuraminic acid, hereafter referred to as sialic acid, to the terminating end of the IgG-Fc *N*-glycan has a similar anti-inflammatory effect to the addition of core fucose (Scallon et al., 2007). Sialylated IgG-Fc *N*-glycans have a lower affinity for Fcγ-RIIIa on natural killer cells leading to an anti-inflammatory effect (Böhm et al., 2012; Scallon et al., 2007). Anthony (2011) postulated that the mechanism by which sialylated, particularly α2-6 sialylated, IgG-Fc glycans can have an anti-inflammatory effect is by binding dendritic cell-specific intercellular adhesion molecule-3-grabbing non-integrin (DC-SIGN), a C-type lectin which is present on dendritic cells, to the protein portion of the IgG-Fc which causes the production of more FcγRIIb receptors on natural killer cells. FcγRIIb are inhibitory receptors that act to reduce inflammation by preventing the activation of FcγRIIIa and other excitatory receptors (Anthony, 2011). However, it has not been reported whether its absence leads to such a high increase in antibody-dependent cell cytotoxicity (ADCC) as seen with the lack of core fucose.

Figure 3: A summary of the biosynthesis of IgG glycoprotein. ① *N*-glycan biosynthesis begins on the endoplasmic reticulum membrane where two *N*-acetylglucosamines (UDP-GlcNAc) and five mannose (GDP-Man) sugar nucleotides are attached to a dolichol-phosphate (Dolichol-P) donor molecule on the cytoplasmic side. ② The whole Dolichol-P attached *N*-glycan is flipped so it is on the luminal side of the endoplasmic reticulum. ③ Dolichol-P flips individual sugar nucleotides from the cytoplasm to the lumen. ④ In tandem, the ribosomes biosynthesise the polypeptide structure of the IgG. ⑤ Oligosaccharyltransferase transfers *N*-glycan moiety from Dolichol-P to Asparagine (Asn) 297 on the growing polypeptide. ⑥ Following the correct folding of the IgG heavy chain, three *N*-acetylglucosamines sugarnucelotides are removed and this signals the transfer of the IgG heavy chain from the endoplasmic reticulum to the Golgi apparatus. ⑦-⑧ The IgG components move through the Golgi apparatus where different glycosyltransferases and glycosidases add and remove (respectively) different sugar nucleotides to the glycan moiety. ⑨ All four components of the IgG, two heavy chains (purple) and two light chains (orange), are assembled following excretion from the *trans* Golgi, with the final IgG glycoprotein been secreted from the B-cell lymphocyte or attaching to the plasma membrane of the B-cell.

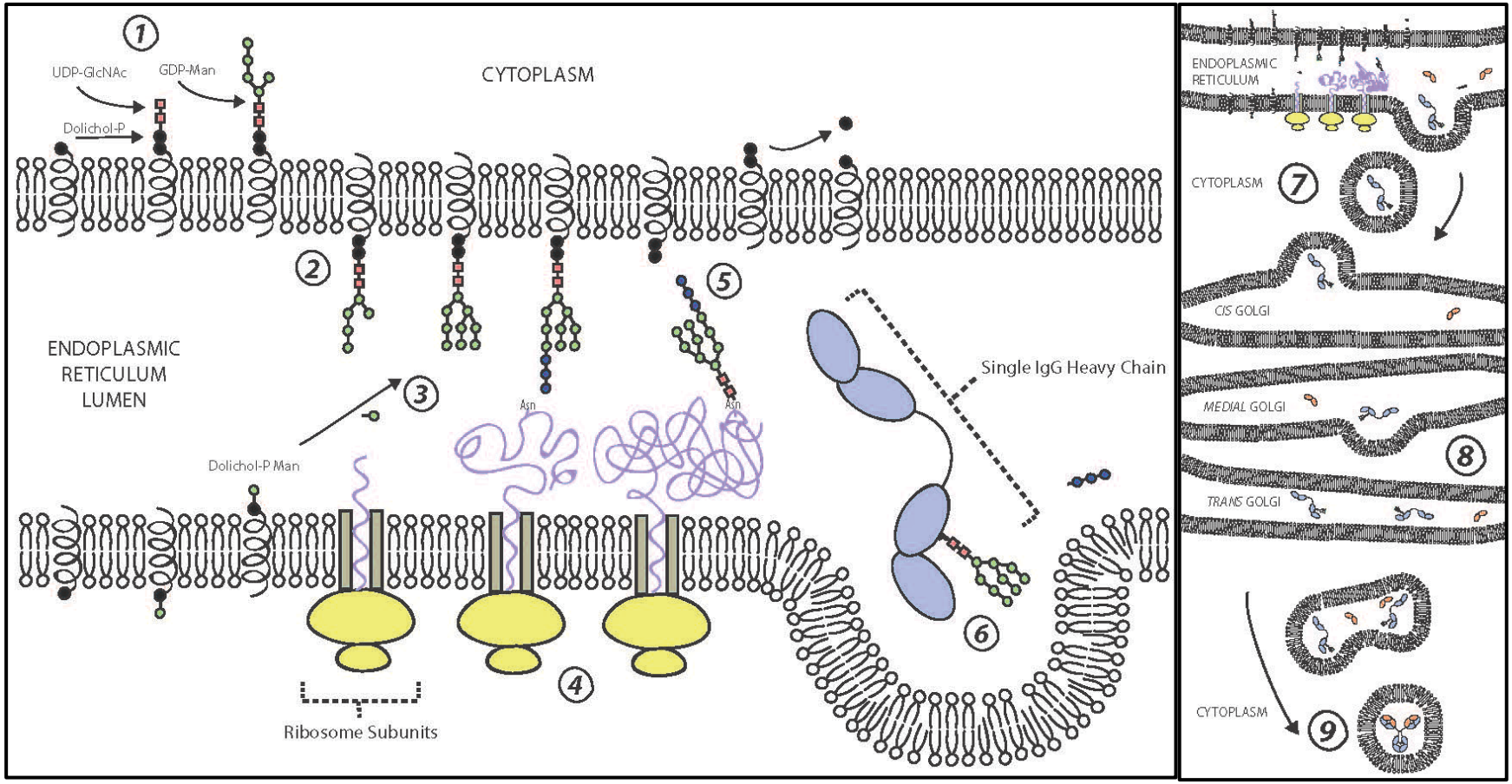
1
UDP-GlcNAc
GDP-Man
Dolichol-P
CYTOPLASM
2
5
ENDOPLASMIC
RETICULUM
LUMEN
3
Asn
Asn
Single IgG Heavy Chain
Dolichol-P Man
6
4
Ribosome Subunits
ENDOPLASMIC
RETICULUM
CYTOPLASM
7
CIS GOLGI
MEDIAL GOLGI
8
TRANS GOLGI
CYTOPLASM
9

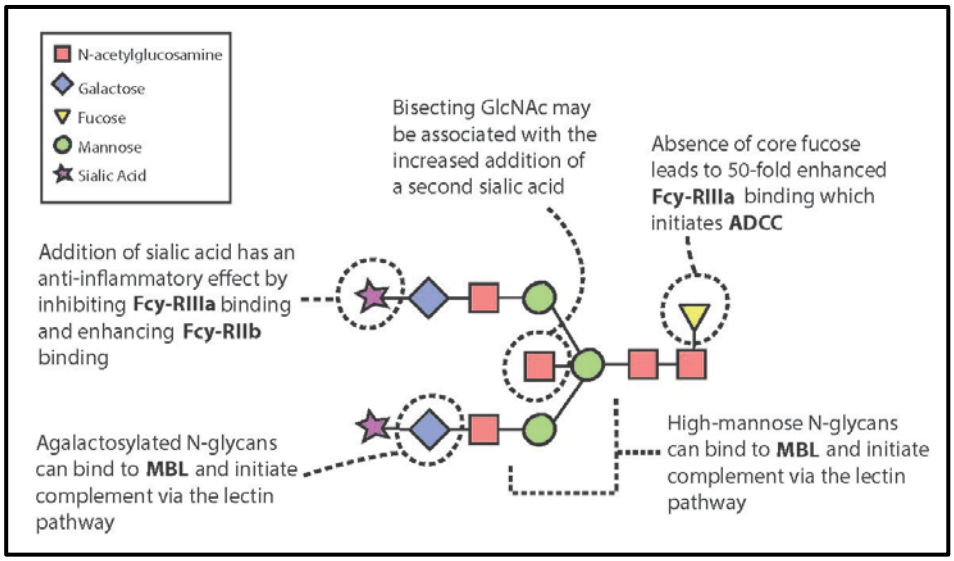

Figure 4: Effector functions caused by modifications to IgG glycosylation.

A lack of core fucose leads to a 100-fold increase in ADCC making these IgG more pro-inflammatory (Shields et al., 2002). Conversely, the addition of fucose to the asparagine-attached core *N*-acetylglucosamine (GlcNAc) of the IgG-Fc *N*-glycan has an anti-inflammatory effect by inhibiting Fcγ-RIIIa receptor binding (Shields et al., 2002). Fcγ-RIIIa are expressed on the surface of natural killer cells (Pucic et al., 2011) and have a role in initiating ADCC (Shields et al., 2002). Previous studies (Lauc et al., 2013; Pucic et al., 2011) have shown that the vast majority of IgG *N*-glycans are core fucosylated, hence they are designed to inhibit ADCC activation subsequent to many IgG binding to an antigen (via the antigen-binding cleft; see **Fig. 1**). However, structural analysis of the IgG-Fc/FcγRIIIa complex has demonstrated that specific glycans on FcγRIIIa are also essential for the effect of core fucose (Ferrara et al., 2011). The presence of a bisecting GlcNAc has also been associated with enhanced ADCC activation via Fcγ-RIIIa binding (Zou et al., 2011) but to a lesser degree than the absence of core fucose (Shields et al., 2002).

Mannose-rich glycans have an increased affinity for MBL which initiates the lectin complement cascade via opsonisation of IgG and the cells to which they are bound (Fujita, 2002; Malhotra et al., 1995). Both mannose and GlcNAc (GlcNAc to a lesser degree than mannose) are

prominent ligands for MBL and are usually found on the surface of pathogens, such as bacteria and viruses (Fujita, 2002; Maupin et al., 2012). Other monosaccharides, such as sialic acid and galactose, normally decorate mammalian glycoproteins and have undetectable affinity for MBL (Fujita, 2002; Maupin et al., 2012). This enables the specific recognition of glycans on pathogen cell surfaces. However, this innate immunity system can malfunction and has been implicated in many disease processes due to an increase in agalactosylated and mannose-rich *N*-glycans. In rheumatoid arthritis, MBL recognises clusters of agalactosylated IgG within the synovial joints and activates the lectin complement cascade which contributes to inflammation by damaging the surrounding tissue (Arnold et al., 2007). Additionally, an increase in agalactosylated *N*-glycans is correlated with an increase in disease severity in rheumatoid arthritis patients (Malhotra et al., 1995). Therefore, both IgG with high-mannose glycans and agalactosylated glycans could cause an increased activation of complement-caused inflammation.

Glycan biomarkers used for Alzheimer's disease have already been researched, with some examples of success (Angata et al., 2012; Chen et al., 2010; Lundström et al., 2014; Rensburg et al., 2004). In the case of PD and PD dementia, both age and disease related glycan biomarkers would be useful. One of the main risk factors for PD and PD dementia is age, suggesting that evidence of early ageing in the glycome may be connected to PD presence. Also, motor impairments are thought to be apparent at stage three to four of the Braak staging hypothesis (Braak, Bohl, et al., 2006; Braak et al., 2003), and mild cognitive symptoms are frequently present at the time of diagnosis, thus increasing the risk of progression to dementia (Shi et al., 2010). The variability seen in the glycome could provide novel glycan biomarkers for PD, not just detecting disease presence but also differentiating between subtypes and predicting progression to cognitive impairment.

1.3 Overview, Specific Aims and Hypotheses

Studies on genetically complex diseases, such as idiopathic PD, have led to discoveries of gene mutations that increase the risk of disease development. However, the contribution of these risk gene mutations to disease development in certain people but not others is less known. It is evident that an interaction between the genome and the environment exists. Glycomics is emerging as a prominent field of science in the quest for biomarker discovery, and

modifications to the glycosylation of many proteins, including IgG, are proposed to contribute to the holistic picture of a disease phenotype. Solely, these modifications will provide an interphenotype of disease: a link between the genome, the environment and the disease phenotype.

Study 1 – IgG *N*-glycans as a Novel Biomarker of Disease Presence

Aim: To identify changes in the peripheral IgG glycome in a PD patient cohort compared with an age- and gender-matched control cohort representative of a 'normally' aged population that represent an interphenotype of the disease.

Therefore, the hypotheses are:

- The peripheral IgG glycome profile will be different in people with PD compared with a control population.
- Modifications to the peripheral IgG glycome in people with PD will be pro-inflammation in nature.

Study 2 – Utility of IgG *N*-glycans in Identifying Risk of Cognitive Decline

Aim: To determine whether the peripheral IgG glycome has utility in identifying risk of cognitive decline in people with PD.

Therefore, the hypotheses are:

- Modifications to the peripheral IgG glycome profile will reflect different clinical motor subtypes of PD, specifically the PIGD motor subtype which infers a high risk of cognitive impairment.
- Modifications to the peripheral IgG glycome profile will be different in people with PD who have semantic fluency impairment, and hence are at a high risk of developing cognitive impairment.

2.0 Methods

2.1 Study Samples

2.1.1 Ethics Approval

Before participating in the larger cohort studies, all individuals gave informed consent. This including consenting to their de-identified data and blood samples being used in related studies. The longitudinal ParkC study was approved by the Edith Cowan University Human Research Ethics Committee [Project 2736], and the larger study of the control group was approved by the appropriate Ethics Board of the University of Zagreb Medical School, Croatia. This thesis conformed to the ethical guidelines of the 1975 Declaration of Helsinki and was approved by the Edith Cowan University Human Research Ethics Committee [Project 9927].

2.1.2 Participants

In total, the plasma samples of 196 participants were utilised in this study; 94 PD cases and 102 individuals as a matched control group.

The PD cases are a subgroup of the Parkinson's Centre (ParkC) ongoing community-based longitudinal study (n=243) investigating the "c*ognitive and motor heterogeneity in idiopathic Parkinson's disease*" (Bucks et al., 2011; Cruise et al., 2011). As part of the study participants are asked to complete a demographic questionnaire as well as numerous validated questionnaires assessing mood, sleep, quality of life, cognitive assessments and a motor assessment. Participants are given the option to provide a sample of their blood for genetic and related analyses, and hence there was no control on the final number of PD cases obtained.

The control participants were age- and gender-matched to the PD cases and are a part of a larger longitudinal study (n=969), described elsewhere (Knezevic et al., 2009). The controls represent a 'normally-aged' comparative Caucasian population in this study, with some individuals who have mild to chronic diseases other than dementia included among the healthy. This information was considered in the interpretation of the results.

2.1.3 Acquired Data

De-identified data from both cohorts was provided for this study including: age, gender, height and weight, and comorbidities. Specific comorbidities acquired from each cohort were slightly

different and as such were not comparable. Hence, they are not reported here. However, the fact that comorbidities existed within each cohort is worth mentioning. Further information provided on the subset of ParkC participants included: age at clinical PD diagnosis, animal naming task score, and raw MDS-UPDRS data. This information was utilised in **Study 2**.

2.1.4 Collection of Blood Samples

Blood samples were collected, processed and stored in the freezer at -80°C until analysis. Plasma (50 µL) was used for glycan analysis by ultra performance liquid chromatography (UPLC).

2.2 Glycan Analysis

2.2.1 Site of Analysis

The analysis of the plasma IgG glycans was outsourced to Genos, Ltd; a research-intensive small to medium enterprise based in Zagreb, Croatia. Genos Ltd has expertise in molecular genetics and glycomics. They perform contract research, analysis and service for universities, hospitals and private individuals within Europe and overseas. The following are the procedures (entire section **2.2 Glycan Analysis**) used for the analyses in the study, which have been used previously by Genos Ltd (Knezevic et al., 2009; Lauc et al., 2013; Pucic et al., 2011).

2.2.2 IgG Isolation

Plasma samples (50 µL) were diluted 10 × with binding buffer and applied to the 96-well Protein G monolithic plate (BIA Separations, Ajdovščina, Slovenia; Pucic et al., 2011). The plate was then washed five times with 5 column volumes of binding buffer (1X PBS, pH 7.4) to remove unbound proteins. IgG was released from the protein G monoliths using 5 column volumes of elution solvent (0.1 M formic acid, pH 2.5). Eluates were collected in a 96-deep-well plate and immediately neutralised to pH 7.0 with neutralisation buffer (1 M ammonium bicarbonate) to maintain the IgG stability.

2.2.3 N-glycans Release and Labelling

Isolated IgG samples were dried in a vacuum centrifuge. After drying, proteins were denatured with the addition of 30 µL 1.33% sodium dodecyl sulfate (w/v) (Invitrogen, Carlsbad, CA, USA) and incubated at 60 °C for 10 min. Subsequently, 10 µL 4% Igepal-CA630 (Sigma-Aldrich, St. Louis, MO, USA) and 0.5 mU of PNGase F (ProZyme, Hayward, CA) in 10 µL 5× PBS were added to the samples. The samples were incubated overnight at 37 °C for *N*-glycan release.

The released *N*-glycans were subsequently labelled with 2-aminobenzamide (2-AB). The labelling mixture was freshly prepared by dissolving 2-AB (Sigma-Aldrich, St. Louis, MO, USA) in dimethyl sulphoxide (DMSO; Sigma-Aldrich, St. Louis, MO, USA) and glacial acetic acid (Merck, Darmstadt, Germany) mixture (17:3 (v/v)) to a final concentration of 48 mg/mL. A volume of 25 µL of labelling mixture was added to each *N*-glycan release sample in the 96-well plate. Also, 25 µL of freshly prepared reducing agent solution (2-picoline borane (Sigma-Aldrich, St. Louis, MO, USA) in DMSO – concentration of 106.96 mg/ml) was added and the plate was sealed using adhesive tape. Mixing was achieved by shaking for 10 min, followed by incubation at 65 °C for 2 hr. Samples were brought to 80% acetonitrile (ACN) (v/v) by adding 400 µL of ACN (J.T. Baker, Phillipsburg, NJ).

2.2.4 Cleaning and Elution of Labelled Glycans using Hydrophilic Interaction Chromatography - Solid Phase Extraction (HILIC-SPE)

Free label and reducing agent were removed from the samples using HILIC-SPE. An amount of 200 µL of a 0.1 g/mL suspension of microcrystalline cellulose (Merck, Darmstadt, Germany) in water was applied to each well of a 0.45 µm GHP filter plate (Pall Corporation, Ann Arbor, MI, USA). Solvent was removed by application of vacuum using a vacuum manifold (Millipore Corporation, Billerica, MA, USA). All wells were prewashed using 5 × 200 µL water, followed by equilibration using 3 × 200 µL acetonitrile/water (80:20, v/v). The samples were loaded in to the wells and subsequently washed 7 × using 200 µL of acetonitrile/water (80:20, v/v).

Glycans were eluted 2 × with 100 µL of water and combined eluates were stored at –20 °C until analysis.

2.2.5 Ultra-Performance Liquid Chromatography (UPLC)

Fluorescently labelled *N*-glycans were separated by UPLC on a Waters Acquity UPLC instrument (Waters, Milford, MA) consisting of a quaternary solvent manager, sample

manager and a FLR fluorescence detector set with excitation and emission wavelengths of 330 nm and 420 nm, respectively. The UPLC instrument utilised Empower 2 software (Waters, Milford, MA). Labelled *N*-glycans were separated on a Waters BEH Glycan chromatography column, 100 × 2.1 mm i.d., 1.7 µm BEH particles, with 100 mM ammonium formate, pH 4.4, as solvent A and acetonitrile as solvent B. The UPLC separation method used a linear gradient of 75–62% acetonitrile at a flow rate of 0.4 ml/min in a 25 min analytical run. Samples were maintained at 5 °C before injection, and the separation temperature was 60 °C.

The system was calibrated using an external standard of hydrolyzed and 2-AB labelled glucose oligomers from which the retention times for the individual glycans were converted to glucose units. Data processing was performed using an automatic processing method with a traditional integration algorithm after which each chromatogram was manually corrected to maintain the same intervals of integration for all the samples.

The chromatograms obtained were all separated in the same manner into 24 glycan peaks for the total glycome and 15 peaks in the neutral glycome. The neutral glycome is the sum of all the neutral glycans in the total glycome, i.e. $GPn_{total} = \Sigma\ GP1{:}15_{raw\ values}$. The relative abundances of glycan peak (GP) were normalised to the total integrated area, e.g. $GP1 = GP1_{raw\ value} / GP_{total} * 100$.

2.2.6 Derived Traits

Derived traits were approximated from the ratios of glycan peaks, as previously described (Pucic et al., 2011). The minor glycan peak GP3 was excluded from all the calculations because in some samples it co-eluted with a contaminant that significantly affected its value.

Derived traits were defined as: the percentage of sialylation of fucosylated galactosylated structures without bisecting GlcNAc in total IgG glycans, FGS/(FG + FGS) = SUM(GP16 + GP18 + GP23)/SUM(GP16 + GP18 + GP23 + GP8 + GP9 + GP14)* 100; the percentage of sialylation of fucosylated galactosylated structures with bisecting GlcNAc in total IgG glycans, FBGS/(FBG + FBGS) = SUM(GP19 + GP24)/SUM(GP19 + GP24 + GP10 + GP11 + GP15)* 100; the percentage of sialylation of all fucosylated structures without bisecting GlcNAc in total IgG glycans, FGS/(F + FG + FGS) = SUM(GP16 + GP18 + GP23)/SUM(GP16 + GP18 + GP23 + GP4 + GP8 + GP9 + GP14)* 100; the percentage of sialylation of all fucosylated structures with bisecting GlcNAc in total IgG glycans, FBGS/(FB + FBG + FBGS) = SUM(GP19 + GP24)/SUM(GP19 + GP24 + GP6 + GP10 + GP11 + GP15)* 100; the percentage of monosialylation of fucosylated

monogalactosylated structures in total IgG glycans, FG1S1/(FG1 + FG1S1) = GP16/SUM(GP16 + GP8 + GP9)* 100; the percentage of monosialylation of fucosylated digalactosylated structures in total IgG glycans, FG2S1/(FG2+FG2S1+FG2S2) = GP18/SUM(GP18 + GP14 + GP23)* 100; the percentage of disialylation of fucosylated digalactosylated structures in total IgG glycans, FG2S2/(FG2 + FG2S1 + FG2S2) = GP23/SUM(GP23 + GP14 + GP18)* 100; the percentage of monosialylation of fucosylated digalactosylated structures with bisecting GlcNAc in total IgG glycans, FBG2S1/(FBG2 + FBG2S1 + FBG2S2) = GP19/SUM(GP19 + GP15 + GP24)* 100; the percentage of disialylation of fucosylated digalactosylated structures with bisecting GlcNAc in total IgG glycans, FBG2S2/(FBG2 + FBG2S1 + FBG2S2) = GP24/SUM(GP24 + GP15 + GP19)* 100; ratio of all fucosylated (± bisecting GlcNAc) monosialylated and disialylated structures in total IgG glycans, $F^{total}S1/F^{total}S2$ = SUM(GP16 + GP18 + GP19)/SUM(GP23 + GP24); ratio of fucosylated (without bisecting GlcNAc) monosialylated and disialylated structures in total IgG glycans, FS1/FS2 = SUM(GP16 + GP18)/GP23; ratio of fucosylated (with bisecting GlcNAc) monosialylated and disialylated structures in total IgG glycans, FBS1/FBS2 = GP19/GP24; ratio of all fucosylated sialylated structures with and without bisecting GlcNAc, FBS^{total}/FS^{total} = SUM(GP19 + GP24)/SUM(GP16 + GP18 + GP23); ratio of fucosylated monosialylated structures with and without bisecting GlcNAc, FBS1/FS1 = GP19/SUM(GP16 + GP18); the incidence of bisecting GlcNAc in all fucosylated monosialylated structures in total IgG glycans, FBS1/(FS1 + FBS1) = GP19/SUM(GP16 + GP18 + GP19); ratio of fucosylated disialylated structures with and without bisecting GlcNAc, FBS2/FS2 = GP24/GP23; the incidence of bisecting GlcNAc in all fucosylated disialylated structures in total IgG glycans, FBS2/(FS2 + FBS2) = GP24/SUM(GP23 + GP24).

The following derived traits were approximated only from the ratios of glycan peaks containing neutral glycan as a major structure. First, the relative abundance of each neutral glycan peak ($GP1^n$ - $GP15^n$) was calculated from the total neutral glycan fraction (SUM(GP1:GP15)) and then traits were defined as: the percentage of agalactosylated structures in total neutral glycan fraction, $G0^n$ = SUM($GP1^n$ + $GP2^n$ + $GP4^n$ + $GP6^n$); the percentage of monogalactosylated structures in total neutral glycan fraction, $G1^n$ = SUM($GP7^n$ + $GP8^n$ + $GP9^n$ + $GP10^n$ + $GP11^n$); the percentage of digalactosylated structures in total neutral glycan fraction, $G2^n$ = SUM($GP12^n$ + $GP13^n$ + $GP14^n$ + $GP15^n$); the percentage of all fucosylated (±bisecting GlcNAc) structures in total neutral glycan fraction, $F^{n\ total}$ = SUM($GP1^n$ + $GP4^n$ + $GP6^n$ + $GP8^n$ + $GP9^n$ + $GP10^n$ + $GP11^n$ + $GP14^n$ + $GP15^n$); the percentage of fucosylation of agalactosylated structures, $FG0^{n\ total}/G0^n$ = SUM($GP1^n$ + $GP4^n$ + $GP6^n$)/$G0^n$ * 100; the percentage of fucosylation of monogalactosylated structures, $FG1^{n\ total}/G1^n$ = SUM($GP8^n$ + $GP9^n$ + $GP10^n$ + $GP11^n$)/$G1^n$ * 100; the percentage of

fucosylation of digalactosylated structures, $FG2^{n\ total}/G2^{n} = SUM(GP14^{n} + GP15^{n})/G2^{n} * 100$; the percentage of fucosylated (without bisecting GlcNAc) structures in total neutral glycan fraction, $F^{n} = SUM(GP1^{n} + GP4^{n} + GP8^{n} + GP9^{n} + GP14^{n})$; the percentage of fucosylation (without bisecting GlcNAc) of agalactosylated structures, $FG0^{n}/G0^{n} = SUM(GP1^{n} + GP4^{n})/G0^{n} * 100$; the percentage of fucosylation (without bisecting GlcNAc) of monogalactosylated structures, $FG1^{n}/G1^{n} = SUM(GP8^{n} + GP9^{n})/G1^{n} * 100$; the percentage of fucosylation (without bisecting GlcNAc) of digalactosylated structures, $FG2^{n}/G2^{n} = GP14^{n}/G2^{n} * 100$; the percentage of fucosylated (with bisecting GlcNAc) structures in total neutral glycan fraction, $FB^{n} = SUM(GP6^{n} + GP10^{n} + GP11^{n} + GP15^{n})$; the percentage of fucosylation (with bisecting GlcNAc) of agalactosylated structures, $FBG0^{n}/G0^{n} = GP6^{n}/G0^{n} * 100$; the percentage of fucosylation (with bisecting GlcNAc) of monogalactosylated structures, $FBG1^{n}/G1^{n} = SUM(GP10^{n} + GP11^{n})/G1^{n} * 100$; the percentage of fucosylation (with bisecting GlcNAc) of digalactosylated structures, $FBG2^{n}/GP2^{n} = GP15^{n}/G2^{n} * 100$; ratio of fucosylated structures with and without bisecting GlcNAc, $FB^{n}/F^{n} = FB^{n}/F^{n}$; the incidence of bisecting GlcNAc in all fucosylated structures in total neutral glycan fraction, $FB^{n}/F^{n\ total} = FB^{n}/F^{n\ total} * 100$; ratio of fucosylated non-bisecting GlcNAc structures and all structures with bisecting GlcNAc, $F^{n}/(B^{n} + FB^{n}) = F^{n}/(GP13^{n} + FB^{n})$; ratio of structures with bisecting GlcNAc and all fucosylated structures (± bisecting GlcNAc), $B^{n}/(F^{n} + FB^{n})$ (‰) = $GP13^{n}/(F^{n}+ \% FB^{n}) * 1000$; ratio of fucosylated digalactosylated structures with and without bisecting GlcNAc, $FBG2^{n}/FG2^{n} = GP15^{n}/GP14^{n}$; the incidence of bisecting GlcNAc in all fucosylated digalactosylated structures in total neutral glycan fraction, $FBG2^{n}/(FG2^{n} + FBG2^{n}) = GP15^{n}/(GP14^{n} + GP15^{n}) \times 100$; ratio of fucosylated digalactosylated nonbisecting GlcNAc structures and all digalactosylated structures with bisecting GlcNAc, $FG2^{n}/(BG2^{n} + FBG2^{n}) = GP14^{n}/(GP13^{n} + GP15^{n})$; ratio of digalactosylated structures with bisecting GlcNAc and all fucosylated digalactosylated structures (±bisecting GlcNAc), $BG2^{n}/(FG2^{n} + FBG2^{n})$ (‰) = $GP13^{n}/(GP14^{n} + GP15^{n}) * 1000$.

2.3 Statistical Analysis

All analyses were performed using R statistical programming language (R Core Team, 2014) through the R studio console (RStudio, 2014). Package details can be found next to each mentioned statistical method.

2.3.1 Batch Effects

One often overlooked aspect of high-throughput data analysis is batch effects, defined as "*…sub-groups of measurements that have qualitatively different behaviour across conditions and are unrelated to the biological or scientific variables in the study*" (Leek et al., 2010). It exists because laboratory conditions, reagents and technicians vary between different batches, and can compound the biological effects within the data (Leek et al., 2010). Blocking, organising samples for analysis so there is the same distribution of case/controls, gender or age on plates (i.e. plates are comparable), was used to control batch effects within the study (for blocking data, see **Appendix 3**).

To explore batch effects, data tables were created for each plate that compared case status, age and gender. Boxplots were then created for visual inspection of batch effects (see **Appendix 4**) with case status faceted to see whether any common patterns of change existed for each individual GP. Principal component analysis (PCA; 'stats' package) was performed to check for clustering of plate samples. If batch effects existed, the principal components would predict groupings that would be according to plates rather than case status.

2.3.2 Study 1: IgG *N*-Glycans as a Novel Biomarker of PD

Q-Q plots, created using the 'qqnorm' function of the *stats* package (R Core Team, 2014), were employed to test the normality of each variable (participant characteristics, GPs and derived traits). Q-Q plots of untransformed variables are in **Appendix 5**.

The vast majority of the glycan variables were non-normally distributed. Therefore, log-transformations were applied to each of the non-normal glycan variables so that parametric tests could be utilised (**Appendix 6**). All variables, with the exception of three, were log-normal. To qualify for a Students t-test ('t.test' function of the *stats* package with 'var.equal' argument equal to 'TRUE'; R Core Team, 2014), the variables must fulfil the assumptions of independence, normality and homogeneity of variances. Both groups were independent of each other. Therefore, all variables that were normally (or log-normally) distributed were subjected to Levene's test for homogeneity of variances, using 'leveneTest' function in the *car* package (Fox & Weisberg, 2011). Results of Levene's test are in **Appendix 7**. Student's t-tests could be performed on each GP and derived trait that met these assumption criteria. For glycan variables that met assumptions for independence and normality but not homoscedasticity, Welch's t-test ('t.test' function of the *stats* package with 'var.equal' argument equal to 'FALSE'; R Core Team, 2014) could be utilised which adjusts the degrees of

freedom (df) according to the unequal variances between the independent groups. The non-parametric equivalent, Mann-Whitney U test ('wilcox.test' function in the *stats* package; R Core Team, 2014) was used for comparisons of means of the non-normal glycan variables; GP1, GP1n and GP22. The Chi-squared test ('chisq.test' function in the *stats* package; R Core Team, 2014) was used for comparing gender frequency in each group.

Correlation matrices were calculated for both groups independently using the 'rcorr' function in the *Hmisc* package (Harrell, 2014). Spearman's correlation coefficient (r_s) was the method used as not all variables could be successfully transformed ('type' argument of the 'rcorr' function equal to 'spearman'). r_s is also more robust to strong outliers than the parametric equivalent, Pearson's product-moment correlation coefficient (Niven & Deutsch, 2012). These coefficients will provide the effect size of an association.

To test for statistically significant differences in effect sizes between the independent groups, Fisher's r-to-z transformation was performed for each bivariate correlation, using the 'cocor.indep.groups' function in the *cocor* package (Diedenhofen, 2013), where there was at least a moderate correlation ($r_s > |0.5|$, $P < 0.05$) in one of the groups. A strong correlation was considered to be an $r_s > |0.7|$ ($P < 0.05$).

Statistical significance was set at $P < 8.06 \times 10^{-4}$ for Student's and Welch's t-test, Mann-Whitney U tests and Spearman's correlation coefficient for each of the GPs and derived traits. This reflects the probability of committing a type I error controlling for multiple testing, i.e. a P-value with Bonferroni correction. There were 62 tests of means performed in this study, therefore $P \leq \frac{0.05}{62} \approx 0.000806$ (i.e. $P < 8.06 \times 10^{-4}$). For Fisher's r-to-z, P was colour coded for values less than 0.05, 0.01 and 0.001 (red, yellow and green, respectively) in the correlation matrices (see **Appendix 8**).

All graphical representations of the statistics were performed using the 'ggplot' function of the *ggplot2* package in R (Wickham, 2009).

2.3.3 Study 2: Utility of IgG *N*-Glycans in Identifying Risk of Cognitive Decline

Non-parametric testing was used to analyse the different GPs and derived traits within the PD cases for the evaluated motor subtypes and risk of cognitive decline (animal naming task). Kruskal-Wallis one-way analysis of variance ('kruskal.test' function of the *stats* package; R Core

Team, 2014) was used to evaluate the variables with two or more groups. Statistical significance was set as above at $P < 8.06 \times 10^{-4}$ to control for multiple tests of means.

2.3.3.1 Motor Subtype Evaluation

The MDS-UPDRS parts II and III were used to calculate a clinical motor subtype of PD for the purpose of this study, as previously described (Stebbins et al., 2013). Based on the score on particular items (0 for normal to 4 for severe), the PD cases were grouped into one of three clinical motor subtypes; tremor dominant (TD), postural instability and gait dysfunction (PIGD) dominant, or an indeterminate (ID) subtype for those that fell into neither of the TD or PIGD motor subtypes.

Total tremor score was defined as the mean MDS-UPDRS tremor score at the items listed in **Table 1**. Likewise, total PIGD score was defined as the MDS-UPDRS PIGD score at the items listed in **Table 1**. Motor subtype was classified as PIGD when the ratio total tremor score/total PIGD score was equal to or less than 1.0, whereas those with a ratio of 1.5 or more were defined as TD. When tremor/PIGD was more than 1.0 and less than 1.5, they were classified as an ID. Moreover, participants with a positive mean tremor score in the numerator but a zero mean PIGD score in the denominator were classified as TD; participants with a zero mean tremor score in the numerator and a positive mean PIGD score in the denominator were classified as PIGD; and participants with zeros in both the numerator and denominator were classified as ID.

2.3.3.2 Risk of Cognitive Decline

Semantic fluency dysfunction is associated with a higher risk of cognitive impairment and dementia development (Hu et al., 2014; Pereira et al., 2014; Williams-Gray et al., 2009). Therefore, the risk of cognitive decline was determined using the animal naming task. Briefly, ParkC participants are instructed to name as many types of animals as they can in 60 seconds. A single score is given for each correct type of animal. Repetitions or age variants of animals (cow, then calf) are two examples of responses that would not receive a score. Full conditions and scoring are included as **Appendix 2**. For this study and similar to a previous study (Williams-Gray et al., 2009), impaired semantic fluency was defined as a score less than 20.

Hence, a factor was created for statistical analyses whereby those who scored less than 20 had a level of '0' and those who scored 20 or more had a level of '1'.

Table 1: MDS-UPDRS items used to evaluate motor subtype. Mean tremor score is calculated by summing the given score at each of the listed tremor items and dividing by 11. Likewise, mean PIGD score is calculated by summing the given score at each of the listed PIGD items and dividing by 5.

Tremor Score Items	PIGD Score Items
MDS-UPDRS Part II	
2.10 Tremor	2.12 Walking and balance
	2.13 Freezing
MDS-UPDRS Part III	
3.15 Postural tremor right UE	3.10 Gait
3.15 Postural tremor left UE	3.11 Freezing of gait
3.16 Kinetic tremor right UE	3.12 Postural stability
3.16 Kinetic tremor left UE	
3.17 Rest tremor right UE	
3.17 Rest tremor left UE	
3.17 Rest tremor right LE	
3.17 Rest tremor left LE	
3.17 Rest tremor lip/jaw	
3.18 Rest constancy	

LE: Lower Extremity; PIGD: postural instability and gait disturbance dominant; UE: Upper Extremity.

3.0 Results

3.1 Study 1: IgG *N*-Glycans as a Novel Biomarker of PD

3.1.1 Participants

Summary statistics for the participants in this study are shown in **Table 2**. Controls were matched for age and gender; therefore, there was not a statistically significant difference ($P < 8.06 \times 10^{-4}$) in age (t [194] = 0.4683, $P = 0.640$) or gender (χ^2 [1, n=196] = 0.0048, $P = 0.945$) between the two independent groups (**Fig. 5a**). However, there was a statistically significant difference in BMI (t [194] = 3.7622, $P = 0.0002$) (**Fig. 5b**).

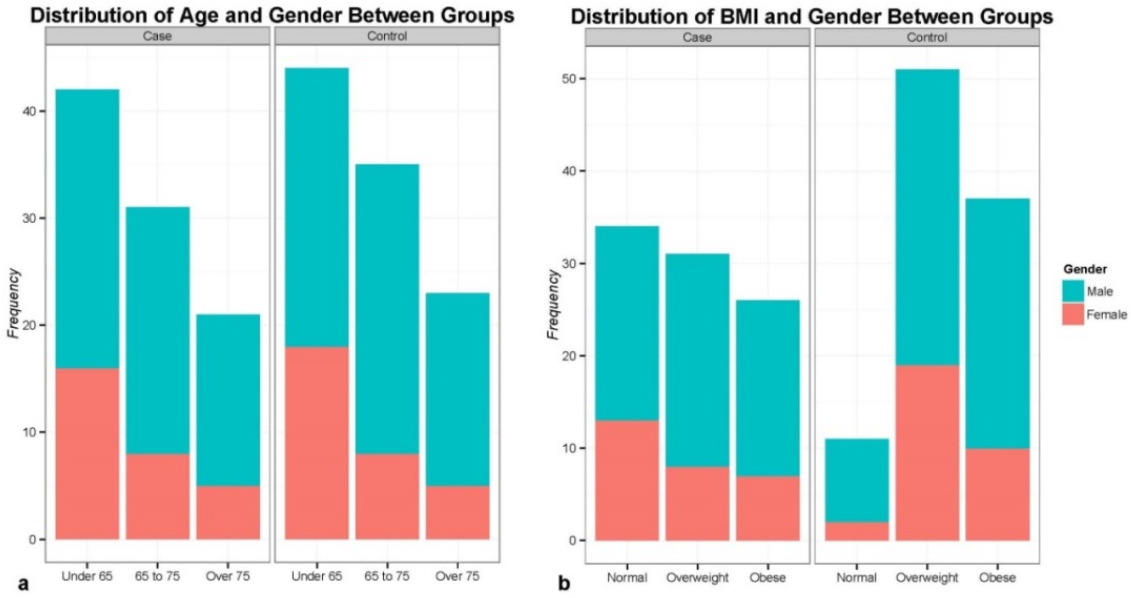

Figure 5: Stacked bar graphs for summary statistics between groups, a) age and b) BMI. Age is in years. Normal, BMI 18 to 25; Overweight, BMI 25 to 30; Obese, BMI above 30.

Inspecting the PD cases, there was not a statistically significant difference between the gender (χ^2 [1, n=337] = 0.002, $P = 0.9679$) or age at entry to the study (t [1, 335] = 1.0424, $P = 0.298$) between the subgroup and the whole cohort of ParkC participants. Unfortunately height and weight data was not available for the entire ParkC cohort. As such, it was not possible to test differences in BMI between the subgroup and the whole ParkC cohort.

Table 2: Summary statistics for the participants in the Study 1.

	PD Cases	Controls	Between Group Differences	
			t-statistic	*P*-value
Participants *n*	94	102		
Age $\bar{x}$ (S)	66.65 (8.99)	67.26 (9.22)	0.4683	0.640
Gender *n* male (%)	65 (69.1%)	71 (69.6%)	0.0048	0.945
BMI $\bar{x}$ (S)	26.40 (4.76)	28.61 (3.40)	3.7622	**0.0002**

*χ^2 statistic

BMI, body mass index; $\bar{x}$, sample mean; S, sample standard deviation

3.1.2 Batch Effects

Summary statistics for each of the plates used for UPLC analysis are shown in **Table 3**. Blocking was performed to randomly place matched-samples on the same plate, i.e. those with the same gender and similar age, along with blanks (for blocking data, see **Appendix 3**). Samples were unevenly distributed between the plates; considerably fewer samples were on plate 3 due to one plate being filled before the next. Boxplots were created for each of the GPs and are included as **Appendix 4**. However, overall there were only mild batch effects and these did not appear to translate through the study.

Table 3: Summary statistics for the distribution of Study 1 samples on plates for UPLC analysis.

	Age $\bar{x}$ (S)	M n (%)	Age $\bar{x}$ (S)	M n (%)
Plate 1	**PD Case (n=42)**		**Control (n=45)**	
	64.12 (10.82)	26 (61.9%)	65.04 (11.49)	28 (62.2%)
Plate 2	**PD Case (n=42)**		**Control (n=44)**	
	68.98 (5.89)	30 (71.4%)	69.30 (5.99)	31 (70.5%)
Plate 3	**PD Case (n=10)**		**Control (n=13)**	
	67.50 (9.35)	9 (90.0%)	68.08 (8.27)	12 (92.3%)

PCA was used to explore whether the first two principal components could cluster according to plate number (see **Fig. 6a**), and case status (see **Fig. 6b**). The first two principal components explained 43.84% of the variance in this study. No clustering was seen for plate number in this study; however, it appeared that the first two principal components of GP1 to GP24 could be used to cluster case status.

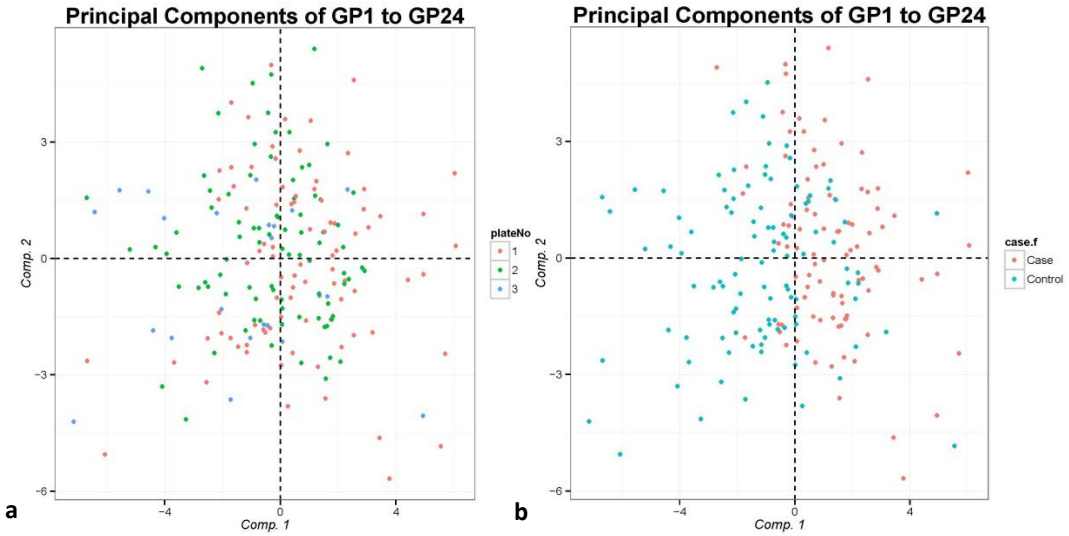

Figure 6: Scatters showing the first two principal components in terms of: a) plate number; and b) case status.

3.1.3 Case-Control Comparisons

Overall, 12 GPs and six derived traits in the total and neutral IgG glycome had statistically significant differences ($P < 8.06 \times 10^{-4}$) between cases and controls on performing Students t-test.

In the total IgG glycome, there were seven statistically significant differences ($P < 8.06 \times 10^{-4}$) between groups. The relative abundances of the following five GPs were significantly lower in the PD cases compared to the controls (see **Fig. 7** and **Table 4**):

- GP5, a high-mannose glycan (t [160.289] = -13.7128, $P < 2.2 \times 10^{-16}$);
- GP17, a biantennary digalactosylated monosialylated glycan (t [163.601] = -13.6209, $P < 2.2 \times 10^{-16}$);
- GP20, an unknown glycan structure (t [134.135] = -14.0479, $P < 2.2 \times 10^{-16}$);
- GP21, a biantennary digalactosylated disialylated glycan (t [149.140] = -9.4946, $P < 2.2 \times 10^{-16}$);
- GP22, a biantennary digalactosylated disialylated glycan with bisecting GlcNAc (U = 3142.5, $P = 3.046 \times 10^{-5}$).

The relative abundances of the following two GPs were significantly higher in the PD cases compared to the controls (see **Table 4**):

- GP8, a biantennary core fucosylated monogalactosylated glycan (t [194] = 5.2345, $P = 4.279 \times 10^{-7}$);
- GP14, a biantennary core fucosylated digalactosylated glycan (t [194] = 4.2332 $P = 3.275 \times 10^{-5}$).

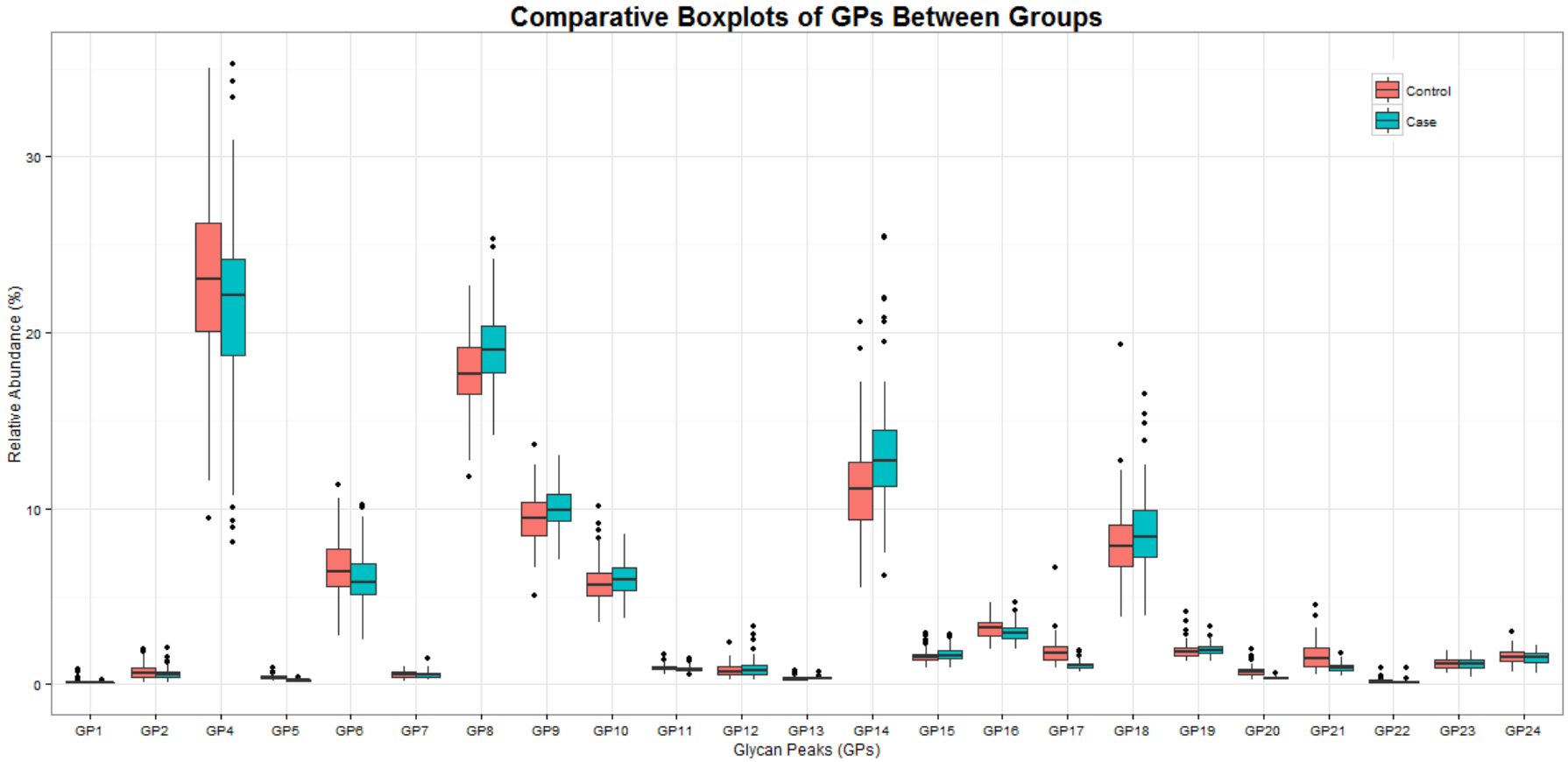

Figure 7: Boxplots showing total glycan peaks (GPs) between PD cases and controls.

Table 4: Descriptive statistics for the GPs within the total IgG glycome.

N-glycan peak	PD cases		Controls		Between Group Difference	
	Median (IQR)	Range	Median (IQR)	Range	t-statistic *U statistic	*P* - value
GP1	0.080 (0.040)	0.030 - 0.280	0.080 (0.048)	0.030 - 0.830	4655.5*	0.727
GP2	0.555 (0.328)	0.130 - 2.090	0.615 (0.575)	0.120 - 2.010	-2.4310	0.016
GP4	22.120 (5.460)	8.100 - 35.310	23.050 (6.110)	9.440 - 35.070	-2.0661	0.040
GP5	0.240 (0.075)	0.150 - 0.440	0.410 (0.128)	0.190 - 0.950	-13.7128#	**< 2.2 x10^{-16}**
GP6	5.805 (1.773)	2.550 - 10.240	6.415 (2.153)	2.790 - 11.350	-3.3072	0.001
GP7	0.545 (0.260)	0.230 - 1.460	0.575 (0.340)	0.180 - 0.980	-0.8352	0.405
GP8	19.030 (2.670)	14.170 - 25.300	17.660 (2.620)	11.830 - 22.700	5.2345	**4.279 x10^{-7}**
GP9	9.885 (1.527)	7.080 - 13.050	9.445 (1.872)	5.080 - 13.620	3.0931	0.002
GP10	5.945 (1.328)	3.780 - 8.510	5.630 (1.307)	3.490 - 10.160	1.4165	0.158
GP11	0.880 (0.160)	0.540 - 1.450	0.905 (0.218)	0.580 - 1.670	-3.0866	0.002
GP12	0.785 (0.518)	0.240 - 3.310	0.745 (0.458)	0.240 - 2.410	0.9122	0.363
GP13	0.340 (0.080)	0.220 - 0.700	0.340 (0.100)	0.220 - 0.800	-0.9727	0.332
GP14	12.720 (3.190)	6.180 - 25.470	11.150 (3.208)	5.520 - 20.650	4.2532	**3.275 x10^{-5}**
GP15	1.660 (0.445)	0.930 - 2.860	1.530 (0.358)	0.910 - 2.880	2.8166	0.005
GP16	2.905 (0.622)	2.020 - 4.630	3.215 (0.788)	2.000 - 4.650	-3.2509	0.001
GP17	1.080 (0.265)	0.720 - 1.940	1.795 (0.733)	0.950 - 6.600	-13.6209#	**< 2.2 x10^{-16}**
GP18	8.395 (2.617)	3.940 - 16.520	7.885 (2.377)	3.850 - 19.320	2.1213	0.035
GP19	1.895 (0.397)	1.320 - 3.310	1.875 (0.442)	1.300 - 4.150	0.4212	0.674
GP20	0.350 (0.108)	0.220 - 0.670	0.700 (0.315)	0.280 - 2.020	-14.0479#	**< 2.2 x10^{-16}**
GP21	0.915 (0.328)	0.460 - 1.740	1.500 (1.063)	0.560 - 4.500	-9.4946#	**< 2.2 x10^{-16}**
GP22	0.120 (0.065)	0.050 - 0.930	0.150 (0.088)	0.060 - 0.930	3142.5*	**3.046 x10^{-5}**
GP23	1.145 (0.488)	0.430 - 1.950	1.160 (0.448)	0.600 - 1.940	-0.0580	0.954
GP24	1.535 (0.535)	0.640 - 2.250	1.560 (0.525)	0.750 - 2.990	-1.6844	0.094

GPx: glycan peak with 'x' corresponding to number; IQR: interquartile range; # Welch's t-test for unequal variances utilised. The degrees of freedom (df) used for each t-test are found in **Appendix 7** next to the respective GPs.

GP values are presented as percentages of the total IgG glycome, i.e. GP1 = GP1/GP * 100. Statistically significant differences ($P < 8.06 \times 10^{-4}$) were determined using Student's t-test [df = 194] and bold. Those variables that did not have a normal (or log-normal) distribution were analysed using the Mann-Whitney U test.

In the neutral IgG glycome (see **Table 5**), there were five statistically significant differences ($P < 8.06 \times 10^{-4}$) between groups. The relative abundances of the following three GPs were significantly lower in the PD cases compared to the controls:

- $GP5^n$, a high-mannose glycan (t [153.062] = -14.4049, $P < 2.2 \times 10^{-16}$);
- $GP6^n$, a biantennary core fucosylated glycan with bisecting GlcNAc (t [194] = -4.2282, $P = 3.676 \times 10^{-5}$);
- $GP11^n$, a biantennary core fucosylated monogalactosylated glycan with bisecting GlcNAc (t [194] = -4.0865, $P = 6.406 \times 10^{-5}$).

The relative abundances of the following two GPs were significantly higher in the PD cases compared to the controls:

- $GP8^n$, a biantennary core fucosylated monogalactosylated glycan (t [194] = 3.6267, $P = 3.670 \times 10^{-4}$);
- $GP14^n$, a biantennary core fucosylated digalactosylated glycan (t [194] = 3.4356, $P = 7.230 \times 10^{-4}$).

The differences with GP6 and GP11 between groups did not reach statistically significance in the total IgG glycome. However, with all the GPs that had glycan structures without terminal sialic acid removed in the neutral IgG glycome (i.e. GP16 to GP24), there were statistical significant differences for both $GP6^n$ and $GP11^n$. Interestingly the major glycan moieties were similar in each GP (see **Appendix 1**), with the addition of a terminal galactose in $GP11^n$.

Table 5: Descriptive statistics for the GPs within the neutral IgG glycome.

N-glycan peak	PD cases		Controls		Between Group Difference	
	Median (IQR)	Range	Median (IQR)	Range	t-statistic *U statistic	*P* - value
$GP1^n$	0.100 (0.040)	0.040 - 0.350	0.105 (0.068)	0.040 - 0.990	4553.5*	0.544
$GP2^n$	0.685 (0.428)	0.170 - 2.540	0.765 (0.680)	0.180 - 2.420	-2.7593	0.006
$GP4^n$	26.580 (6.310)	10.770 - 41.970	28.890 (7.010)	13.900 - 42.380	-2.9342	0.004
$GP5^n$	0.295 (0.080)	0.190 - 0.520	0.520 (0.155)	0.260 - 1.130	-14.4049#	**< 2.2 x10^{-16}**
$GP6^n$	7.210 (1.855)	3.390 - 12.210	8.180 (2.332)	4.110 - 13.970	-4.2458	**3.376 x10^{-5}**
$GP7^n$	0.660 (0.310)	0.270 - 1.830	0.720 (0.428)	0.270 - 1.250	-1.2463	0.214
$GP8^n$	23.430 (2.570)	16.280 - 31.310	22.140 (3.610)	14.570 - 33.440	3.6267	**3.670 x10^{-4}**
$GP9^n$	12.300 (1.830)	8.820 - 16.350	11.780 (2.320)	7.490 - 17.720	2.062	0.041
$GP10^n$	7.215 (1.650)	4.500 - 10.090	7.030 (1.603)	4.560 - 14.960	0.6522	0.515
$GP11^n$	1.085 (0.218)	0.670 - 1.690	1.150 (0.250)	0.830 - 2.090	-4.0865	**6.406 x10^{-5}**
$GP12^n$	0.970 (0.640)	0.290 - 4.140	0.930 (0.568)	0.350 - 3.010	0.6033	0.547
$GP13^n$	0.420 (0.108)	0.260 - 0.880	0.430 (0.118)	0.290 - 1.100	4413.5*	0.3378
$GP14^n$	2.745 (0.279)	1.960 - 3.543	2.650 (0.328)	1.917 - 3.249	3.4356	**7.230 x10^{-4}**
$GP15^n$	0.735 (0.288)	0.104 - 1.295	0.645 (0.244)	0.113 - 1.411	2.0664	0.040

GP^nx: glycan peak with 'x' corresponding to number; IQR: interquartile range; # Welch's t-test for unequal variances utilised. The degrees of freedom (df) used for each t-test are found in **Appendix 7** next to the respective GPs.

GP values are presented as percentages of the neutral glycan pool, i.e. $GP1^n = GP1^n/GP^n * 100$. Statistically significant differences ($P < 8.06 \times 10^{-4}$) were determined using Students t-test [df = 194] and bold. Those variables that did not have a normal (or log-normal) distribution were analysed using the Mann-Whitney U test.

Derived traits (see **Table 6**) were calculated using formulas of the different GPs (see **Section 2.2.6**). The statistically significant differences ($P < 8.06 \times 10^{-4}$) observed between the PD cases and controls in the total IgG glycome were associated with a lower percentage of sialylation of core fucosylated glycans without bisecting GlcNAc overall (FGS/(FG+FGS); t [194] = -3.5372, $P = 5.058 \times 10^{-4}$) which is associated with less anti-inflammatory activity. In the derived traits using the GPs of the neutral IgG glycome, statistically significant differences were observed between the levels of galactosylated glycans; lower levels of agalactosylation ($G0^n$; t [194] = -3.6370, $P = 3.535 \times 10^{-4}$) and higher levels of monogalactosylation ($G1^n$; t [189.123] = 3.8576, $P = 1.569 \times 10^{-4}$) in the PD cases compared to the controls. PD cases also had a lower ratio of digalactosylated glycans with bisecting GlcNAc divided by all core fucosylated digalactosylated glycans with and without bisecting GlcNAc ($BG2^n/(FG2^n+FBG2^n)$; t [194] = -3.9751, $P = 9.919 \times 10^{-5}$). This was interpreted as a higher level of core fucosylated digalactosylated glycans in the neutral IgG glycome of PD cases compared to the control group.

Table 6: Descriptive statistics for the derived traits from the total and neutral IgG glycome.

Glycan trait	PD cases		Controls		Between Group Difference	
	Median (IQR)	Range	Median (IQR)	Range	t-statistic	*P* - value
Percentage of Sialylation of Fucosylated Structures with Bisecting GlcNAc						
FBGS/(FBG+FBGS)	28.690 (7.290)	15.880 - 44.870	29.460 (7.310)	18.190 - 45.530	-1.427	0.140
Percentage of Sialylation of Fucosylated Structures without Bisecting GlcNAc						
FGS/(FG+FGS)	23.380 (3.670)	17.240 - 31.380	24.500 (3.640)	18.980 - 37.320	-3.5372	**5.058 x10^{-4}**
Percentage of Sialylation of Fucosylated Galactosylated Glycans with Bisecting GlcNAc						
FBG2S1/(FBG2 +FBG2S1+FBG2S2)	37.600 (4.940)	26.890 - 50.300	37.530 (4.970)	30.400 - 51.110	-0.2801	0.780
FBG2S2/(FBG2 +FBG2S1+FBG2S2)	29.610 (6.600)	15.370 - 38.520	30.930 (6.780)	14.660 - 42.750	-3.0348	0.003
Percentage of Sialylation of Fucosylated Galactosylated Glycans without Bisecting GlcNAc						
FG1S1/(FG1+FG1S1 +FG2S2+FG2S2)	9.105 (2.082)	5.700 - 13.610	10.790 (2.400)	6.680 - 15.080	-5.8788	**1.777 x10^{-8}**
FG2S1/(FG1+FG1S1 +FG2S2+FG2S2)	38.030 (3.450)	31.260 - 43.430	39.120 (3.640)	33.440 - 57.870	-3.9504	**1.091 x10^{-4}**
FG2S2/(FG1+FG1S1 +FG2S2+FG2S2)	4.950 (1.897)	1.720 - 9.580	5.830 (2.409)	1.920 - 12.800	-2.7751	0.006
Percentage of Galactosylation						
G0^{n}	34.740 (7.790)	14.470 - 53.110	38.130 (8.310)	18.270 - 55.530	-3.6370	**3.535 x10^{-4}**
G1^{n}	45.230 (3.330)	36.340 - 52.010	43.770 (4.570)	34.460 - 57.010	3.8576$^{\#}$	**1.569 x10^{-4}**
G2^{n}	19.260 (5.140)	10.100 - 41.460	17.400 (5.460)	9.290 - 32.470	3.2262	0.001
Percentage of Fucosylation (+/- Bisecting GlcNAc)						
F$^{n\ total}$	96.910 (1.330)	91.910 - 98.650	96.440 (1.770)	93.990 - 98.510	-2.6030	0.010
FG0^{n}/G0$^{n\ total}$	97.970 (1.240)	94.490 - 99.450	97.930 (1.780)	94.210 - 99.550	-1.3187	0.189
FG1^{n}/G1$^{n\ total}$	98.560 (0.720)	95.900 - 99.320	98.310 (1.000)	97.110 - 99.530	-1.9937	0.048
FG2^{n}/G2$^{n\ total}$	92.590 (3.050)	80.520 - 96.460	91.410 (3.940)	84.680 - 96.860	-2.5195	0.013
Percentage of Fucosylation with Bisecting GlcNAc						
FB^{n}	17.820 (3.490)	11.970 - 24.220	18.340 (3.910)	14.360 - 26.470	-2.4126	0.017
FBG0^{n}/G0^{n}	21.290 (4.660)	11.650 - 32.750	21.720 (5.040)	14.370 - 31.850	-1.0821	0.281
FBG1^{n}/G1^{n}	18.460 (3.900)	11.980 - 25.760	19.200 (3.860)	14.600 - 28.620	-1.7795	0.077
FBG2^{n}/G2^{n}	10.695 (1.856)	7.520 - 17.430	10.820 (2.568)	8.360 - 17.970	-2.0838	0.038
Percentage of Fucosylation without Bisecting GlcNAc						
F^{n}	79.090 (4.530)	69.650 - 86.680	77.670 (4.380)	68.890 - 83.620	2.9265	0.004
FG0^{n}/G0^{n}	76.610 (5.420)	63.480 - 87.800	75.640 (5.220)	64.490 - 85.030	1.3953	0.165
FG1^{n}/G1^{n}	80.220 (4.490)	71.610 - 86.940	79.210 (4.170)	69.310 - 84.490	2.0542	0.041
FG2^{n}/G2^{n}	81.860 (3.880)	70.270 - 87.500	80.240 (4.910)	67.400 - 85.670	-3.1790	0.002
Other Traits						
FB^{n}/(F^{n}+FB^{n})	18.400 (3.740)	12.140 - 25.780	19.200 (3.980)	14.650 - 27.760	-2.4793	0.014
FG2^{n}/(BG2^{n}/FBG2^{n})	6.345 (1.183)	3.350 - 9.530	5.990 (1.748)	3.060 - 8.200	3.0569	0.003
BG2^{n}/(FG2^{n}+FBG2^{n})	23.070 (9.130)	11.720 - 42.250	27.430 (9.900)	14.120 - 83.330	-3.9751	**9.919 x10^{-5}**

B, bisecting GlcNAc; F, core fucose; G, galactose; S, sialic acid; $^{\#}$ Welch's t-test for unequal variances utilised. The degrees of freedom (df) used for each t-test are found in **Appendix 7** next to the respective GPs.

See 2.2.6 Derived Traits for further details. Statistically significant differences ($P < 8.06 \times 10^{-4}$) were determined using Students t-test [df = 194] and bold.

3.1.4 Associations of Age, BMI, and GPs to other GPs and Derived Traits

Correlation matrices were conducted for both groups independently. On observing bivariate associations in the PD cases, age (see **Table 7** and **8**) was significantly ($P < 8.06 \times 10^{-4}$) and positively correlated with:

- GP4 (r_s [194] = 0.37, P = 0.0002),
- GP5 (r_s [194] = 0.41, P = 0.0000),
- GP6 (r_s [194] = 0.36, P = 0.0003),
- Agalactosylated glycans ($G0^n$; r_s [194] = 0.38, P = 0.0002),
- Core fucosylated digalactosylated glycans with bisecting GlcNAc ($FBG2^n/G2^n$; r_s [194] = 0.40, P = 0.0000).

Moreover, in the PD cases, age was significantly and negatively correlated with:

- GP14 (r_s [194] = -0.38, P = 0.0002),
- GP18 (r_s [194] = -0.39, P = 0.0001),
- Digalactosylated glycans ($G2^n$; r_s [194] = -0.37, P = 0.0002).

Age, however, was not significantly correlated with any GP or derived trait in the control group. Furthermore, no statistically significant association was found between BMI (see **Tables 9** and **10**) and any GP or derived trait within this study.

Table 7: Correlation between age and GPs in both the PD cases and controls.

N-glycan peak	PD cases		Controls	
	r_s	*P* - value	r_s	*P* - value
GP1	0.32	0.0017	0.26	0.0073
GP2	0.13	0.2162	0.03	0.7917
GP4	**0.37**	**0.0002**	0.31	0.0014
GP5	**0.41**	**0.0000**	0.19	0.0554
GP6	**0.36**	**0.0003**	0.13	0.1788
GP7	0.00	0.9851	-0.03	0.7590
GP8	-0.10	0.3513	-0.22	0.0235
GP9	-0.04	0.7240	0.01	0.9051
GP10	0.21	0.0423	-0.21	0.0363
GP11	0.34	0.0009	-0.05	0.6371
GP12	-0.12	0.2680	-0.17	0.0806
GP13	0.02	0.8263	-0.14	0.1493
GP14	**-0.38**	**0.0002**	-0.32	0.0009
GP15	-0.10	0.3407	-0.33	0.0008
GP16	0.00	0.9662	0.18	0.0696
GP17	-0.05	0.6313	0.00	0.9766
GP18	**-0.39**	**0.0001**	-0.22	0.0237
GP19	-0.11	0.2864	-0.01	0.9111
GP20	-0.08	0.4237	0.01	0.9377
GP21	-0.05	0.6064	0.10	0.3221
GP22	-0.10	0.3498	0.09	0.3843
GP23	-0.24	0.0189	0.10	0.3350
GP24	-0.07	0.5282	0.09	0.3426

r_s, Spearman's Rho correlation coefficient

Table 8: Correlation between age and derived traits in both the PD cases and controls.

Glycan trait	PD cases		Controls	
	r_s	*P* - value	r_s	*P* - value
Percentage of Sialylation of Fucosylated Structures with Bisecting GlcNAc				
FBGS/(FBG+FBGS)	-0.18	0.0867	0.20	0.0400
Percentage of Sialylation of Fucosylated Structures without Bisecting GlcNAc				
FGS/(FG+FGS)	-0.17	0.1016	0.07	0.4715
Percentage of Sialylation of Fucosylated Galactosylated Glycans with Bisecting GlcNAc				
FBG2S1/(FBG2 +FBG2S1+FBG2S2)	0.02	0.8178	0.08	0.4441
FBG2S2/(FBG2 +FBG2S1+FBG2S2)	-0.05	0.6650	0.27	0.0062
Percentage of Sialylation of Fucosylated Galactosylated Glycans without Bisecting GlcNAc				
FG1S1/(FG1+FG1S1 +FG2S2+FG2S2)	0.06	0.5693	0.23	0.0197
FG2S1/(FG1+FG1S1 +FG2S2+FG2S2)	0.11	0.2906	0.18	0.0707
FG2S2/(FG1+FG1S1 +FG2S2+FG2S2)	0.01	0.9115	0.27	0.0066
Percentage of Galactosylation				
$G0^n$	**0.38**	**0.0002**	0.32	0.0009
$G1^n$	-0.21	0.0385	-0.29	0.0033
$G2^n$	**-0.37**	**0.0002**	-0.32	0.0011
Percentage of Fucosylation (+/- Bisecting GlcNAc)				
F^{total}	0.03	0.7382	0.07	0.4842
$FG0^n/G0^{n\ total}$	0.08	0.4186	0.10	0.3066
$FG1^n/G1^{n\ total}$	-0.01	0.9165	-0.04	0.7162
$FG2^n/G2^{n\ total}$	-0.13	0.2243	-0.04	0.6633
Percentage of Fucosylation with Bisecting GlcNAc				
FB^n	0.24	0.0179	-0.09	0.3801
$FBG0^n/G0^n$	-0.06	0.5631	-0.24	0.0173
$FBG1^n/G1^n$	0.26	0.0100	-0.11	0.2893
$FBG2^n/G2^n$	**0.40**	**0.0000**	0.06	0.5758
Percentage of Fucosylation without Bisecting GlcNAc				
F^n	-0.19	0.0739	0.08	0.4138
$FG0^n/G0^n$	0.06	0.5465	0.22	0.0280
$FG1^n/G1^n$	-0.22	0.0299	0.07	0.4555
$FG2^n/G2^n$	-0.30	0.0032	-0.08	0.4222
Other Traits				
$FB^n/(F^n+FB^n)$	0.22	0.0294	-0.08	0.4286
$FG2^n/(BG2^n/FBG2^n)$	**-0.39**	**0.0001**	-0.12	0.2363
$BG2^n/(FG2^n+FBG2^n)$	**0.35**	**0.0006**	0.21	0.0373

B, bisecting GlcNAc; F, core fucose; G, galactose; S, sialic acid

Table 9: Correlation between BMI and GPs in both the PD cases and controls.

N-glycan peak	PD cases		Controls	
	r_s	*P* - value	r_s	*P* - value
GP1	0.09	0.3988	0.04	0.6629
GP2	0.12	0.2666	-0.14	0.1768
GP4	0.27	0.0111	0.06	0.5644
GP5	0.13	0.2325	-0.03	0.7772
GP6	0.12	0.2774	0.06	0.5715
GP7	-0.01	0.9276	-0.13	0.1872
GP8	0.06	0.5587	-0.06	0.5779
GP9	0.07	0.4902	-0.10	0.3468
GP10	-0.02	0.8323	0.08	0.4588
GP11	0.03	0.7635	0.02	0.8152
GP12	-0.08	0.4265	-0.09	0.3508
GP13	-0.12	0.2534	0.07	0.5171
GP14	-0.24	0.0210	0.00	0.9765
GP15	-0.24	0.0211	0.03	0.7519
GP16	-0.08	0.4381	-0.03	0.7907
GP17	-0.22	0.0383	0.01	0.9407
GP18	-0.27	0.0110	-0.01	0.8854
GP19	-0.08	0.4675	-0.01	0.9112
GP20	-0.18	0.0960	-0.01	0.9538
GP21	-0.07	0.5240	0.06	0.5397
GP22	-0.08	0.4647	-0.02	0.8661
GP23	-0.17	0.0972	0.13	0.2138
GP24	-0.11	0.2886	0.02	0.8307

r_s, Spearman's Rho correlation coefficient

Table 10: Correlation between BMI and derived traits in both the PD cases and controls.

Glycan trait	PD cases		Controls	
	r_s	*P* - value	r_s	*P* - value
Percentage of Sialylation of Fucosylated Structures with Bisecting GlcNAc				
FBGS/(FBG+FBGS)	-0.07	0.5004	-0.03	0.7364
Percentage of Sialylation of Fucosylated Structures without Bisecting GlcNAc				
FGS/(FG+FGS)	-0.26	0.0120	0.04	0.7141
Percentage of Sialylation of Fucosylated Galactosylated Glycans with Bisecting GlcNAc				
FBG2S1/(FBG2 +FBG2S1+FBG2S2)	0.16	0.1287	-0.04	0.7134
FBG2S2/(FBG2 +FBG2S1+FBG2S2)	0.02	0.8616	0.03	0.7436
Percentage of Sialylation of Fucosylated Galactosylated Glycans without Bisecting GlcNAc				
FG1S1/(FG1+FG1S1 +FG2S2+FG2S2)	-0.14	0.1823	0.01	0.9060
FG2S1/(FG1+FG1S1 +FG2S2+FG2S2)	-0.13	0.2339	-0.02	0.8413
FG2S2/(FG1+FG1S1 +FG2S2+FG2S2)	0.02	0.8760	0.07	0.4688
Percentage of Galactosylation				
$G0^n$	0.24	0.0202	0.05	0.5941
$G1^n$	-0.08	0.4603	-0.09	0.3998
$G2^n$	-0.26	0.0135	0.00	0.9715
Percentage of Fucosylation (+/- Bisecting GlcNAc)				
$F^{n\ total}$	0.05	0.6148	0.16	0.1196
$FG0^n/G0^{n\ total}$	0.02	0.8251	0.16	0.1087
$FG1^n/G1^{n\ total}$	0.04	0.7371	0.12	0.2511
$FG2^n/G2^{n\ total}$	-0.02	0.8217	0.12	0.2338
Percentage of Fucosylation with Bisecting GlcNAc				
FB^n	-0.03	0.7642	0.09	0.3605
$FBG0^n/G0^n$	-0.17	0.1085	0.02	0.8107
$FBG1^n/G1^n$	-0.02	0.8728	0.10	0.3240
$FBG2^n/G2^n$	0.05	0.6570	0.07	0.5131
Percentage of Fucosylation without Bisecting GlcNAc				
F^n	0.06	0.5530	-0.01	0.9089
$FG0^n/G0^n$	0.16	0.1420	0.07	0.4917
$FG1^n/G1^n$	0.03	0.7545	-0.08	0.4475
$FG2^n/G2^n$	-0.02	0.8464	0.06	0.5323
Other Traits				
$FB^n/(F^n+FB^n)$	-0.04	0.7128	0.08	0.4547
$FG2^n/(BG2^n/FBG2^n)$	-0.07	0.4873	-0.06	0.5293
$BG2^n/(FG2^n+FBG2^n)$	0.10	0.3239	0.06	0.5454

B, bisecting GlcNAc; F, core fucose; G, galactose; S, sialic acid

Comparisons based on independent groups were made between each coefficient representative of at least a moderate correlation ($r_s > |0.5|$) in one of the groups. There were less statistically significant differences in the correlations of GPs between the groups in the neutral IgG glycome (see **Appendix 6c**) compared to the total IgG glycome (see **Appendix 6a**). Of interest were the statistically significant differences between the PD cases and controls where at least one coefficient was suggestive of a strong relationship ($r_s > |0.7|$). In the total IgG glycome, GP17 and GP20 had the most differences where at least one coefficient was suggestive of a strong relationship (see **Appendix 6a**). In the neutral IgG glycome, GP8n had the most significant differences (see **Appendix 6c**). The glycan with the most significant different correlations between groups was GP5; its correlation with GP20 was the most different between the groups in this study (see **Fig. 8**).

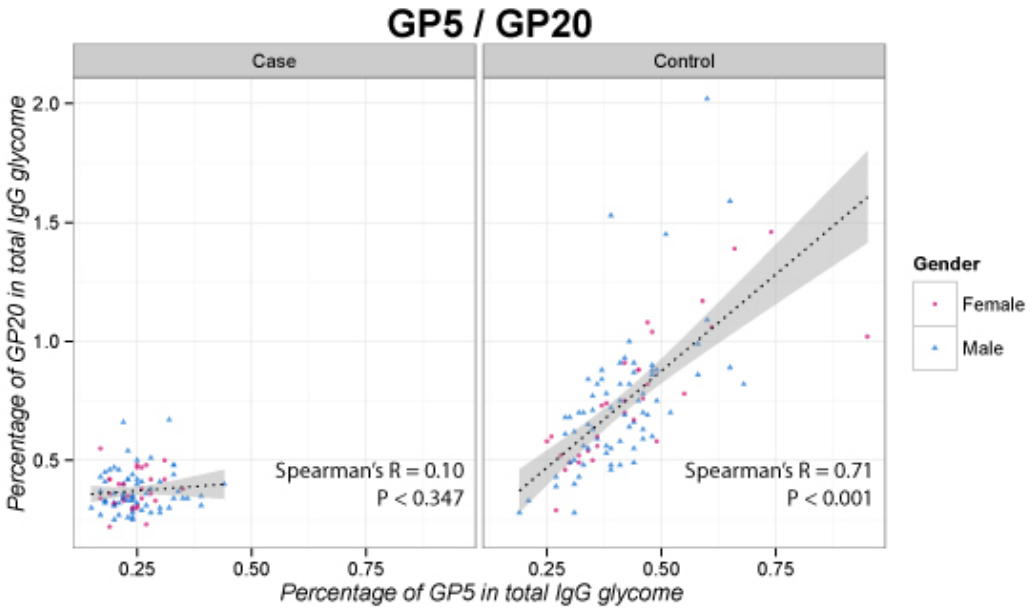

Figure 8: Two-way scatters of the relative abundance of GP5 and GP20. Correlations according to Spearman's Rho included. Fisher's r-to-z results confirmed this difference to be highly significant (z = 5.42, P = 0.0000).

3.2 Study 2: Utility of IgG *N*-Glycans in Identifying Risk of Cognitive Decline

3.2.1 Participants

Summary statistics for the PD cases with motor subtype data are shown in **Table 11**. In total there were 11 cases with no or incomplete motor subtype data in this study. However, there was not a statistically significant difference ($P < 8.06 \times 10^{-4}$) between those with and without motor subtype data in terms of age (χ^2 [1, n=94] = 0.2109, P = 0.646), gender (χ^2 [1, n=94] = 0.9273, P = 0.336) or BMI (χ^2 [1, n=94] = 1.7528, P = 0.186). Considering the motor subtype comparisons, there was not a statistically significant difference in age (χ^2 [1, n=83] = 1.0383, P = 0.595), gender (χ^2 [1, n=83] = 0.1373, P = 0.934) or BMI (χ^2 [1, n=83] = 0.1542, P = 0.926) between the three independent groups. As expected, there were far fewer participants classified as having an indeterminate (ID) motor subtype (n=9) compared to tremor dominant (TD; n=30) and postural instability and gait dysfunction dominant (PIGD; n=44).

Table 11: Summary statistics in terms of PD motor subtype.

	TD	PIGD	ID	Between Group Differences	
				χ2-statistic	*P*-value
Participants *n*	30	44	9		
Age $\bar{x}$ (S)	65.33 (10.78)	67.43 (7.33)	65.56 (12.29)	1.0383	0.595
Gender *n* male (%)	21 (70.0%)	29 (65.9%)	6 (66.7%)	0.1373	0.934
BMI $\bar{x}$ (S)	26.48 (3.89)	26.93 (5.19)	25.89 (4.91)	0.1542	0.926

ID, indeterminate; PIGD, postural instability and gait disturbance dominant; TD, tremor dominant; BMI, body mass index; $\bar{\mathbf{x}}$, sample mean; S, sample standard deviation

Summary statistics for the cases with an animal naming task score for semantic fluency are shown in **Table 12**. In total, there were three cases with no animal naming task score in this study. However, there was not a statistically significant difference ($P < 8.06 \times 10^{-4}$) between those with and without animal naming task data in terms of age (χ^2 [1, n=94] = 2.3705, P = 0.124), gender (χ^2 [1, n=94] = 1.3679, P = 0.242) or BMI (χ^2 [1, n=94] = 0.3753, P = 0.540). Similarly, there was not a statistically significant difference in gender (χ^2 [1, n=91] = 0.1514,

P = 0.697) or BMI (χ^2 [1, n=91] = 0.0920, P = 0.762) between the two independent groups. However, participants with an animal naming task score of less than 20 were significantly older than those with an animal naming task score equal to or greater than 20 (χ^2 [1, n=91] = 13.1491, P = 0.0003).

Table 12: Summary statistics in terms of animal naming task (ANT) score.

	ANT < 20	ANT ≥ 20	Between Group Differences	
			χ2-statistic	*P*-value
Participants *n*	56	35		
Age $\bar{x}$ (S)	69.21 (7.61)	61.91 (9.40)	13.1491	**0.0003**
Gender *n* male (%)	39 (69.6%)	23 (65.7%)	0.1514	0.697
BMI $\bar{x}$ (S)	26.28 (4.87)	26.46 (4.58)	0.0920	0.762

BMI, body mass index; $\bar{\mathbf{x}}$, sample mean; S, sample standard deviation

3.2.2 Batch Effects

Summary statistics for the distribution of PD case samples over the plates used for UPLC analysis are shown below for: motor subtype (see **Table 13**) and animal naming task score (see **Table 14**). Batch effects were also explored within the cases using PCA (Euclidean distance) in terms of motor subtype and animal naming task score. The first two principal components explained 44.00% of the variance in this study; however, these principal components could not be used to cluster the PD cases according to plate number (see **Fig. 9a**), motor subtype (see **Fig. 9b**) or animal naming task score (see **Fig. 9c**). This result is in stark comparison to **Fig6b** in **Study 1** where the PD cases and controls had almost separate clusters.

Table 13: Summary statistics for the distribution of Study 2 samples on plates for UPLC analysis.

	Age $\bar{x}$ (S)	M n (%)	Age $\bar{x}$ (S)	M n (%)	Age $\bar{x}$ (S)	M n (%)
Plate 1	**TD (n=15)**		**PIGD (n=17)**		**ID (n=6)**	
	62.60 (11.95)	9 (60.0%)	65.12 (9.23)	11 (64.7%)	64.50 (14.87)	4 (66.7%)
Plate 2	**TD (n=10)**		**PIGD (n=23)**		**ID (n=3)**	
	69.90 (6.59)	8 (80.0%)	68.70 (5.90)	14 (60.9%)	67.67 (6.43)	2 (66.7%)
Plate 3	**TD (n=5)**		**PIGD (n=4)**		**ID (n=0)**	
	64.40 (12.82)	4 (80.0%)	70.00 (2.94)	4 (100.0%)		

ID, indeterminate; PIGD, postural instability and gait disturbance dominant; TD, tremor dominant; $\bar{x}$, sample mean; S, sample standard deviation

Table 14: Summary statistics for the distribution of Study 2 samples on plates for UPLC analysis.

	Age $\bar{x}$ (S)	M n (%)	Age $\bar{x}$ (S)	M n (%)
Plate 1	**ANT score < 20 (n=23)**		**ANT score ≥ 20 (n=19)**	
	68.70 (10.08)	15 (65.2%)	58.58 (9.11)	11 (57.9%)
Plate 2	**ANT score < 20 (n=27)**		**ANT score ≥ 20 (n=13)**	
	69.52 (5.67)	19 (70.4%)	67.00 (6.24)	9 (69.2%)
Plate 3	**ANT score < 20 (n=6)**		**ANT score ≥ 20 (n=3)**	
	69.83 (4.54)	5 (83.3%)	61.00 (15.72)	3 (100.0%)

ANT, Animal Naming Task; $\bar{x}$, sample mean; S, sample standard deviation

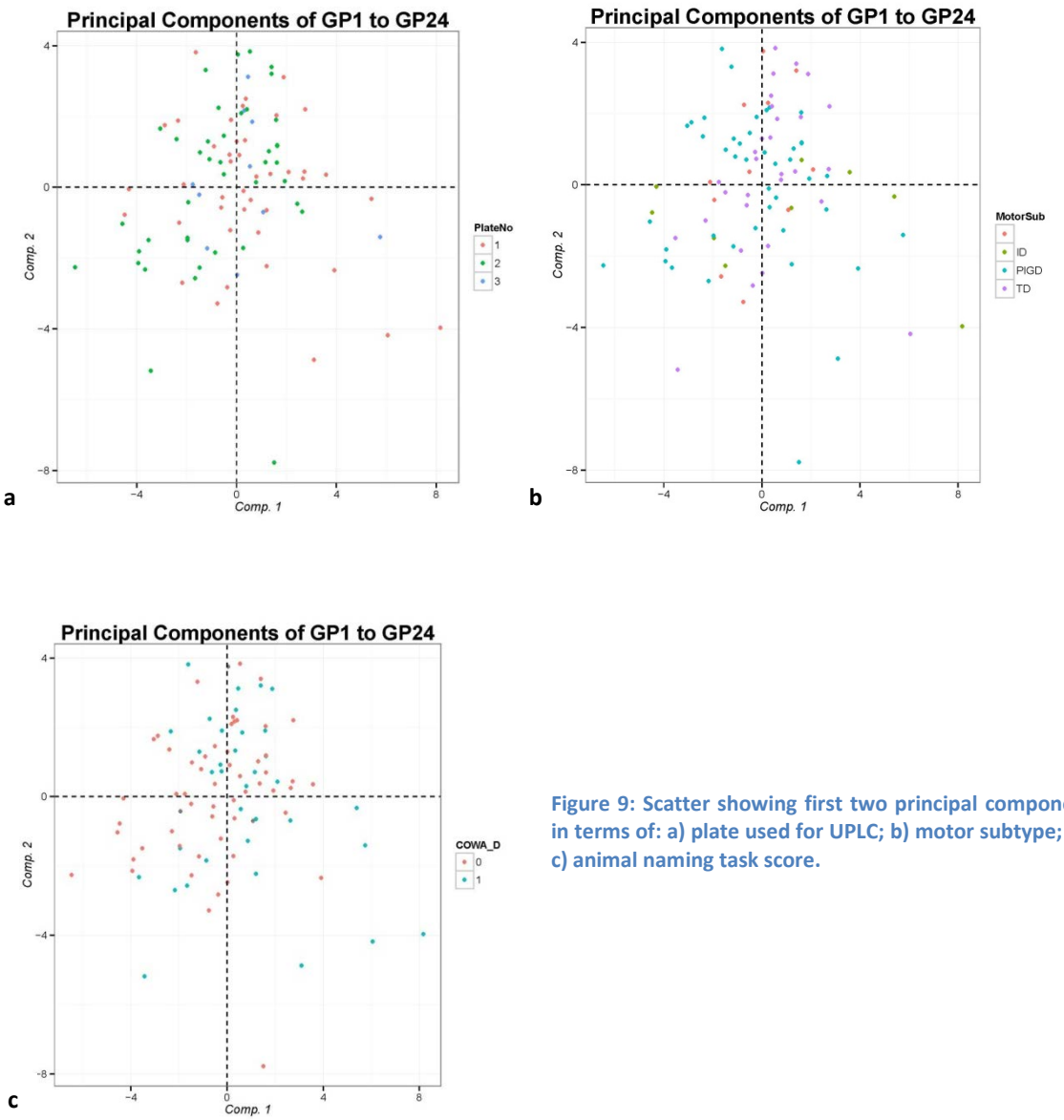

Figure 9: Scatter showing first two principal components in terms of: a) plate used for UPLC; b) motor subtype; and c) animal naming task score.

3.2.3 Motor Subtypes Comparisons

Comparisons between the PD cases in terms of motor subtype in the total IgG glycome (see **Table 15**), the neutral IgG glycome (see **Table 16**), and derived traits (see **Table 17**) are shown below. There were no statistically significant differences ($P < 8.06 \times 10^{-4}$) for either the total or neutral IgG glycome, or the derived traits of these.

Page intentionally left blank

Table 15: Descriptive statistics for the GPs within the total IgG glycome according to PD motor subtype.

N-glycan peak	Tremor Dominant		PIGD Dominant		Indeterminate Type		Between Group Difference	
	Median (IQR)	Range	Median (IQR)	Range	Median (IQR)	Range	χ2 statistic	P - value
GP1	0.08 (0.18)	0.04 - 0.22	0.09 (0.25)	0.03 - 0.28	0.08 (0.08)	0.04 - 0.12	2.2230	0.527
GP2	0.47 (1.93)	0.16 - 2.09	0.58 (1.44)	0.13 - 1.57	0.66 (0.79)	0.19 - 0.98	1.3553	0.716
GP4	20.86 (16.86)	10.72 - 27.58	22.61 (26.03)	9.28 - 35.31	19.18 (22.28)	8.10 - 30.38	0.6503	0.199
GP5	0.23 (0.27)	0.17 - 0.44	0.24 (0.22)	0.17 - 0.39	0.23 (0.24)	0.15 - 0.39	2.6753	0.444
GP6	5.82 (6.27)	3.78 - 10.05	5.77 (6.19)	4.05 - 10.24	4.70 (6.99)	2.55 - 9.54	1.1231	0.772
GP7	0.51 (0.69)	0.27 - 0.96	0.56 (1.23)	0.23 - 1.46	0.60 (0.34)	0.38 - 0.72	0.7241	0.868
GP8	19.06 (9.52)	15.78 - 25.30	18.87 (7.35)	14.17 - 21.52	19.29 (8.77)	15.39 - 24.16	2.0626	0.560
GP9	9.88 (5.79)	7.26 - 13.05	9.96 (5.75)	7.08 - 12.83	9.47 (2.19)	8.02 - 10.21	5.8514	0.119
GP10	6.08 (3.89)	4.22 - 8.11	5.94 (4.73)	3.78 - 8.51	6.21 (3.53)	4.58 - 8.11	1.2631	0.738
GP11	0.90 (0.56)	0.54 - 1.10	0.85 (0.82)	0.63 - 1.45	0.92 (0.50)	0.61 - 1.11	0.9429	0.815
GP12	0.78 (2.17)	0.40 - 2.57	0.80 (3.07)	0.24 - 3.31	1.05 (1.41)	0.56 - 1.97	2.9664	0.397
GP13	0.34 (0.23)	0.23 - 0.46	0.33 (0.48)	0.22 - 0.70	0.33 (0.16)	0.27 - 0.43	1.1388	0.768
GP14	13.13 (11.43)	8.01 - 19.44	12.50 (15.70)	6.18 - 21.88	14.20 (18.00)	7.47 - 25.47	3.2563	0.354
GP15	1.71 (1.46)	1.09 - 2.55	1.56 (1.93)	0.93 - 2.86	1.94 (1.34)	1.40 - 2.74	3.3797	0.337
GP16	2.92 (2.56)	2.07 - 4.63	2.86 (2.07)	2.07 - 4.14	2.70 (1.40)	2.02 - 3.42	9.2705	0.026
GP17	1.08 (1.14)	0.74 - 1.88	1.10 (1.22)	0.72 - 1.94	1.09 (0.76)	0.81 - 1.57	0.1828	0.980
GP18	8.70 (7.60)	6.23 - 13.83	8.22 (12.58)	3.94 - 16.52	9.05 (10.00)	5.37 - 15.37	2.9195	0.404
GP19	2.02 (1.36)	1.38 - 2.74	1.84 (1.99)	1.32 - 3.31	1.79 (1.03)	1.73 - 2.76	5.4112	0.144
GP20	0.35 (0.29)	0.22 - 0.51	0.34 (0.44)	0.23 - 0.67	0.41 (0.25)	0.30 - 0.55	2.6296	0.452
GP21	0.92 (0.88)	0.52 - 1.40	0.92 (1.28)	0.46 - 1.74	0.74 (0.44)	0.49 - 0.93	6.8917	0.075
GP22	0.12 (0.26)	0.05 - 0.31	0.11 (0.16)	0.05 - 0.21	0.10 (0.86)	0.07 - 0.93	1.9771	0.577
GP23	1.21 (1.44)	0.51 - 1.95	1.12 (1.33)	0.43 - 1.76	0.85 (1.01)	0.54 - 1.55	7.4973	0.058
GP24	1.68 (1.61)	0.64 - 2.25	1.40 (1.47)	0.71 - 2.18	1.33 (0.84)	0.88 - 1.72	11.9966	0.007

GP values are presented as percentages of the total IgG glycome, i.e. GP1 = GP1/GP * 100. Statistically significant differences ($P < 8.06 \times 10^{-4}$) were determined using the Mann-Whitney U test.

Page intentionally left blank

Table 16: Descriptive statistics for the GPs within the neutral IgG glycome according to PD motor subtype.

N-glycan peak	Tremor Dominant		PIGD Dominant		Indeterminate Type		Between Group Difference	
	Median (IQR)	Range	Median (IQR)	Range	Median (IQR)	Range	χ2 statistic	P - value
$GP1^n$	0.09 (0.22)	0.05 - 0.27	0.11 (0.31)	0.04 - 0.35	0.10 (0.09)	0.05 - 0.14	2.0333	0.566
$GP2^n$	0.58 (2.34)	0.20 - 2.54	0.72 (1.64)	0.17 - 1.81	0.80 (0.88)	0.25 - 1.13	1.4485	0.694
$GP4^n$	25.61 (19.02)	14.63 - 33.65	27.84 (29.63)	12.34 - 41.97	23.17 (25.51)	10.77 - 36.28	4.9731	0.174
$GP5^n$	0.28 (0.31)	0.21 - 0.52	0.29 (0.24)	0.21 - 0.45	0.28 (0.28)	0.19 - 0.47	3.2756	0.351
$GP6^n$	7.25 (7.53)	4.68 - 12.21	7.08 (6.62)	5.15 - 11.77	5.89 (7.58)	3.39 - 10.97	1.0655	0.785
$GP7^n$	0.64 (0.84)	0.35 - 1.19	0.71 (1.56)	0.27 - 1.83	0.71 (0.40)	0.47 - 0.87	0.7160	0.865
$GP8^n$	23.58 (11.92)	19.39 - 31.31	23.34 (10.36)	16.28 - 26.64	23.28 (9.01)	20.19 - 29.20	2.3018	0.512
$GP9^n$	12.20 (7.53)	8.82 - 16.35	12.23 (6.25)	8.94 - 15.19	11.30 (4.00)	9.58 - 13.58	5.0515	0.168
$GP10^n$	7.60 (4.96)	5.13 - 10.09	7.09 (5.39)	4.50 - 9.89	7.36 (3.87)	5.83 - 9.70	1.6804	0.641
$GP11^n$	1.12 (0.68)	0.67 - 1.35	1.05 (0.90)	0.79 - 1.69	1.16 (0.59)	0.74 - 1.33	1.3628	0.714
$GP12^n$	0.96 (3.02)	0.49 - 3.51	1.00 (3.85)	0.29 - 4.14	1.28 (2.01)	0.67 - 2.68	2.9768	0.395
$GP13^n$	0.42 (0.31)	0.28 - 0.59	0.41 (0.62)	0.26 - 0.88	0.44 (0.26)	0.32 - 0.58	1.3517	0.717
$GP14^n$	16.35 (16.81)	9.73 - 26.54	15.32 (21.38)	7.10 - 28.48	17.81 (25.65)	8.92 - 34.57	3.1218	0.373
$GP15^n$	2.12 (2.15)	1.33 - 3.48	1.96 (2.52)	1.11 - 3.63	2.39 (2.03)	1.62 - 3.65	2.0333	0.566

GP^nx: glycan peak with 'x' corresponding to number; IQR: interquartile range

GP values are presented as percentages of the neutral glycan pool, i.e. $GP1^n = GP1^n/GP^n * 100$. Statistically significant differences ($P < 8.06 \times 10^{-4}$) were using the Mann-Whitney U test.

Page intentionally left blank

Table 17: Descriptive statistics for the derived traits from the total and neutral IgG glycome according to PD motor subtype.

N-glycan peak	Tremor Dominant		PIGD Dominant		Indeterminate Type		Between Group Difference	
	Median (IQR)	Range	Median (IQR)	Range	Median (IQR)	Range	χ2 statistic	P - value
Percentage of Sialylation of Fucosylated Structures with Bisecting GlcNAc								
FBGS/(FBG+FBGS)	29.52 (24.28)	15.88 – 40.16	28.55 (28.76)	16.11 – 44.87	24.93 (12.97)	21.91 – 34.88	5.6691	0.129
Percentage of Sialylation of Fucosylated Structures without Bisecting GlcNAc								
FGS/(FG+FGS)	23.63 (12.14)	17.24 – 29.38	22.05 (14.14)	17.24 – 31.38	22.61 (9.00)	18.30 – 27.30	3.7153	0.294
Percentage of Sialylation of Fucosylated Galactosylated Glycans with Bisecting GlcNAc								
FBG2S1/(FBG2 +FBG2S1+FBG2S2)	37.14 (13.62)	30.64 – 44.26	37.66 (23.41)	26.89 – 50.30	36.21 (16.45)	33.46 – 49.91	0.2168	0.975
FBG2S2/(FBG2 +FBG2S1+FBG2S2)	30.84 (20.24)	15.88 – 36.12	28.95 (23.15)	15.37 – 38.52	24.77 (12.61)	17.67 – 30.28	14.6426	0.002
Percentage of Sialylation of Fucosylated Galactosylated Glycans without Bisecting GlcNAc								
FG1S1/(FG1+FG1S1 +FG2S2+FG2S2)	9.24 (7.53)	6.08 – 13.61	8.94 (6.28)	6.08 – 12.36	8.88 (4.26)	5.70 – 9.96	6.5143	0.089
FG2S1/(FG1+FG1S1 +FG2S2+FG2S2)	38.42 (12.17)	31.26 – 43.43	36.95 (12.03)	31.26 – 43.29	36.60 (7.06)	35.31 – 42.37	3.0054	0.391
FG2S2/(FG1+FG1S1 +FG2S2+FG2S2)	4.95 (5.19)	2.28 – 7.47	5.09 (7.86)	1.72 – 9.58	3.71 (2.98)	2.41 – 5.39	14.7113	0.002
Percentage of Galactosylation								
$G0^n$	33.62 (24.55)	21.59 – 46.14	36.25 (34.10)	19.01 – 53.11	29.17 (33.53)	14.47 – 48.00	4.2337	0.237
$G1^n$	45.69 (12.16)	39.85 – 52.01	44.61 (13.49)	36.34 – 49.83	45.94 (10.56)	39.94 – 50.50	4.6870	0.196
$G2^n$	19.76 (20.48)	13.64 – 34.12	18.62 (24.36)	10.10 – 34.46	21.64 (29.87)	11.59 – 41.46	3.1522	0.369

B, bisecting N-acetylglucosamine; F, core fucose; G, galactose; S, sialic acid.

See 2.2.6 Derived Traits for further details. Statistically significant differences ($P < 8.06 \times 10^{-4}$) were determined using the Mann-Whitney U test.

Page intentionally left blank

Table 17 cont: Descriptive statistics for the derived traits from the total and neutral IgG glycome according to PD motor subtype.

N-glycan peak	Tremor Dominant		PIGD Dominant		Indeterminate Type		Between Group Difference	
	Median (IQR)	Range	Median (IQR)	Range	Median (IQR)	Range	χ2 statistic	P - value
Percentage of Fucosylation (+/- Bisecting GlcNAc)								
$F^{n\ total}$	97.17 (4.50)	93.66 – 98.16	96.80 (6.74)	91.91 – 98.65	96.65 (1.95)	95.27 – 97.22	1.9089	0.592
$FG0^{n}/G0^{n\ total}$	98.24 (4.85)	94.49 – 99.34	97.82 (4.45)	95.00 – 99.45	97.82 (1.35)	97.26 – 98.61	1.2529	0.740
$FG1^{n}/G1^{n\ total}$	98.64 (2.16)	97.07 – 99.23	98.45 (3.42)	95.90 – 99.32	98.24 (0.96)	98.04 – 99.00	1.1786	0.758
$FG2^{n}/G2^{n\ total}$	93.12 (11.08)	84.83 – 95.91	92.59 (15.48)	80.52 – 96.00	91.43 (5.05)	90.28 – 95.33	1.0366	0.792
Percentage of Fucosylation with Bisecting GlcNAc								
FB^{n}	17.95 (12.08)	12.11 – 24.19	17.82 (12.25)	11.97 – 24.22	18.79 (9.41)	13.51 – 22.92	0.1528	0.985
$FBG0^{n}/G0^{n}$	21.57 (14.28)	14.79 – 29.07	20.73 (21.10)	11.65 – 32.75	23.46 (10.85)	17.58 – 28.43	2.5095	0.474
$FBG1^{n}/G1^{n}$	18.72 (13.48)	11.98 – 25.46	18.39 (12.73)	13.03 – 25.76	20.72 (9.37)	13.72 – 23.09	1.3476	0.718
$FBG2^{n}/G2^{n}$	10.89 (6.47)	7.53 – 14.00	10.54 (9.91)	7.52 – 17.43	11.26 (6.45)	8.00 – 14.45	0.3746	0.945
Percentage of Fucosylation without Bisecting GlcNAc								
F^{n}	78.88 (15.92)	69.65 – 85.57	79.09 (14.14)	72.54 – 86.68	78.45 (9.15)	73.28 – 82.43	0.2533	0.969
$FG0^{n}/G0^{n}$	76.47 (15.44)	68.02 – 83.45	76.92 (24.32)	63.48 – 87.80	74.79 (10.48)	69.20 – 79.68	2.3811	0.497
$FG1^{n}/G1^{n}$	79.86 (15.33)	71.61 – 86.94	80.23 (13.63)	72.66 – 86.29	78.03 (9.33)	75.13 – 84.46	1.2121	0.750
$FG2^{n}/G2^{n}$	81.94 (16.14)	71.36 – 87.50	81.76 (16.88)	70.27 – 87.15	82.30 (9.06)	76.99 – 86.05	0.2839	0.963
Other Traits								
$FB^{n}/(F^{n}+FB^{n})$	0.23 (0.21)	0.14 – 0.35	0.23 (0.19)	0.14 – 0.33	0.24 (0.15)	0.16 – 0.31	0.1392	0.987
$FG2^{n}/(BG2^{n}/FBG2^{n})$	6.35 (5.25)	4.28 – 9.53	6.37 (6.09)	3.35 – 9.44	6.11 (4.05)	4.47 – 8.52	0.3919	0.942
$BG2^{n}/(FG2^{n}+FBG2^{n})$	22.01 (22.10)	15.75 – 37.85	23.52 (28.55)	13.70 – 42.25	23.57 (22.57)	11.72 – 34.29	1.7484	0.626

B, bisecting N-acetylglucosamine; F, core fucose; G, galactose; S, sialic acid.

See 2.2.6 Derived Traits for further details. Statistically significant differences ($P < 8.06 \times 10^{-4}$) were determined using the Mann-Whitney U test.

3.2.4 Risk of Cognitive Decline

Comparisons between the PD cases in terms of animal naming task score in the total IgG glycome (see **Table 18**), the neutral IgG glycome (see **Table 19**), and derived traits (see **Table 20**) are shown below. There were no statistically significant differences ($P < 8.06 \times 10^{-4}$) in either the total or neutral IgG glycome, or the derived traits of these.

Table 18: Descriptive statistics for the GPs within the total IgG glycome according to animal naming task (ANT) score.

N-glycan peak	ANT < 20		ANT ≥ 20		Between Group Difference	
	Median (IQR)	Range	Median (IQR)	Range	U-statistic	*P* - value
GP1	0.09 (0.25)	0.03 - 0.28	0.08 (0.19)	0.03 - 0.22	1200.50	0.071
GP2	0.56 (1.44)	0.13 - 1.57	0.48 (1.92)	0.17 - 2.09	1113.50	0.278
GP4	22.28 (22.58)	11.74 - 34.32	20.25 (27.21)	8.10 - 35.31	1184.00	0.097
GP5	0.25 (0.29)	0.15 - 0.44	0.22 (0.15)	0.17 - 0.32	1251.00	0.027
GP6	5.88 (6.63)	3.61 - 10.24	5.66 (7.50)	2.55 - 10.05	1133.00	0.214
GP7	0.55 (1.15)	0.31 - 1.46	0.50 (0.80)	0.23 - 1.03	1040.00	0.627
GP8	19.23 (11.13)	14.17 - 25.30	18.67 (8.77)	15.39 - 24.16	1138.00	0.199
GP9	9.84 (5.01)	7.82 - 12.83	9.99 (5.97)	7.08 - 13.05	991.00	0.932
GP10	6.04 (4.34)	4.17 - 8.51	5.81 (4.33	0.61 - 1.35	1077.00	0.431
GP11	0.89 (0.91)	0.54 - 1.45	0.86 (0.74)	0.61 - 1.35	1088.50	0.378
GP12	0.76 (2.94)	0.37 - 3.31	0.89 (2.59)	0.24 - 2.83	890.00	0.465
GP13	0.34 (0.47)	0.23 - 0.70	0.33 (0.26)	0.22 - 0.48	1038.00	0.638
GP14	12.08 (15.82)	6.18 - 22.00	13.63 (17.46)	8.01 - 25.47	696.00	0.021
GP15	1.62 (1.77)	1.09 - 2.86	1.71 (1.81)	0.93 - 2.74	804.00	0.152
GP16	2.90 (2.07)	2.07 - 4.14	2.90 (2.61)	2.02 - 4.63	1033.50	0.665
GP17	1.08 (1.22)	0.72 - 1.94	1.07 (1.09)	0.79 - 1.88	914.50	0.596
GP18	8.28 (8.53)	3.94 - 12.47	8.93 (10.29)	6.23 - 16.52	742.00	0.053
GP19	1.86 (1.99)	1.32 - 3.31	1.94 (1.35)	1.39 - 2.74	888.50	0.458
GP20	0.34 (0.44)	0.22 - 0.66	0.35 (0.44)	0.23 - 0.67	953.00	0.829
GP21	0.91 (1.25)	0.49 - 1.74	0.91 (0.94)	0.46 - 1.40	944.50	0.775
GP22	0.12 (0.26)	0.05 - 0.31	0.11 (0.87)	0.06 - 0.93	993.50	0.915
GP23	1.12 (1.47)	0.43 - 1.90	1.19 (1.39)	0.56 - 1.95	847.50	0.282
GP24	1.52 (1.54)	0.64 - 2.18	1.53 (1.54)	0.71 - 2.25	946.50	0.788

ANT, animal naming task; GPx: glycan peak with 'x' corresponding to number; IQR: interquartile range

GP values are presented as percentages of the total IgG glycome, i.e. GP1 = GP1/GP * 100. Statistically significant differences ($P < 8.06 \times 10^{-4}$) were determined using the Mann-Whitney U test.

Table 19: Descriptive statistics for the GPs within the neutral IgG glycome according to animal naming task (ANT) score.

	ANT < 20		ANT ≥ 20		Between Group Difference	
N-glycan peak	Median (IQR)	Range	Median (IQR)	Range	U-statistic	*P* - value
$GP1^n$	0.11 (0.31)	0.04 - 0.35	0.10 (0.23)	0.04 - 0.27	1163.50	0.134
$GP2^n$	0.70 (1.64)	0.17 - 1.81	0.59 (2.33)	0.21 - 2.54	1099.50	0.332
$GP4^n$	27.46 (24.54)	14.89 - 39.43	25.62 (31.20)	10.77 - 41.97	1182.50	0.099
$GP5^n$	0.30 (0.33)	0.19 - 0.52	0.27 (0.17)	0.21 - 0.38	1224.50	0.046
$GP6^n$	7.24 (7.26)	4.51 - 11.77	7.04 (8.82)	3.39 - 12.21	1116.00	0.269
$GP7^n$	0.66 (1.44)	0.39 - 1.83	0.64 (0.99)	0.27 - 1.26	1008.50	0.819
$GP8^n$	23.46 (15.03)	16.28 - 31.31	23.32 (10.19)	19.01 - 29.20	1008.50	0.819
$GP9^n$	12.27 (7.00)	8.94 - 15.94	12.59 (7.53)	8.82 - 16.35	937.50	0.732
$GP10^n$	7.28 (4.78)	5.11 - 9.89	7.13 (5.59)	4.50 - 10.09	1016.50	0.769
$GP11^n$	1.08 (1.02)	0.67 - 1.69	1.09 (0.88)	0.74 - 1.62	1059.00	0.522
$GP12^n$	0.92 (3.70)	0.44 - 4.14	1.10 (3.22)	0.29 - 3.51	880.50	0.419
$GP13^n$	0.42 (0.59)	0.29 - 0.88	0.43 (0.33)	0.26 - 0.59	979.00	0.997
$GP14^n$	15.00 (20.65)	7.10 - 27.75	16.95 (24.96)	9.61 - 34.57	684.50	0.016
$GP15^n$	2.03 (2.34)	1.29 - 3.63	2.12 (2.54)	1.11 - 3.65	791.00	0.124

ANT, animal naming task; GPx: glycan peak with 'x' corresponding to number; IQR: interquartile range

GP values are presented as percentages of the neutral glycan pool, i.e. $GP1^n = GP1^n/GP^n * 100$. Statistically significant differences ($P < 8.06 \times 10^{-4}$) were using the Mann-Whitney U test.

Table 20: Descriptive statistics for the derived traits from the total and neutral IgG glycome according to animal naming task (ANT) score.

Glycan trait	ANT < 20		ANT ≥ 20		Between Group Difference	
	Median (IQR)	Range	Median (IQR)	Range	U-statistic	*P* - value
Percentage of Sialylation of Fucosylated Structures with Bisecting GlcNAc						
FBGS/(FBG+FBGS)	28.52 (28.99)	15.88 - 44.87	29.76 (21.01)	16.84 - 37.85	903	0.533
Percentage of Sialylation of Fucosylated Structures without Bisecting GlcNAc						
FGS/(FG+FGS)	23.30 (10.54)	17.24 - 27.78	23.48 (12.58)	18.80 - 31.38	804	0.152
Percentage of Sialylation of Fucosylated Galactosylated Glycans with Bisecting GlcNAc						
FBG2S1/(FBG2 +FBG2S1+FBG2S2)	37.61 (19.32)	2.28 - 9.58	37.05 (18.82)	26.89 - 45.71	1042	0.616
FBG2S2/(FBG2 +FBG2S1+FBG2S2)	29.69 (22.64)	30.98 - 50.30	29.20 (20.36)	15.37 - 35.73	1020.5	0.744
Percentage of Sialylation of Fucosylated Galactosylated Glycans without Bisecting GlcNAc						
FG1S1/(FG1+FG1S1 +FG2S2+FG2S2)	9.00 (6.28)	6.08 - 12.36	9.23 (7.91)	5.70 - 13.61	951.5	0.819
FG2S1/(FG1+FG1S1 +FG2S2+FG2S2)	38.08 (12.03)	31.26 - 43.29	37.22 (10.78)	32.65 - 43.43	973.5	0.961
FG2S2/(FG1+FG1S1 +FG2S2+FG2S2)	4.88 (7.30)	2.28 - 9.58	5.07 (6.61)	1.72 - 8.33	1029	0.692
Percentage of Galactosylation						
$G0^n$	35.67 (33.28)	19.83 - 53.11	32.87 (33.45)	14.47 - 47.92	1178	0.107
$G1^n$	45.09 (15.67)	36.34 - 52.01	45.62 (8.50)	39.85 - 48.35	1036.5	0.648
$G2^n$	18.61 (23.92)	10.10 - 34.02	20.66 (30.20)	11.26 - 41.46	701	0.023
Percentage of Fucosylation (+/- Bisecting GlcNAc)						
$F^{n\ total}$	96.96 (6.35)	91.91 - 98.26	96.90 (4.99)	93.66 - 98.65	992.5	0.922
$FG0^n/G0^{n\ total}$	98.03 (3.25)	96.15 - 99.40	97.97 (4.96)	94.49 - 99.45	1018.5	0.757
$FG1^n/G1^{n\ total}$	98.56 (3.30)	95.90 - 99.20	98.66 (2.25)	97.07 - 99.32	946.5	0.788
$FG2^n/G2^{n\ total}$	92.38 (15.48)	80.52 - 96.00	92.91 (11.72)	84.74 - 96.46	854	0.306
Percentage of Fucosylation with Bisecting GlcNAc						
FB^n	17.94 (12.10)	12.11 - 24.21	17.70 (12.25)	11.97 - 24.22	1019	0.754
$FBG0^n/G0^n$	20.68 (14.28)	14.79 - 29.07	22.21 (21.10)	11.65 - 32.75	831.5	0.227
$FBG1^n/G1^n$	18.71 (13.78)	11.98 - 25.76	18.52 (12.43)	13.03 - 25.46	1047	0.588
$FBG2^n/G2^n$	10.77 (9.90)	7.53 - 17.43	10.48 (6.48)	7.52 - 14.00	1136.5	0.203
Percentage of Fucosylation without Bisecting GlcNAc						
F^n	78.97 (13.82)	71.75 - 85.57	79.39 (17.03)	69.65 - 86.68	938.5	0.738
$FG0^n/G0^n$	77.02 (14.62)	68.84 - 83.46	76.11 (24.32)	63.48 - 87.80	1116	0.269
$FG1^n/G1^n$	79.35 (14.28)	72.66 - 86.94	80.27 (14.68)	71.61 - 86.29	916	0.604
$FG2^n/G2^n$	81.57 (17.23)	70.27 - 87.50	82.90 (15.48)	71.36 - 86.84	766	0.082
Other Traits						
$FB^n/(F^n+FB^n)$	18.59 (12.63)	12.4 – 25.03	18.19 (13.64)	14.12 – 25.78	1019.5	0.75
$FG2^n/(BG2^n/FBG2^n)$	6.14 (6.18)	3.35 – 9.53	6.63 (4.99)	4.28 – 9.27	728.5	0.041
$BG2^n/(FG2^n+FBG2^n)$	25.10 (29.93)	12.32 – 42.25	20.27 (27.22)	11.72 – 38.94	1333.5	0.004

ANT, animal naming task; B, bisecting N-acetylglucosamine; F, core fucose; G, galactose; S, sialic acid.

See 2.2.6 Derived Traits for further details. Statistically significant differences ($P < 8.06 \times 10^{-4}$) were determined using the Mann-Whitney U test.

4.0 Discussion

4.1 Study 1: IgG *N*-Glycans as a Novel Biomarker of PD

This was the first study, to our knowledge, that investigated the potential of using IgG glycomic biomarkers to identify people with PD using a case-control epidemiological approach. It was hypothesised that the peripheral IgG glycome would be different in people with PD compared with a control population, and that these modifications would infer a more pro-inflammatory fraction of IgG. Therefore, the purpose of **Study 1** was to identify changes present in the peripheral IgG glycome of people with PD that may represent an interphenotype of the disorder: a link between the genome, the environment and the disease phenotype. PD has a heterogeneous presentation of clinical symptoms, and many genetic and environmental factors contribute to the development of the disease. Whether this clinical heterogeneity between PD patients had an influence on the peripheral glycosylation of IgG was the motivation of **Study 2**. It was evident from the current study that the PD cases did have a different glycosylation profile to the controls.

4.1.1 Batch Effects

Batch effects exist because laboratory conditions, reagents and technicians vary between different batches, and can compound the biological effects within the data (Leek et al., 2010). Importantly, batch effects can be detrimental to results of a study as incorrect conclusions can be made. Mild batch effects were present, as indicated by some of the boxplots of GPs separated according to plate number (see **Appendix 4**). However, blocking appeared to be effective in averting the influence of batch effects in this study, as evident by the inability of PCA to cluster samples according to plate number (see **Fig. 6a**). This is a positive finding as PCA would have been effective, even if only partially, in clustering participant samples according to plate number if batch effects were detrimental to the results of this study. There was, however, evidence of some separation of the samples according to case status (see **Fig. 6b**), thus indicating that the glycan variables in this study were able to segregate samples according to whether a participant was a PD case or a control.

4.1.2 Influence of Age and BMI on GPs and Derived Traits

Advancing age has previously been associated with changes in the glycosylation of IgG that alter the effector functions of these glycoproteins, making them pro-inflammatory. Pro-

inflammatory modifications to the peripheral IgG glycome infer the presence of low-grade inflammation which is capable of fuelling an inflammatory vicious loop (Dall'Olio et al., 2013). Specifically, an increase in agalactosylated biantennary glycans and a concurrent decrease in digalactosylated biantennary glycans, with or without bisecting GlcNAc (Pucic et al., 2011; Ruhaak et al., 2010), has been found to be associated with advancing age. The current study corroborates these associations; however, the association between advancing age and an increase in agalactosylation ($G0^n$) or a decrease in digalactosylation ($G2^n$) only reached statistical significance in the PD cases and not in the controls (see **Table 8**). Therefore, these associations were greater in the PD cases. Hence, people with PD may have an accelerated development of pro-inflammatory IgG with advancing age.

This may be an expected result for an age-related chronic disease population. What was not expected, however, was an overall difference indicative of a decreased pro-inflammatory capacity of peripheral IgG in the PD cases (see **Table 6**). In the current study, a significant decrease in agalactosylated biantennary glycans ($G0^n$) and an increase in digalactosylated biantennary glycans ($G2^n$) were found in the PD cases compared to controls, though the latter result did not reach statistical significance. This perceived decrease in pro-inflammatory capacity, albeit perplexing, may be under genetic influence and a result of inter-population allelic frequency differences rather than associated to PD. Although the overall trend of the PD cases was to have lower levels of pro-inflammatory IgG, there was a sharper increase in the pro-inflammatory capacity of peripheral IgG as people with PD aged, at least in the context of a cross-sectional study. Though this will need to be further validated in a longitudinal study, it may be resolved that the peripheral IgG in people with PD have a propensity to become more pro-inflammatory faster than what would be expected as they aged. This would therefore support the hypothesis that modifications to the peripheral IgG glycome would infer more pro-inflammatory ability through the presence of low-grade inflammation.

As well as the overall levels of agalactosylated and digalactosylated biantennary glycans, alterations in many individual GPs have been found to be associated with advancing age, both biological and chronological (Krištić et al., 2014). Individual GP changes associated with age were only found to be statistically significant in the PD cases in this study: five in total and four of these previously associated with advancing age (Krištić et al., 2014). The lack of a significant association in the control population may be a result of the small sample size in the current study, and hence reduced power, compared with the sample size used in Krištić and colleagues study (2014). Though this is the circumstance, the associations of age and these GPs were greater in the PD cases. The three GPs that were associated with a moderate increase as a

result of advancing age in people with PD were GP4, GP5, and GP6, all of which are GPs with agalactosylated biantennary glycan moieties (see **Appendix 1**). Likewise, the two GPs that were associated with a moderate decrease with advancing age in people with PD were GP14 and GP18, both of which are GPs containing digalactosylated biantennary glycan moieties (see **Appendix 1**). Although GP5 is indeed an agalactosylated glycan, it was not associated with advancing age in previous studies and may therefore be unique to PD.

It has been demonstrated that changes in BMI can alter plasma protein glycosylation. Significant increases in triantennary glycan structures and significant decreases in core fucosylated glycans, monosialylated glycans and biantennary glycans have been connected to an increase in BMI (Knezevic et al., 2010; Nikolac Perkovic et al., 2014). Nikolac Perkovic and colleagues (2014) reported an increase in BMI to be associated with an increase in agalactosylated biantennary glycans, and hence a tendency for more pro-inflammatory IgG. Nevertheless, BMI did not have a statistical influence over the interpretation of the GPs and derived traits in the current study. Though BMI was significantly different (t [194] = 3.7622, P = 0.0002) between the PD cases and controls, whereby the control group had a higher average BMI (28.61; SD=3.40) compared with the PD cases (26.40; SD=4.76), it did not have a statistically significant association to any of the GPs or derived traits in either of the groups (see **Tables 9** and **10**). This was unsurprising given that Nikolac Perkovic et al. (2014) only found an increase in BMI to have a weak positive association with agalactosylated glycans of IgG, BMI explaining only 2% of the variation in their study, with statistical significance due to increased sample size and therefore increased power in the study.

4.1.3 Differing Glycosylation Profiles of IgG in People with PD

Changes in peripheral IgG glycosylation are associated with a number of chronic diseases, including: rheumatoid arthritis (Gindzienska-Sieskiewicz et al., 2007; Malhotra et al., 1995; Troelsen et al., 2012), metabolic syndrome (Lauc et al., 2013; Lu et al., 2011), inflammatory bowel disease (Lauc et al., 2013; Nakajima et al., 2011), systemic lupus erythematosus (Lauc et al., 2013), haematological cancers (Lauc et al., 2013), thyroid cancer (Chen et al., 2012), gastric cancer (Kodar et al., 2012), lung cancer (Chen et al., 2013), ovarian cancer (Saldova et al., 2007), multiple sclerosis (Lauc et al., 2013), and more recently AD and progressive MCI (Lundström et al., 2014). In the current study, several deviations in the peripheral IgG glycome were seen in the PD cases compared with the controls. The majority of the between group GP differences were reflected as trends in the derived traits. For example, lower relative

abundances of GPs primarily comprised of monosialylated and disialylated digalactosylated biantennary glycans without bisecting GlcNAc (GP17 and GP21, respectively) occurred in parallel to lower relative abundances of the same glycan structures that were additionally core fucosylated in the derived traits. These derived traits are used to sum up the trends in the whole IgG glycome; that is, an overall increase or decrease in sialylation, core fucosylation, galactosylation or bisecting GlcNAc, and any combination of these traits (see **2.2.6 Derived Traits**). The derived traits are useful for inferring whether a change of an individual GP has a downstream change on the IgG glycome and whether this change causes the IgG glycoprotein as a whole to become more anti-inflammatory or pro-inflammatory.

A reduced level of sialylation, particularly monosialylation, was seen in the PD cases compared with the controls. GP17, comprised predominantly of monosialylated digalactosylated biantennary glycans without bisecting GlcNAc (see **Appendix 1**), was significantly reduced in the PD cases. GP21, comprised of disialylated digalactosylated biantennary glycans without bisecting GlcNAc (see **Appendix 1)** was also significantly reduced in the PD cases. Parallel to this, there was an overall reduction in sialylation of fucosylated galactosylated glycans within the PD cases (FGS/(FG+FGS). Following further inspection, this reduction was significant specifically for lower levels of monosialylation in fucosylated monogalactosylated (FG1S1/(FG1 + FG1S1 + FG2S1 + FG2S2) and digalactosylated (FG2S1/(FG1 + FG1S1 + FG2S1 + FG2S2)) biantennary glycans without a bisecting GlcNAc. However, there was no statistically significant difference in disialylated fucosylated digalactosylated biantennary glycans without a bisecting GlcNAc (FG2S2/(FG1 + FG1S1 + FG2S1 + FG2S2)). Disialylated digalactosylated biantennary glycans with a bisecting GlcNAc (GP22; see **Appendix 1**) were reduced in the PD cases. However, this was not reflected as an overall effect in the core fucosylated galactosylated biantennary glycans with bisecting GlcNAc (FBGS/(FBG + FBGS)). Higher levels of sialylation are associated with an increased anti-inflammatory fraction of IgG due to a reduced capacity to bind to FcγRIIIa receptors on natural killer cells thereby lowering inflammatory activity via ADCC (Böhm et al., 2012; Scallon et al., 2007). It has been postulated that the mechanism by which sialylated, particularly α2-6 sialylated, IgG-Fc glycans can have an anti-inflammatory effect is by binding DC-SIGN, a C-type lectin which is present on dendritic cells, to the protein portion of the IgG-Fc which causes the production of more FcγRIIb receptors on natural killer cells (Anthony, 2011). FcγRIIb are inhibitory receptors that act to reduce inflammation by preventing the activation of FcγRIIIa and other excitatory receptors (Anthony, 2011). Therefore, these results suggest a reduced capacity for people with PD compared with controls in the current study to prevent ADCC caused inflammation, at least in terms of sialylation.

There was no significant difference overall in core fucosylation (see **Table 6**), despite the fact that two of the three GPs which contain core fucosylated glycan moieties and together constitute more than half of the IgG glycome were significantly increased in the PD cases compared to the controls, i.e. GP8 and GP14, but not GP4 (see **Table 4**). Interestingly, all three of these GPs contain glycans that are structurally similar, the only difference being the number of galactoses terminally attached (see **Appendix 1**). GP8, comprised predominantly of core fucosylated monogalactosylated biantennary glycans, was significantly increased in the PD cases. Likewise, GP14, comprised of core fucosylated digalactosylated biantennary glycans, was significantly increased in the PD cases. The attachment of core fucose is very important for the pro-inflammatory capability of IgG and its absence leads to a 50-fold enhanced ability to cause ADCC (Pucic et al., 2011; Shields et al., 2002). As expected for IgG, there was a large proportion of *N*-glycans that were core fucosylated in both the PD cases and controls, ~97% and ~96.5%, respectively ($F^{n\ total}$; see **Table 6**). Therefore, core fucosylation was not significantly different between groups and thus ADCC activation was no different in the PD cases compared with the controls in this study.

GP5 and GP20 were the most significantly different GPs between PD cases and controls in this study (see **Table 4**). GP5 is predominantly comprised of a high-mannose glycan moiety that constitutes a small proportion of the total IgG glycome (<1%). This small percentage has been replicated in other studies (Lauc et al., 2013; Pucic et al., 2011). Although it may present as a small difference in terms of the total IgG glycome, the majority of the PD cases had a lower value than the controls in this study and this difference was highly significant (GP5). Mannose-rich glycans have an increased affinity for MBL which initiates the lectin complement cascade via opsonisation of IgG and the cells to which they are bound (Fujita, 2002; Malhotra et al., 1995). Both mannose and GlcNAc (GlcNAc to a lesser degree than mannose) are prominent ligands for MBL and are usually found on the surface of pathogens, such as bacteria and viruses (Fujita, 2002; Malhotra et al., 1995). Other monosaccharides, such as sialic acid and galactose, normally attach to mammalian glycoproteins and have undetectable affinity for MBL (Fujita, 2002; Malhotra et al., 1995). This enables the specific recognition of glycans on pathogen cell surfaces. However, this innate immunity system can malfunction and has been implicated in many disease processes due to an increase in agalactosylated and mannose-rich *N*-glycans. For example, MBL recognises clusters of agalactosylated IgG within the synovial joints of rheumatoid arthritis patients and activates the lectin complement cascade which contributes to inflammation by damaging the surrounding tissue (Arnold et al., 2007; Malhotra

et al., 1995). Therefore, both IgG with high-mannose glycans and agalactosylated glycans could cause an increased activation of complement-caused inflammation.

Interestingly in the current study, both high-mannose glycans (GP5) and agalactosylated glycans ($G0^n$) had lower relative abundances in the PD cases compared with the controls. Moreover, a higher relative abundance of GP5 in the neutral glycome ($GP5^n$) was associated with a higher relative abundance of agalactosylated glycans ($G0^n$) in both the PD cases and controls. GP5 is an agalactosylated glycan structure. Consequently an increase in GP5 was expected to cause an increase in total agalactosylated structures. As previously discussed (see **Section 4.1.2**), advancing age was significantly associated with both an increase in GP5 and other agalactosylated ($G0^n$) biantennary glycans in the PD cases but not the controls. Due to age and gender-matching of PD cases and controls in the current study, differences between the two independent groups associated with advancing age may indicate a propensity for the IgG in people with PD to become more pro-inflammatory at a faster rate than those in the general population. Therefore, the presence of PD appears to be associated with more rapid biologically ageing, as evidenced by the modifications of peripheral IgG glycosylation.

GP20 was another peak that was found to be significantly different between groups. As illustrated in **Appendix 1,** and reported previously (Krištić et al., 2014; Lauc et al., 2013; Pucic et al., 2011), it is unknown what type of *N*-glycans contribute to GP20. However, similar to GP5, GP20 was significantly reduced in nearly all PD cases compared to the controls. Furthermore, GP5 and GP20 were significantly and strongly correlated in the control group (r_s = 0.71, *P* = 0.0000) but there was no significant correlation found in the PD cases (r_s = 0.10, *P* = 0.347), mainly due to both GPs having small relative abundances in these individuals. Unsurprising, these two correlations produced a highly significant difference when analysing with Fisher's r-to-z transformation (z = 5.42, *P* = 0.0000). While the inflammatory influence of GP20 on IgG cannot be deduced for the purpose of this study, this may be the first evidence that the *N*-glycans of GP20 are produced out of a similar biosynthetic pathway as GP5. It was unclear from the current study how different genetic or environmental factors contributed to this observation, but further investigation may be warranted.

The addition of terminal sialic acid and the lack of core fucose are two modifications in the IgG glycome that can be considered as being in equilibrium, at least in terms of ADCC activation. Increased sialic acid leads to an increased inhibition of ADCC and decreased core fucose leads to a significant increase in ADCC activation, up to 50-fold in *in vitro* studies (Pucic et al., 2011; Shields et al., 2002). Thus the results in **Study 1** support the hypothesis that the peripheral IgG

glycome profile is different in people with PD compared with the control population, and this difference infers an increased pro-inflammatory capacity by activating complement-caused inflammation rather than inflammation caused by activating ADCC, as people with PD age. Longitudinal studies are required for validation of this hypothesis.

4.2 Study 2: Utility of IgG *N*-Glycans in Identifying Risk of Cognitive Decline

Owing to the clinical heterogeneity of the disease, it was hypothesised that the peripheral IgG glycome within a population of people with PD would have a different glycosylation profile between different clinical motor subtypes. Specifically, the PIGD motor subtype infers a high risk of cognitive impairment and therefore would have utility in identifying people with PD who are at risk of developing cognitive impairment. Moreover, it was hypothesised that differences would exist in the peripheral IgG glycome of people with PD who have semantic fluency impairment, and hence are at higher risk of developing cognitive impairment. Therefore, the purpose of **Study 2** was to determine whether the IgG glycome had utility in identifying risk of cognitive decline in people with PD. In order to achieve this, PD cases were separated into respective clinical motor subtypes, according to MDS-UPDRS guidelines (Goetz et al., 2008), or separated on how they performed on the animal naming task. Semantic fluency impairment for the purpose of the current was study defined as a score of less than 20 which was congruent with previous studies (Pereira et al., 2014; Williams-Gray et al., 2009).

4.2.1 Batch Effects

Mild batch effects may have been present, as indicated by some of the boxplots of GPs separated according to plate number in **Study 1** (see **Appendix 4**) and the inability to block for clinical motor subtype and animal naming task score as well as case status. However, batch effects did not have an influence in this study, as evident by the inability of PCA to cluster samples according to plate number in section **3.2.2 Batch Effects** (see **Fig. 9a**). There was also no evidence of separation in the PD case according to motor subtype (see **Fig. 9b**) or animal naming task score (see **Fig. 9c**), thus indicating that the peripheral IgG glycome may not be useful in identifying risk of cognitive decline.

4.2.2 Influence of Motor Subtype on the IgG Glycome

Previous studies have indicated the differential progression of PD according to clinical motor subtype using longitudinal study designs and also [^{123}I]FP-CIT-SPECT (Alves et al., 2006; Eggers et al., 2011; Eggers et al., 2012). In particular, the speed of disease progression and subsequent development of dementia have been linked to people classified as having a PIGD, non-tremor dominant motor subtype (Alves et al., 2006). This suggests that these subtypes have different aetiopathological pathways leading to the development of PD, thereby warranting the interest in analysing the IgG glycome in terms of motor subtype. The same statistical comparisons were performed in terms of motor subtype. However, as earlier indicated by PCA, no difference in the relative abundances of either GPs or derived traits reached statistical significance ($P < 8.06 \times 10^{-4}$) in this component of **Study 2**. Thus, the glycosylation of peripheral IgG cannot be used to class people with PD according to their motor subtype, and therefore rejects the hypothesis that it has utility in identifying people with PD who are at risk of cognitive decline as determined by their clinical motor subtype.

4.2.3 Influence of the Animal Naming Task Score on the IgG Glycome

Impairment of semantic fluency is associated with a higher risk of cognitive impairment and dementia development in people with PD (Hu et al., 2014; Pereira et al., 2014; Williams-Gray et al., 2009). Therefore, the risk of cognitive impairment was determined using the animal naming task, with impaired semantic fluency defined as a score less than 20 (Williams-Gray et al., 2009). In unison with the evaluation of the peripheral IgG glycome in terms of clinical motor subtype, similar comparisons were performed in terms of impaired (score less than 20) or normal (score equal to or greater than 20) semantic fluency in people with PD. However, as indicated by PCA, no difference in either GPs or derived traits reached statistical significance in this component of **Study 2** (see **Section 3.2.4**). Thus, the glycosylation of peripheral IgG cannot be used to identify people with PD that may be at risk of dementia development, and therefore rejects the hypothesis that it has utility in identifying people with PD who are at risk of cognitive decline as determined by impaired semantic fluency.

Using the results of **Study 2**, it can be hypothesised that the peripheral IgG glycome profile in people with PD was affected by factors outside the CNS or close to sites of bi-directional interaction between the CNS and the periphery. Consequently, the modifications in the peripheral IgG glycome profiles presented in **Study 1** may have utility of not only identifying clinical PD presence, but rather prodromal disease presence, as alpha-synuclein inclusions are

hypothesised to begin in the ENS and progress along the vagal nerve to the CNS during the prodromal phase.

4.3 A Novel Biomarker of PD Presence but not Risk of Cognitive Decline

Given the results presented in **Studies 1** and **2**, the IgG glycome may be useful as a novel biomarker of idiopathic PD presence but not risk of cognitive decline. It was demonstrated in **Study 1** that the peripheral IgG glycome in the PD cases was indicative of an increased capacity to biologically age, as evident by the significant association of advancing age and an increase in the relative abundance of agalactosylated biantennary glycans, as well as a concurrent decrease in the relative abundance of digalactosylated biantennary glycans, in the PD cases but not the controls. These two modifications in IgG-Fc glycosylation make the IgG more pro-inflammatory, a hallmark feature in a number of chronic diseases. In PD, the severity of the underlying pathology increases as the disease progresses, which occurs as an individual ages and, therefore, was a confounder of the effect of advancing age on pro-inflammation. There were no statistically significant differences between the PD cases and controls in terms of age and gender. Consequently, any association related to age alone should have been measured concurrently in the control population. However, advancing age did not reach a significant association with any GP or derived trait in the control group of the study. Thus it may be considered that the peripheral IgG in people with PD have a propensity to become more pro-inflammatory at a faster rate as they age, and this may be linked to the severity of pathology during the course of the disorder.

One could then wonder whether the propensity of IgG to become more pro-inflammatory was associated with specific motor subtypes of PD. For example, people with a PIGD dominant motor subtype are more likely to develop PD dementia and other disturbances, such as depression and sleep disorders, as the disease progresses (Alves et al., 2006; Thenganatt & Jankovic, 2014). Indeed, imaging studies have shown that different sections of the brain are affected during the progression of these motor subtypes (Eggers et al., 2011; Eggers et al., 2012). Additionally, longitudinal studies have also implicated a low animal naming score as identifying people with PD that have impaired semantic memory, and are therefore at an increased risk for cognitive impairment and dementia development (Hu et al., 2014; Pereira et al., 2014; Williams-Gray et al., 2009). This is an important point as approximately 80% of

people with PD will develop dementia in due course (Aarsland et al., 2003; Hely et al., 2008). However, when analysing the IgG glycome in terms of these factors, there were no significant differences evident.

Inflammation may facilitate the neuron-to-neuron propagation of PD pathology (Holmes et al., 2009; Menza 2010; Reale et al, 2009; Rocha et al., 2014; Lema Tome 2013). It has been demonstrated that CSF IgG from people with PD can induce dopaminergic neuron injury after stereotaxic injection into the SN of mice. Furthermore, dopaminergic neurons within PD brains show strong immunolabelling for IgG, and IgG specific for alpha-synuclein have been found in both CSF and blood plasma (Sanchez-Guajardo et al., 2013). The proportion of IgG immunolabelled neurons within the brain is positively associated with the number of activated microglia and negatively associated with the number of dopaminergic neurons (Sanchez-Guajardo et al., 2013). Consequently, as PD progresses an increase in pro-inflammatory IgG would be expected. While the overall trend of the PD cases in the current study was to have lower relative abundances of *N*-glycans that infer a larger fraction of pro-inflammatory IgG, they had IgG that pertain to an increased activation of complement-caused inflammation as they aged in the context of a cross-sectional study. This will need to be validated in a longitudinal study.

It would be expected that the level of neuroinflammation within the CNS would be different between clinical motor subtypes of PD, as evident by the interaction of CNS IgG with peripheral IgG. However, as shown in **Study 2** this is not the case. Taken together, these results may be indicative of the peripheral IgG interacting with PD pathology in the ENS and as it propagates from the ENS to the CNS along the vagal nerve, a known bi-directional interaction site (Takeda et al., 2014). This conjecture is based on the notion that although the clinical motor subtypes of PD have different aetiopathological pathways of neurodegeneration within the CNS, and consequently the neurons containing alpha-synuclein aggregates are differentially exposed to the known sites of bi-directional interaction between the CNS and the periphery, there was no evidence of a more severe motor subtype in terms of modifications to the glycosylation of peripheral IgG. The ENS has no protective layer like the BBB and contains one of two vulnerable nervous tissues, in terms of risk to environmental exposure, in the body. Due to this lack of a protective layer, the ENS also interacts with the peripheral inflammatory system. Furthermore, alpha-synuclein inclusions, particularly Lewy neurites, increase in severity as PD pathology progresses, much like the staging of alpha-synuclein inclusions in the brain (Braak, de Vos, et al., 2006). Thus the increases in pro-inflammatory IgG associated with

age in people with PD presented in **Study 1** are reasonable in terms of the hypothesised disease process.

Interestingly, GP5 was not previously associated with advancing age and may therefore be unique to PD. GP5 contains predominantly high mannose glycans that are classed as agalactosylated biantennary glycan moieties. Therefore, an increase in GP5 was expected to cause an increase in total agalactosylated biantennary *N*-glycans. GP5 and GP20 were significantly reduced in nearly all PD cases compared to the matched controls. Subsequently, GP5 and GP20 were significantly and strongly correlated in the control group but there was no significant correlation found in the PD cases (see **Fig. 8**). Furthermore, GP20 was not associated with advancing age in either group, unlike GP5 or agalactosylated biantennary glycans ($G0^n$). It is not known what glycan moieties constitute GP20, and therefore, the inflammatory influence that the GP20 *N*-glycans have on IgG cannot be deduced for the purpose of this thesis. Even so, this may be the first evidence that the *N*-glycans of GP20 are involved in a similar biosynthetic pathway as GP5. Whether this is under genetic or environmental control is unclear from **Study 1**, but it warrants further investigation.

The modifications of peripheral IgG glycosylation in people with PD may represent an interphenotype of the disease: the mutual interaction between the genetic makeup, the environment and the disease phenotype. Therefore, a reasonable explanation for the peripheral IgG glycome not having utility in indicating risk of cognitive decline in people with PD is that the peripheral IgG glycoproteins are interacting with the ENS and vagal nerve neurons that have alpha-synuclein inclusions, and the increase in peripheral pro-inflammatory IgG is due to the increase in severity of these inclusions. Hence, peripheral IgG *N*-glycans may be useful biomarkers in identifying people with prodromal PD, which is hypothesised to begin in the ENS.

5.0 Summary

5.1 Findings

It was demonstrated in **Study 1** that the peripheral IgG glycome in the PD cases was indicative of an increased capacity to biologically age. This was evident by the significant association of advancing age and an increase in the relative abundance of agalactosylated biantennary glycans, and a concurrent decrease in the relative abundance of digalactosylated biantennary glycans in the PD cases but not the controls. While advancing age has previously been associated with modifications to the glycosylation of IgG, making them more pro-inflammatory, advancing age was only associated with significant increases in modifications to IgG glycosylation that infer more pro-inflammatory IgG in the PD cases and not the controls. Thus, the peripheral IgG of people with PD has a propensity to become more pro-inflammatory and lead to an increased activation of complement-caused inflammation as they aged.

PD has a heterogeneous presentation of clinical symptoms, and many genetic and environmental factors contribute to the development of the disease. While this is true, it was demonstrated in **Study 2** that the peripheral IgG glycome does not have utility in differentiating between clinical motor subtypes of PD, which result from different aetiopathological pathways of PD development and progression within the CNS, particularly from the SN to the neocortex. Combined, these results are indicative of the peripheral IgG interacting with PD pathology in the ENS as well as when it propagates from the ENS to the CNS along the vagal nerve. Inflammation may facilitate the neuron-to-neuron propagation of PD inclusions along this pathway and thus be a contributor to PD development during the prodromal phase. Hence, the peripheral IgG glycome may be useful as a novel biomarker of PD presence in the prodromal phase of the disease and may represent an interphenotype of PD.

5.2 Strengths

The innovation and strength of this thesis was that for the first time the potential of using peripheral IgG glycomic biomarkers to identify people with PD, as well as identify people with PD who are at risk of cognitive decline, was investigated. This was done using an established PD cohort based in Perth, Western Australia; another strength of the thesis. A further strength was that the technology used to analyse the glycans, i.e. UPLC, is a validated method that is utilised in research worldwide and published frequently (Knezevic et al., 2009; Krištić et al.,

2014; Lauc et al., 2013; Lu et al., 2011; Pucic et al., 2011). Furthermore, the statistical methods used in these studies influenced the way data was analysed in this thesis.

5.3 Limitations

Although this thesis presented some strong results, there were some limitations. Firstly, the sample size included in this thesis was relatively small compared to other studies analysing modifications to the glycosylation of IgG. This may have contributed to some of the deviation from previous findings, such as a weak but statistically insignificant correlation between BMI and agalactosylated glycans. Secondly, although both populations are Caucasian in descent, they are from different geographical parts: Australia and Croatia. This was a predetermined aspect of the study out of the control of the researcher. Plasma glycome variability has been reported between different populations in previous studies (Knezevic et al., 2009). However, this inter-population variability has not been fully explored in terms of the peripheral IgG glycome. Therefore, the consequence of using Caucasian controls from a different population in this thesis is unknown. Lastly, due to time constraints not all non-motor aspects of clinical PD were explored, such as depression and sleep disorders. Thus the peripheral IgG glycome may have utility as a biomarker of these non-motor aspects of PD as well.

5.4 Implications for Future Research

The utility in using the peripheral IgG glycome as a means of identifying people with PD, particularly in the prodromal phase, needs to be further investigated. This will involve a longitudinal study design with at-risk, suboptimally healthy individuals who do not have any current signs of PD. Moreover, the contribution of environmental or genetic influences to the changes reported in this thesis needs to be further investigated. Importantly, it would be recommended that future studies analysing the IgG glycome for use as a biomarker of an interphenotype of disease utilise intra-population controls and a larger study sample.

6.0 References

Aarsland, D., Andersen, K., Larsen, J. P., Lolk, A., & Kragh-Sorensen, P. (2003). Prevalence and Characteristics of Dementia in Parkinson's Disease. *Archives of Neurology, 60*, 387-392.

Aarsland, D., Bronnick, K., Williams-Gray, C., Weintraub, D., Marder, K., Kulisevsky, J., . . . Emre, M. (2010). Mild cognitive impairment in Parkinson disease: A multicenter pooled analysis. *Neurology, 75*, 1062-1069.

Alves, G., Larsen, J. P., Emre, M., Wentzel-Larsen, T., & Aarsland, D. (2006). Changes in motor subtype and risk for incident dementia in Parkinson's disease. *Movement Disorders, 21*(8), 1123-1130.

Angata, T., Fujinawa, R., Kurimoto, A., Nakajima, K., Kato, M., Takamatsu, S., . . . Taniguchi, N. (2012). Intergrated approach toward the discovery of glyco-biomarkers of inflammatory-related diseases. *Annals of the New York Academy of Science, 1253*, 159-169.

Angot, E., Steiner, J. A., Tomé, C. M. L., Ekström, P., Mattsson, B., Björklund, A., & Brundin, P. (2012). Alpha-synuclein cell-to-cell transfer and seeding in grafted dopaminergic neurons in vivo. *PLoS One, 7*(6), e39465.

Anthony, R. M. (2011). The role of differential IgG glycosylation in the interaction of antibodies with FcγRs in vivo. *Current Opinion in Organ Transplantation, 16*(1), 7-14.

Anthony, R. M., Wermeling, F., & Ravetch, J. V. (2012). Novel roles for the IgG Fc glycan. *Annals of the New York Academy of Sciences, 1253*(1), 170-180.

Arnold, J. N., Wormald, M. R., Sim, R. B., Rudd, P. M., & Dwek, R. A. (2007). The impact of glycosylation on the biological function and structure of human immunoglobulins. *Annu. Rev. Immunol., 25*, 21-50.

Atkinson, A. J., Colburn, W. A., DeGruttola, V. G., DeMets, D. L., Downing, G. J., Hoth, D. F., . . . Spilker, B. A. (2001). Biomarkers and surrogate endpoints: Preferred definitions and conceptual framework*. *Clinical Pharmacology & Therapeutics, 69*(3), 89-95.

Baldivia, B., Brucki, S. M. D., Batistela, S., Esper, J. C., Augusto, C. D., & Rocha, M. S. G. (2011). Dementia in Parkinson's disease: a Brazilian sample. *Arquivos De Neuro-Psiquiatria, 69*(5), 733-738.

Blow, N. (2009). A spoonful of sugar. *Nature, 457*(7229), 617.

Böhm, S., Schwab, I., Lux, A., & Nimmerjahn, F. (2012). *The role of sialic acid as a modulator of the anti-inflammatory activity of IgG.* Paper presented at the Seminars in immunopathology.

Braak, H., Bohl, J. R., Muller, C. M., Rub, U., Vos, R. A. I. d., & Tredici, K. D. (2006). Stanley Fahn Lecture 2005: The Staging Procedure for the Inclusion Body Pathology Associated with Sporadic Parkinson's Disease Reconsidered. *Movement Disorders, 21*(12), 2042-2051. doi: 10.1002/mds.21065

Braak, H., de Vos, R. A., Bohl, J., & Del Tredici, K. (2006). Gastric α-synuclein immunoreactive inclusions in Meissner's and Auerbach's plexuses in cases staged for Parkinson's disease-related brain pathology. *Neuroscience Letters, 396*(1), 67-72.

Braak, H., Tredici, K. D., Rub, U., Vos, R. A. I. d., Steur, E. N. H. J., & Braak, E. (2003). Staging of brain pathology related to sporadic Parkinson's disease. *Neurobiology of Aging, 24*(2), 197-211.

Bucks, R., Cruise, K., Skinner, T., Loftus, A., Barker, R., & Thomas, M. (2011). Coping processes and health-related quality of life in Parkinson's disease. *International Journal of Geriatric Psychiatry, 26*(3), 247-255.

Burré, J., Sharma, M., Tsetsenis, T., Buchman, V., Etherton, M. R., & Südhof, T. C. (2010). α-Synuclein promotes SNARE-complex assembly in vivo and in vitro. *Science, 329*(5999), 1663-1667.

Cersosimo, M. G., & Benarroch, E. E. (2008). Neural control of the gastrointestinal tract: implications for Parkinson disease. *Movement Disorders, 23*(8), 1065-1075.

Chen, C. C., Engelborghs, S., Dewaele, S., Bastard, N. L., Martin, J.-J., Vanhooren, V., . . . Deyn, P. P. D. (2010). Altered Serum Glycomics in Alzheimer Disease: A Potential Blood Biomarker. *Rejuvenation Research, 13*(4), 439-444.

Chen, G., Wang, Y., Qin, X., Li, H., Guo, Y., Wang, Y., . . . Li, F. (2013). Change in IgG1 Fc N-linked glycosylation in human lung cancer: Age-and sex-related diagnostic potential. *Electrophoresis, 34*(16), 2407-2416.

Chen, G., Wang, Y., Qiu, L., Qin, X., Liu, H., Wang, X., . . . Guo, Y. (2012). Human IgG Fc-glycosylation profiling reveals associations with age, sex, female sex hormones and thyroid cancer. *Journal of proteomics, 75*(10), 2824-2834.

Collins, L. M., Toulouse, A., Connor, T. J., & Nolan, Y. M. (2012). Contributions of central and systemic inflammation to the pathophysiology of Parkinson's disease. *Neuropharmacology, 62*(7), 2154-2168.

Cruise, K., Bucks, R., Loftus, A., Newton, R., Pegoraro, R., & Thomas, M. (2011). Exercise and Parkinson's: benefits for cognition and quality of life. *Acta Neurologica Scandinavica, 123*(1), 13-19.

Dall'Olio, F., Vanhooren, V., Chen, C. C., Slagboom, P. E., Wuhrer, M., & Franceschi, C. (2013). N-glycomic biomarkers of biological aging and longevity: a link with inflammaging. *Ageing Research Reviews, 12*(2), 685-698.

de Lau, L. M. L., Schnipper, M. A., Hofman, A., Koudstaal, P. J., & Breteler, M. M. B. (2005). Prognosis of Parkinson's Disease. *Archives of Neurology, 62*, 1265-1269.

Del Tredici, K., & Braak, H. (2012). Lewy pathology and neurodegeneration in premotor Parkinson's disease. *Movement Disorders, 27*(5), 597-607.

Deloitte Access Economics. (2011). Living with Parkinson's Disease - update. Canberra, Australia: Deloitte Access Economics.

DeMarco, M. L., & Woods, R. J. (2008). Structural glycobiology: A game of snakes and ladders. *Glycobiology, 18*(6), 426-440.

Derkinderen, P., Rouaud, T., Lebouvier, T., Des Varannes, S. B., Neunlist, M., & De Giorgio, R. (2011). Parkinson disease The enteric nervous system spills its guts. *Neurology, 77*(19), 1761-1767.

Desplats, P., Lee, H.-J., Bae, E.-J., Patrick, C., Rockenstein, E., Crews, L., . . . Lee, S.-J. (2009). Inclusion formation and neuronal cell death through neuron-to-neuron transmission of α-synuclein. *Proceedings of the National Academy of Sciences, 106*(31), 13010-13015.

Dewey, M. E., & Saz, P. (2001). Dementia, cognitive impairment and mortality in persons aged 65 and over living in the community: a systematic review of the literature. *International journal of geriatric psychiatry, 16*(8), 751-761. doi: 10.1002/gps.397

Diedenhofen, B. (2013). cocor: Comparing Correlations (Version 1.0-0). Retrieved from http://r.birkdiedenhofen.de/pckg/cocor/

Eggers, C., Kahraman, D., Fink, G. R., Schmidt, M., & Timmermann, L. (2011). Akinetic-rigid and tremor-dominant Parkinson's disease patients show different patterns of FP-CIT Single photon emission computed tomography. *Movement Disorders, 26*(3), 416-423.

Eggers, C., Pedrosa, D. J., Kahraman, D., Maier, F., Lewis, C. J., Fink, G. R., . . . Timmermann, L. (2012). Parkinson subtypes progress differently in clinical course and imaging pattern. *PLoS One, 7*(10), e46813.

Emre, M., Aarsland, D., Brown, R., Burn, D. J., Duyckaertz, C., Mizuno, Y., . . . Dubois, B. (2007). Clinical Diagnostic Criteria for Dementia Associated with Parkinson's Disease. *Movement Disorders, 22*(12), 1689-1707.

Ferrara, C., Grau, S., Jäger, C., Sondermann, P., Brünker, P., Waldhauer, I., . . . Stihle, M. (2011). Unique carbohydrate–carbohydrate interactions are required for high affinity binding between FcγRIII and antibodies lacking core fucose. *Proceedings of the National Academy of Sciences, 108*(31), 12669-12674.

Fox, J., & Weisberg, S. (2011). An R Companion to Applied Regression. Thousand Oaks, USA: Sage. Retrieved from http://socserv.socsci.mcmaster.ca/jfox/Books/Companion

Fujita, T. (2002). Evolution of the lectin–complement pathway and its role in innate immunity. *Nature Reviews Immunology, 2*(5), 346-353.

Furness, J. B. (2012). The enteric nervous system and neurogastroenterology. *Nature Reviews Gastroenterology and Hepatology, 9*(5), 286-294.

Galluzzi, L., Vitale, I., Abrams, J., Alnemri, E., Baehrecke, E., Blagosklonny, M., . . . Fulda, S. (2011). Molecular definitions of cell death subroutines: recommendations of the Nomenclature Committee on Cell Death 2012. *Cell Death & Differentiation, 19*(1), 107-120.

Gindzienska-Sieskiewicz, E., Klimiuk, P. A., Kisiel, D. G., Gindzienski, A., & Sierakowski, S. (2007). The changes in monosaccharide composition of immunoglobulin G in the course of rheumatoid arthritis. *Clinical Rheumatology, 26*(5), 685-690.

Goetz, C. G., Tilley, B. C., Shaftman, S. R., Stebbins, G. T., Fahn, S., Martinez-Martin, P., . . . Dodel, R. (2008). Movement Disorder Society-sponsored revision of the Unified Parkinson's Disease Rating Scale (MDS-UPDRS): Scale presentation and clinimetric testing results. *Movement Disorders, 23*(15), 2129-2170.

Gyoneva, S., Davalos, D., Biswas, D., Swanger, S. A., Garnier-Amblard, E., Loth, F., . . . Traynelis, S. F. (2014). Systemic inflammation regulates microglial responses to tissue damage in vivo. *Glia*.

Harrell, F. E. (2014). Hmisc: Harrell Miscellaneous (Version 3.14-15). Retrieved from http://biostat.mc.vanderbilt.edu/Hmisc,https://github.com/harrelfe/Hmisc

Hauser, D. N., & Hastings, T. G. (2013). Mitochondrial dysfunction and oxidative stress in Parkinson's disease and monogenic parkinsonism. *Neurobiology of Disease, 51*, 35-42.

Hawkes, C., Del Tredici, K., & Braak, H. (2007). Parkinson's disease: a dual-hit hypothesis. *Neuropathology and Applied Neurobiology, 33*(6), 599-614.

Hely, M. A., Reid, W. G. J., Adena, M. A., Halliday, G. M., & Morris, J. G. L. (2008). The Sydney Multicentre Study of Parkinson's Disease: The Inevitability of Dementia at 20 years. *Movement Disorders, 23*(6), 837-844.

Henchcliffe, C., & Beal, M. F. (2008). Mitochondrial biology and oxidative stress in Parkinson disease pathogenesis. *Nature Clinical Practice Neurology, 4*(11), 600-609.

Hirsch, E. C., & Hunot, S. (2009). Neuroinflammation in Parkinson's disease: a target for neuroprotection? *The Lancet Neurology, 8*(4), 382-397.

Hobson, P., & Meara, J. (2004). Risk and Incidence of Dementia in a Cohort of Older Subjects With Parkinson's Disease in the United Kingdom. *Movement Disorders, 19*(9), 1043-1049.

Hoegh, M., Ibrahim, A. K., Chibnall, J., Zaidi, B., & Grossberg, G. T. (2013). Prevalence of Parkinson Disease and Parkinson Disease Dementia in Community Nursing Homes. *The American Journal of Geriatric Psychiatry, 21*(6), 529-535.

Holmes, C., Cunningham, C., Zotova, E., Woolford, J., Dean, C., Kerr, S. u., . . . Perry, V. (2009). Systemic inflammation and disease progression in Alzheimer disease. *Neurology, 73*(10), 768-774.

Horvat, T., Zoldos, V., & Lauc, G. (2011). Evolutional and clinical implications of the epigenetic regulation of protein glycosylation. *Clinical Epigenetics, 2*, 425-432.

Hu, M., Szewczyk-Królikowski, K., Tomlinson, P., Nithi, K., Rolinski, M., Murray, C., . . . Ben-Shlomo, Y. (2014). Predictors of cognitive impairment in an early stage Parkinson's disease cohort. *Movement Disorders, 29*(3), 351-359.

Hughes, A. J., Daniel, S. E., Kilford, L., & Lees, A. J. (1992). Accuracy of clinical diagnosis of idiopathic Parkinson's disease: a clinico-pathological study of 100 cases. *Journal of Neurology, Neurosurgery & Psychiatry, 55*(3), 181-184.

Hughes, T. A., Ross, H. F., Mindham, R. H. S., & Spokes, E. G. S. (2004). Mortality in Parkinson's disease and its association with dementia and depression. *Acta Neurologica Scandinavica, 110*(2), 118-123.

Ibarretxe-Bilbao, N., Junque, C., Marti, M. J., & Tolosa, E. (2011). Brain structural MRI correlates of cognitive dysfunctions in Parkinson's disease. *Journal of the Neurological Sciences, 310*(1), 70-74.

Irwin, D. J., White, M. T., Toledo, J. B., Xie, S. X., Robinson, J. L., Deerlin, V. V., . . . Trojanowski, J. Q. (2012). Neuropathologic Substrates of Parkinson's Disease Dementia. *Annals of Neurology, 72*(4), 587-598.

Jang, H., Boltz, D., Sturm-Ramirez, K., Shepherd, K. R., Jiao, Y., Webster, R., & Smeyne, R. J. (2009). Highly pathogenic H5N1 influenza virus can enter the central nervous system and induce neuroinflammation and neurodegeneration. *Proceedings of the National Academy of Sciences, 106*(33), 14063-14068.

Jankovic, J., McDermott, M., Carter, J., Gauthier, S., Goetz, C., Golbe, L., . . . Shoulson, I. (1990). Variable expression of Parkinson's disease A base-line analysis of the DAT ATOP cohort. *Neurology, 40*(10), 1529-1529.

Keane, P., Kurzawa, M., Blain, P., & Morris, C. (2011). Mitochondrial dysfunction in Parkinson's disease. *Parkinson's Disease, 2011*.

Kettenmann, H., Hanisch, U.-K., Noda, M., & Verkhratsky, A. (2011). Physiology of microglia. *Physiological Reviews, 91*(2), 461-553.

Khoury, G. A., Baliban, R. C., & Floudas, C. A. (2011). Proteome-wide post-translational modification statistics: frequency analysis and curation of the swiss-prot database. *Scientific Reports, 1*(90), 1-4.

Knezevic, A., Polasek, O., Gornik, O., Rudan, I., Campbell, H., Hayward, C., . . . Lauc, G. (2009). Variability, Heritability, and Environmental Determinants of Human Plasma N-Glycome. *Journal of Proteome Research, 8*, 694-701.

Knezevic, A., Rudan, I., Lauc, G., Gornik, O., Polasek, O., Pucic, M., . . . Campbell, H. (2010). Effects of aging, body mass index, plasma lipid profiles, and smoking on human plasma N-glycans. *Glycobiology, 20*(8), 959-969.

Kodar, K., Stadlmann, J., Klaamas, K., Sergeyev, B., & Kurtenkov, O. (2012). Immunoglobulin G Fc N-glycan profiling in patients with gastric cancer by LC-ESI-MS: relation to tumor progression and survival. *Glycoconjugate Journal, 29*(1), 57-66.

Kordower, J. H., Chu, Y., Hauser, R. A., Freeman, T. B., & Olanow, C. W. (2008). Lewy body–like pathology in long-term embryonic nigral transplants in Parkinson's disease. *Nature Medicine, 14*(5), 504-506.

Koyama, A., O'Brien, J., Weuve, J., Blacker, D., Metti, A. L., & Yaffe, K. (2012). The role of peripheral inflammatory markers in dementia and Alzheimer's disease: a meta-analysis. *The Journals of Gerontology Series A: Biological Sciences and Medical Sciences*, gls187.

Krapp, S., Mimura, Y., Jefferis, R., Huber, R., & Sondermann, P. (2003). Structural analysis of human IgG-Fc glycoforms reveals a correlation between glycosylation and structural integrity. *Journal of Molecular Biology, 325*(5), 979-989.

Krištić, J., Vučković, F., Menni, C., Klarić, L., Keser, T., Beceheli, I., . . . Lauc, G. (2014). Glycans Are a Novel Biomarker of Chronological and Biological Ages. *The Journals of Gerontology Series A: Biological Sciences and Medical Sciences, 69*(7), 779-789.

Kuo, Y.-M., Li, Z., Jiao, Y., Gaborit, N., Pani, A. K., Orrison, B. M., . . . Gershon, M. D. (2010). Extensive enteric nervous system abnormalities in mice transgenic for artificial chromosomes containing Parkinson disease-associated α-synuclein gene mutations precede central nervous system changes. *Human Molecular Genetics*, ddq038.

Lauc, G., Huffman, J. E., Pučić, M., Zgaga, L., Adamczyk, B., Mužinić, A., . . . Krištić, J. (2013). Loci associated with N-glycosylation of human immunoglobulin G show pleiotropy with autoimmune diseases and haematological cancers. *PLoS Genetics, 9*(1), e1003225.

Lauc, G., & Zoldo, V. (2010). Protein glycosylation - An evolutionary crossroad between genes and environment. *Molecular BioSystems, 6*(12), 2373-2379.

Lebouvier, T., Neunlist, M., des Varannes, S. B., Coron, E., Drouard, A., N'Guyen, J.-M., . . . Flamand, M. (2010). Colonic biopsies to assess the neuropathology of Parkinson's disease and its relationship with symptoms. *PLoS One, 5*(9), e12728.

Lee, V. M. (2013). Transmission of alpha-synuclein in Parkinson's disease. *Molecular Neurodegeneration, 8*(Suppl 1), O25.

Leek, J. T., Scharpf, R. B., Bravo, H. C., Simcha, D., Langmead, B., Johnson, W. E., . . . Irizarry, R. A. (2010). Tackling the widespread and critical impact of batch effects in high-throughput data. *Nature Reviews Genetics, 11*(10), 733-739.

Leroi, I., McDonald, K., Pantula, H., & Harbishettar, V. (2012). Cognitive Impairment in Parkinson Disease: Impact on Quality of Life, Disability, and Caregiver Burden. *Journal of Geriatric Psychiatry and Neurology, 25*(4), 208-214.

Lesage, S., & Brice, A. (2009). Parkinson's disease: from monogenic forms to genetic susceptibility factors. *Human Molecular Genetics, 18*(R1), R48-R59.

Levy, G., Tang, M. X., Louis, E. D., Côté, L. J., Alfaro, B., Mejia, H., . . . Marder, K. (2002). The association of incident dementia with mortality in PD. *Neurology, 59*(11), 1708-1713.

Lewis, S., Foltynie, T., Blackwell, A., Robbins, T., Owen, A., & Barker, R. (2005). Heterogeneity of Parkinson's disease in the early clinical stages using a data driven approach. *Journal of Neurology, Neurosurgery & Psychiatry, 76*(3), 343-348.

Li, J.-Y., Englund, E., Holton, J. L., Soulet, D., Hagell, P., Lees, A. J., . . . Björklund, A. (2008). Lewy bodies in grafted neurons in subjects with Parkinson's disease suggest host-to-graft disease propagation. *Nature Medicine, 14*(5), 501-503.

Li, J. Y., Englund, E., Widner, H., Rehncrona, S., Björklund, A., Lindvall, O., & Brundin, P. (2010). Characterization of Lewy body pathology in 12-and 16-year-old intrastriatal mesencephalic grafts surviving in a patient with Parkinson's disease. *Movement Disorders, 25*(8), 1091-1096.

Litvan, I., Goldman, J. G., Troster, A. I., Schmand, B. A., Weintraub, D., Petersen, R. C., . . . Emre, M. (2012). Diagnostic Criteria for Mild Cognitive Impairment in Parkinson's Disease: Movement Disorder Society Task Force Guidelines. *Movement Disorders, 27*(3), 349-356.

Lu, J.-P., Knezivic, A., Wang, Y.-X., Rudan, I., Campbell, H., Zou, Z.-K., . . . Wang, W. (2011). Screening Novel Biomarkers for Metabolic Syndrome by Profiling Human Plasma N-Glycans in Chinese Han and Croatian Populations. *Journal of Proteome Research, 10*, 4959-4969.

Lundström, S. L., Yang, H., Lyutvinskiy, Y., Rutishauser, D., Herukka, S.-K., Soininen, H., & Zubarev, R. A. (2014). Blood Plasma IgG Fc Glycans are Significantly Altered in Alzheimer's Disease and Progressive Mild Cognitive Impairment. *Journal of Alzheimer's Disease, 38*(3), 567-579.

Malhotra, R., Wormald, M. R., Rudd, P. M., Fischer, P. B., Dwek, R. A., & Sim, R. B. (1995). Glycosylation changes of IgG associated with rheumatooid arthritis can activate complement via the mannose-binding protein. *Nature Medicine, 1*(3), 237-243.

Marder, K., Levy, G., Louis, E. D., Mejia-Santana, H., Cote, L., Andrews, H., . . . Ottman, R. (2003). Familial aggregation of early- and late-onset Parkinson's disease. *Annals of Neurology, 54*(4), 507-513.

Marras, C., Zadikoff, C., Kennedy, N., Marshall, F. J., Mapstone, M., Chou, K. L., . . . Eslinger, P. J. (2013). Measuring mild cognitive impairment in patients with Parkinson's disease. *Movement Disorders, 28*(5), 626-633.

Maupin, K. A., Liden, D., & Haab, B. B. (2012). The fine specificity of mannose-binding and galactose-binding lectins revealed using outlier motif analysis of glycan array data. *Glycobiology, 22*(1), 160-169.

Meissner, W. G., Frasier, M., Gasser, T., Goetz, C. G., Lozano, A., Piccini, P., . . . Bezard, E. (2011). Priorities in Parkinson's disease research. *Nature Reviews, 10*(5), 377 - 393.

Menza, M., DeFronzo Dobkin, R., Marin, H., Mark, M. H., Gara, M., Bienfait, K., . . . Kusnekov, A. (2010). The role of inflammatory cytokines in cognition and other non-motor symptoms of Parkinson's disease. *Psychosomatics, 51*(6), 474-479.

Muller, M. L. T. M., Frey, K. A., Petrou, M., Kotagal, V., Koeppe, R. A., Albin, R. L., & Bohnen, N. I. (2013). B-Amyloid and Postural Instability and Gait Difficulty in Parkinson's Disease at Risk for Dementia. *Movement Disorders, 28*(3), 296-301.

Nakajima, S., Iijima, H., Shinzaki, S., Egawa, S., Inoue, T., Mukai, A., . . . Nishida, T. (2011). Functional analysis of agalactosyl IgG in inflammatory bowel disease patients. *Inflammatory bowel diseases, 17*(4), 927-936.

Nelson, D. L., Lehninger, A. L., Cox, M. M., & Osgood, M. (2008). *Lehninger Principles of Biochemistry*. New York: W.H. Freeman.

Nie, K., Zhang, Y., Wang, L., Zhao, J., Huang, Z., Gan, R., . . . Wang, L. (2012). A pilot study of psychometric properties of the Beijing version of Montreal Cognitive Assessment in patients with idiopathic Parkinson's disease in China. *Journal of Clinical Neuroscience, 19*, 1497-1500.

Nikolac Perkovic, M., Pucic Bakovic, M., Kristic, J., Novokmet, M., Huffman, J. E., Vitart, V., . . . Campbell, H. (2014). The association between galactosylation of immunoglobulin G and body mass index. *Progress in Neuro-Psychopharmacology and Biological Psychiatry, 48*, 20-25.

Nimmerjahn, F., Anthony, R. M., & Ravetch, J. V. (2007). Agalactosylated IgG antibodies depend on cellular Fc receptors for in vivo activity. *Proceedings of the National Academy of Sciences, 104*(20), 8433-8437.

Niven, E. B., & Deutsch, C. V. (2012). Calculating a robust correlation coefficient and quantifying its uncertainty. *Computers & Geosciences, 40*, 1-9.

Olanow, C. W., & Brundin, P. (2013). Parkinson's Disease and Alpha Synuclein: Is Parkinson's Disease a Prion-Like Disorder? *Movement Disorders, 28*(1), 31-40.

Pan-Montojo, F., Anichtchik, O., Dening, Y., Knels, L., Pursche, S., Jung, R., . . . Reichmann, H. (2010). Progression of Parkinson's disease pathology is reproduced by intragastric administration of rotenone in mice. *PloS one, 5*(1), e8762.

Parkinson, J. (1817). *An essay on the shaking palsy*: Whittingham and Rowland.

Patanella, A. K., Zinno, M., Quaranta, D., Nociti, V., Frisullo, G., Gainotti, G., . . . Marra, C. (2010). Correlations between peripheral blood mononuclear cell production of BDNF, TNF-alpha, IL-6, IL-10 and cognitive performances in multiple sclerosis patients. *Journal of Neuroscience Research, 88*(5), 1106-1112.

Pereira, J. B., Svenningsson, P., Weintraub, D., Brønnick, K., Lebedev, A., Westman, E., & Aarsland, D. (2014). Initial cognitive decline is associated with cortical thinning in early Parkinson disease. *Neurology, 82*(22), 2017-2025.

Perry, V. H., Nicoll, J. A., & Holmes, C. (2010). Microglia in neurodegenerative disease. *Nature Reviews Neurology, 6*(4), 193-201.

Pucic, M., Knezevic, A., Vidic, J., Adamczyk, B., Novokmet, M., Polasek, O., . . . Lauc, G. (2011). High Throughput Isolation and Glycosylation Analysis of IgG-Variability and Heritability of the IgG Glycome in Three Isolated Human Populations. *Molecular Cell Proteomics, 10*(10).

Pucic, M., Pinto, S., Novokmet, M., Knezevic, A., Gornik, O., Polasek, O., . . . Lauc, G. (2010). Common aberrations from the normal human plasma N-glycan profile. *Glycobiology, 20*(8), 970-975.

R Core Team. (2014). R: A language and environment for statistical computing Retrieved from http:/www.R-project.org/

Rana, A. Q., Yousuf, M. S., Naz, S., & Qa'aty, N. (2012). Prevalence and relation of dementia to various factors in Parkinson's disease. *Psychiatry and Clinical Neurosciences, 66*(1), 64-68.

RCSB Protein Data Bank. (2013). PDB Current Holdings Breakdown Retrieved 17/04/2013, from http://www.rcsb.org/pdb/statistics/holdings.do

Reale, M., Iarlori, C., Thomas, A., Gambi, D., Perfetti, B., Di Nicola, M., & Onofrj, M. (2009). Peripheral cytokines profile in Parkinson's disease. *Brain, Behavior, and Immunity, 23*(1), 55-63.

Reid, W. G. J., Hely, M. A., Morris, J. G. L., Broe, G. A., Adena, M., Sullivan, D. J. O., & Williamson, P. M. (1996). A longitudinal study of Parkinson's disease: clinical and neuropsychological correlates of dementia. *Journal of Clinical Neuroscience, 3*(4), 327-333.

Rensburg, S. J. v., Berman, P., Potocnik, F., MacGregor, P., Hon, D., & Villiers, N. d. (2004). 5- and 6-Glycosylation of Transferrin in Patients with Alzheimer's Disease. *Metabolic Brain Disease, 19*(1/2), 89-96.

Riedel, O., Klotsche, J., Spottke, A., Deuschl, G., Förstl, H., Henn, F., . . . Riederer, P. (2008). Cognitive impairment in 873 patients with idiopathic Parkinson's disease. *Journal of Neurology, 255*(2), 255-264.

Robinson, L. N., Artpreadit, C., Raman, R., Shriver, Z. H., Ruchirawat, M., & Sasisekharan, R. (2012). Harnessing glycomics technologies: Intergrating structure with function for glycan characterization. *Electrophoresis, 33*, 797-814.

Rocha, N. P., Teixeira, A. L., Scalzo, P. L., Barbosa, I. G., Sousa, M. S., Morato, I. B., . . . Reis, H. J. (2014). Plasma levels of soluble tumor necrosis factor receptors are associated with cognitive performance in Parkinson's disease. *Movement Disorders, 29*(4), 527-531.

RStudio. (2014). RStudio: Integrated development environment for R (Version 3.0.1). Boston, USA. Retrieved from http://www.rstudio.org/

Ruhaak, L. R., Uh, H.-W., Beekman, M., Koeleman, C. A., Hokke, C. H., Westendorp, R. G., . . . Deelder, A. M. (2010). Decreased levels of bisecting GlcNAc glycoforms of IgG are associated with human longevity. *PloS One, 5*(9), e12566.

Russell, A., Drozdova, A., Wang, W., & Thomas, M. (2014). The Impact of Dementia Development Concurrent with Parkinson's Disease: A New Perspective. *CNS & Neurological Disorders - Drug Targets, 13*.

Saldova, R., Huffman, J. E., Adamczyk, B., Muzinic, A., Kattla, J. J., Pucic, M., . . . Rudd, P. M. (2012). Association of Medication with the Human Plasma N-Glycome. *Journal of Proteome Research, 11*, 1821-1831.

Saldova, R., Royle, L., Radcliffe, C. M., Hamid, U. M. A., Evans, R., Arnold, J. N., . . . Antrobus, R. (2007). Ovarian cancer is associated with changes in glycosylation in both acute-phase proteins and IgG. *Glycobiology, 17*(12), 1344-1356.

Sanchez-Guajardo, V., Barnum, C. J., Tansey, M. G., & Romero-Ramos, M. (2013). Neuroimmunological processes in Parkinson's disease and their relation to alpha-synuclein: microglia as the referee between neuronal processes and peripheral immunity. *ASN Neuro, 5*(2), 113-139.

Scallon, B. J., Tam, S. H., McCarthy, S. G., Cai, A. N., & Raju, T. S. (2007). Higher levels of sialylated Fc glycans in immunoglobulin G molecules can adversely impact functionality. *Molecular Immunology, 44*(7), 1524-1534.

Selikhova, M., Williams, D., Kempster, P., Holton, J., Revesz, T., & Lees, A. (2009). A clinico-pathological study of subtypes in Parkinson's disease. *Brain, 132*(11), 2947-2957.

Sellal, F. (2006). Parkinson's disease with dementia and dementia with Lewy body disease: two syndromes, the same disease? *Psychogeriatrics, 6*(s1), S30-S34.

Shade, K.-T. C., & Anthony, R. M. (2013). Antibody Glycosylation and inflammation. *Antibodies, 2*(3), 392-414.

Shi, M., Huber, B. R., & Zhang, J. (2010). Biomarkers for Cognitive Impairment in Parkinson's Disease. *Brain Pathology, 20*(3), 660-671.

Shields, R. L., Lai, J., Keck, R., O'Connell, L. Y., Hong, K., Meng, Y. G., . . . Presta, L. G. (2002). Lack of fucose on human IgG1 N-linked oligosaccharide improves binding to human FcγRIII and antibody-dependent cellular toxicity. *Journal of Biological Chemistry, 277*(30), 26733-26740.

Stebbins, G. T., Goetz, C. G., Burn, D. J., Jankovic, J., Khoo, T. K., & Tilley, B. C. (2013). How to identify tremor dominant and postural instability/gait difficulty groups with the movement disorder society unified Parkinson's disease rating scale: Comparison with the unified Parkinson's disease rating scale. *Movement Disorders, 28*(5), 668-670.

Sveinbjörnsdóttir, S., Hicks, A. A., Jónsson, T., Pétursson, H., Guðmundsson, G., Frigge, M. L., . . . Stefánsson, K. (2000). Familial Aggregation of Parkinson's Disease in Iceland. *New England Journal of Medicine, 343*(24), 1765-1770.

Svenningsson, P., Westman, E., Ballard, C., & Aarsland, D. (2012). Cognitive impairment in patients with Parkinson's disease: diagnosis, biomarkers, and treatment. *Lancet Neurology, 11*(8), 697-707. doi: 10.1016/S1474-4422(12)70152-7

Takeda, S., Sato, N., & Morishita, R. (2014). Systemic inflammation, blood-brain barrier vulnerability and cognitive/non-cognitive symptoms in Alzheimer disease: relevance to pathogenesis and therapy. *Frontiers in Aging Neuroscience, 6*.

Tanner, C. M., Kamel, F., Ross, G., Hoppin, J. A., Goldman, S. M., Korell, M., . . . Chade, A. R. (2011). Rotenone, paraquat, and Parkinson's disease. *Environmental Health Pperspectives, 119*(6), 866-872.

Tansey, M. G., & Goldberg, M. S. (2010). Neuroinflammation in Parkinson's disease: its role in neuronal death and implications for therapeutic intervention. *Neurobiology of Disease, 37*(3), 510-518.

Taylor, J. M., Main, B. S., & Crack, P. J. (2013). Neuroinflammation and oxidative stress: co-conspirators in the pathology of Parkinson's disease. *Neurochemistry International, 62*(5), 803-819.

Tharmalingam, T., Adamczyk, B., Doherty, M. A., Royle, L., & Rudd, P. M. (2013). Strategies for the profiling, characterisation and detailed structural analysis of N-linked oligosaccharides. *Glycoconjugate Journal, 30*(2), 137-146.

Thenganatt, M. A., & Jankovic, J. (2014). Parkinson disease subtypes. *JAMA Neurology, 71*(4), 499.

Tomé, C. M. L., Tyson, T., Rey, N. L., Grathwohl, S., Britschgi, M., & Brundin, P. (2013). Inflammation and α-Synuclein's Prion-like Behavior in Parkinson's Disease—Is There a Link? *Molecular Neurobiology, 47*(2), 561-574.

Troelsen, L. N., Jacobsen, S., Abrahams, J. L., Royle, L., Rudd, P. M., Narvestad, E., . . . Garred, P. (2012). IgG glycosylation changes and MBL2 polymorphisms: associations with markers of systemic inflammation and joint destruction in rheumatoid arthritis. *The Journal of Rheumatology, 39*(3), 463-469.

Varki, A., Cummings, R. D., Esko, J. D., Freeze, H. H., Stanley, P., Bertozzi, C. R., . . . Etzler, M. E. (2009). *Essentials of Glycobiology* (2nd ed.). New York, USA: Cold Spring Harbor Laboratory Press.

Volpicelli-Daley, L. A., Luk, K. C., Patel, T. P., Tanik, S. A., Riddle, D. M., Stieber, A., . . . Lee, V. M.-Y. (2011). Exogenous α-synuclein fibrils induce Lewy body pathology leading to synaptic dysfunction and neuron death. *Neuron, 72*(1), 57-71.

Wang, J., Balog, C. I., Stavenhagen, K., Koeleman, C. A., Scherer, H. U., Selman, M. H., . . . Wuhrer, M. (2011). Fc-glycosylation of IgG1 is modulated by B-cell stimuli. *Molecular & Cellular Proteomics, 10*(5), M110. 004655.

Wang, W., Russell, A., & Yan, Y. (2014). Traditional Chinese medicine and new concepts of predictive, preventive and personalized medicine in diagnosis and treatment of suboptimal health. *EPMA Journal, 5*(1), 1-9.

Wickham, H. (2009). ggplot2: elegant graphics for data analysis: Springer New York.
Williams-Gray, C. H., Evans, J. R., Goris, A., Foltynie, T., Ban, M., Robbins, T. W., . . . Sawcer, S. J. (2009). The distinct cognitive syndromes of Parkinson's disease: 5 year follow-up of the CamPaIGN cohort. *Brain, 132*(11), 2958-2969.
Williams-Gray, C. H., Mason, S. L., Evans, J. R., Foltynie, T., Brayne, C., Robbins, T. W., & Barker, R. A. (2013). The CamPaIGN study of Parkinson's disease: 10-year outlook in an incident population-based cohort. *Journal of Neurology, Neurosurgery, and Psychiatry*.
Yamaguchi, Y., Nishma, W., Re, S., & Sugita, Y. (2012). Confident identification of isometric N-glycan structures by combined ion mobility mass spectrometry and hydrophilic interaction liquid chromatography. *Rapid Communications in Mass Spectrometry, 26*, 2877-2884.
Yarnall, A. J., Rochester, L., & Burn, D. J. (2013). Mild cognitive impairment in Parkinson's disease. *Age and Ageing, 0*, 1-10. doi: 10.1093/ageing/aft085
Zhang, Y., Yin, H., & Lu, H. (2012). Recent progress in quantitative glycoproteomics. *Glycoconjugate Journal, 29*(5-6), 249-258.
Zou, G., Ochiai, H., Huang, W., Yang, Q., Li, C., & Wang, L.-X. (2011). Chemoenzymatic synthesis and Fcγ receptor binding of homogeneous glycoforms of antibody Fc domain. Presence of a bisecting sugar moiety enhances the affinity of Fc to FcγIIIa receptor. *Journal of the American Chemical Society, 133*(46), 18975-18991.

Appendix 1 – The Glycan Moieties of IgG

Below are pictorial representations of the dominant glycan moieties in each peak of UPLC. All exist in the total glycome. However, the neutral glycome is the sum of all the glycans within the IgG glycome that do not have terminal sialic acid, i.e. GP1:15=GP^n. GP3 was excluded from all analyses because in some samples it coeluted with a contaminant that significantly affected its value. GP20 is represented as a question mark as its glycan moiety is yet to be determined.

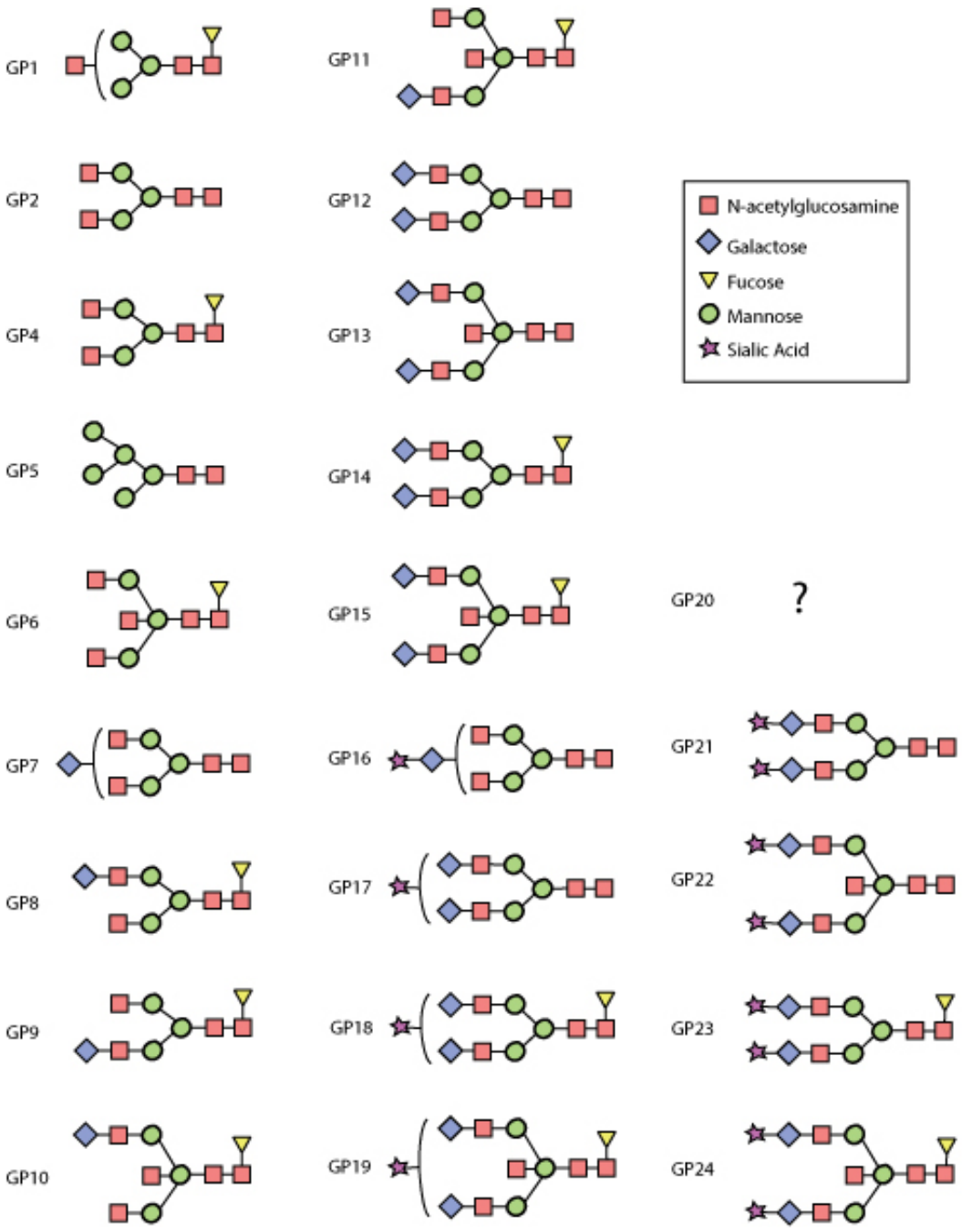

Appendix 2 – Animal Naming Task

Semantic fluency dysfunction is associated with a higher risk of cognitive impairment and dementia development (Hu et al., 2014; Pereira et al., 2014; Williams-Gray et al., 2009). Therefore, the risk of cognitive decline was determined using the animal naming task. Details regarding the animal naming task have been adapted from the Parkinson's Centre procedures manual.

The animal naming task is a timed task whereby participants are asked to name as many animals (the category) as they can in 60 seconds. It is administered to each participant the same way using a script by trained staff within the Parkinson's Centre research group. The task is administered following a similar verbal fluency task that involves specific letters of the alphabet (F, A, S). Therefore, participants are prompted if they are sticking to the previous rules. The score is the total number of correct animals generated in 60 seconds. Rule breaks receive no penalty or score.

Instructions to Participant

Administrator: "*Now we are doing something a little bit different. This time, you will have one minute to think of as many animals as you can. You can name any animal (pause) including mammals, birds, fish, reptiles, and insects and you can use any letter of the alphabet. Again, if you draw a blank, use this time to think*."

(pause)

"*Does that make sense?*"

(wait for response)

"*You have one minute to name as many animals as you can (pause) starting now*."

*If the participant begins to name specific breeds of animals, i.e. Beagle, Labrador, Great Dance, etc. prompt:

"*Try to name different animals rather than breeds of animals*."

*If the participant is sticking to previous rules and using the same letter of the alphabet for all animals, prompt:

"*You can use any letter of the alphabet*."

Scoring Conditions

- **A type of animal**, followed by specific types of animals (e.g. birds, then parrot, cockatoo) is scored as incorrect, but the following specific types are all scored as correct. However, if a type of animal (e.g. birds) but no further specific types are given, the type of animal is scored as one correct answer.
- **Age variants** (e.g. cow, then calf) are not acceptable and scored a rule break.
- **Extinct, imaginary or magic animals** are acceptable (these are animals such as unicorn, not made up animals).
- **Insects, mammals, reptiles**; all types of animals are correct regardless of the category to which they belong.
- **Names of animals** (e.g. Fido or Rover) are not acceptable and are classified as rule breaks.
- **Repetitions** are direct repetitions of previously said animals, and are a rule break.
- **Repetitions and rule breaks** cannot be retracted and are counted as incorrect answers, even if the participant recognises the error has been made.
- **Sexual variants** (e.g. bull, heifer) are acceptable.
- **Species variation**, are acceptable as they are classed as distinct animals (e.g. gorilla, monkey and chimpanzee). This also includes variations such as different possums (e.g. sugar glider possum, ring tail possum). It could be argued that smaller variations (e.g. Appaloosa horse, Arabian horse) may not be acceptable. However, these will also be scored as correct.

Score Card Example

1-15sec	16-30sec
31-45sec	46-60sec

Appendix 3 – Blocking Data

Below are the raw plate layouts, in the format "CaseStatus_Age_Gender". For easy viewing, the PD Cases are in orange boxes and the Controls (Cont) are in the light green boxes. The yellow boxes represent samples that did not pass visual quality control following UPLC. The purple boxes represent samples which were removed from the study due to meeting ParkC exclusion criteria. Reference standards and sample blanks are included as a normal part of quality control for UPLC.

PLATE 1

	1	2	3	4	5	6	7	8	9	10	11	12
A	Case_51_M	Cont_51_M	Case_40_F	Cont_40_F	Case_54_M	Cont_54_M	Case_54_F	Cont_54_F	Case_56_M	Cont_56_M	Case_54_F	Cont_54_F
B	Cont_56_F	STANDARD	Cont_56_M	Case_56_M	Cont_58_F	Case_58_F	Cont_58_M	Case_58_M	Cont_58_F	Case_58_F	Cont_58_M	Case_58_M
C	Case_82_F	Cont_82_F	Case_78_M	Cont_90_M	Case_79_F	Cont_79_F	Case_85_1	Cont_90_M	Case_77_F	Cont_77_F	Case_85_M	Cont_85_M
D	Case_70_M	Cont_70_M	Case_62_M	Cont_62_M	Case	Cont_70_M	STANDARD	Case_66_M	Case_70_M	Cont_70_M	Case_62_M	Cont_62_M
E	Cont_82_M	Case_82_M	Cont_77_F	Case_77_F	Cont_81_M	Case	Cont_76_F	Case_76_F	Cont_81_M	Case_80_M	Cont_73_F	Case_73_F
F	Case_46_F	Cont_46_F	Case_57_M	Cont_57_M	Case_58_F	Cont_58_F	Case_58_M	Cont_58_M	Case_56_F	STANDARD	Case_60_M	Control
G	Cont_60_M	Case_60_M	Cont_59_F	Case_59_F	Cont_60_M	Case_60_M	Cont_59_F	Case_59_F	Cont_61_M	Case_61_M	Cont_62_F	Case
H	Cont_63_M	Case	Cont_66_M	Case_66_M	Cont_63_M	Case_63_M	Cont_66_M	Case_66_M	Cont_63_M	Case_63_M	Cont_66_M	BLANK

PLATE 2

	1	2	3	4	5	6	7	8	9	10	11	12
A	Case_58_F	Cont_58_F	Case_62_M	Cont_62_M	Case_62_F	Cont_62_F	Case_63_M	Cont_63_M	Case_75_M	Cont_75_M	Case_63_M	Cont_63_M
B	Cont_79_M	STANDARD	Cont_70_F	Case_70_F	Cont_79_M	Case_79_M	Cont_70_F	Case_70_F	Cont_78_M	Case_78_M	Cont_69_F	Case_69_F
C	Case_68_F	Cont_68_F	Case	Cont_78_M	Case_67_F	Cont_67_F	Case	Cont_77_M	Case_65_F	Cont_65_F	Case_77_M	Cont_77_M
D	Cont_77_M	Case_77_M	Cont_64_M	Case_63_M	Cont_77_M	Case_77_M	STANDARD	Case_79_M	Cont_64_M	Case_63_M	Cont_76_M	Case_76_M
E	Case_63_F	Cont_63_F	Case_63_M	Cont_64_M	Case	Cont_63_F	Case_64_M	Cont_64_M	Case_64_F	Cont_64_F	Case_64_M	Cont_64_M
F	Cont_76_M	Case_76_M	Cont_76_M	Case_76_M	Cont_74_M	Case_74_M	Cont_72_M	Case_72_M	Control	STANDARD	Cont_74_M	Case_74_M
G	Case_64_M	Cont_64_M	Case_64_F	Cont_64_F	Case_72_M	Cont_72_M	Case_65_F	Cont_65_F	Case_67_M	Control	Case_68_M	Cont_68_M
H	Cont_65_M	Case_65_M	Cont_66_M	Case_66_M	Cont_74_M	Case_74_M	Cont_66_M	Case_66_M	Cont_73_M	Case	Case_75_M	BLANK

PLATE 3

	1	2	3	4	5	6	7	8	9	10	11	12
A	Case	Cont_70_M	Case	Control	Case	Control	Case	Control	Case_68_M	Cont_68_M	Case	Cont_71_M
B	Case	STANDARD	Cont_67_M	Case_73_M	Cont_73_M	Case_67_M	Cont_67_M	Case_71_M	Cont_71_M	Case_72_M	Cont_73_M	Case_74_M
C	Cont_74_M	Case_72_M	Cont_73_M	Case_73_M	Cont_73_M	Case_62_F	Cont_62_F	Case_43_M	Cont_43_M	BLANK	STANDARD	STANDARD
D	STANDARD	STANDARD	STANDARD	STANDARD	STANDARD	STANDARD	STANDARD	STANDARD	STANDARD	STANDARD	STANDARD	STANDARD
E	STANDARD	STANDARD	STANDARD	STANDARD	STANDARD	STANDARD	STANDARD	STANDARD	STANDARD	STANDARD	STANDARD	STANDARD
F	STANDARD	STANDARD	STANDARD	STANDARD	STANDARD	STANDARD	STANDARD	STANDARD	STANDARD	STANDARD	STANDARD	STANDARD
G	STANDARD	STANDARD	STANDARD	STANDARD	STANDARD	STANDARD	STANDARD	STANDARD	STANDARD	STANDARD	STANDARD	STANDARD
H	STANDARD	STANDARD	STANDARD	STANDARD	STANDARD	STANDARD	STANDARD	STANDARD	STANDARD	STANDARD	STANDARD	STANDARD

Appendix 4 – Boxplots of Batch Comparisons

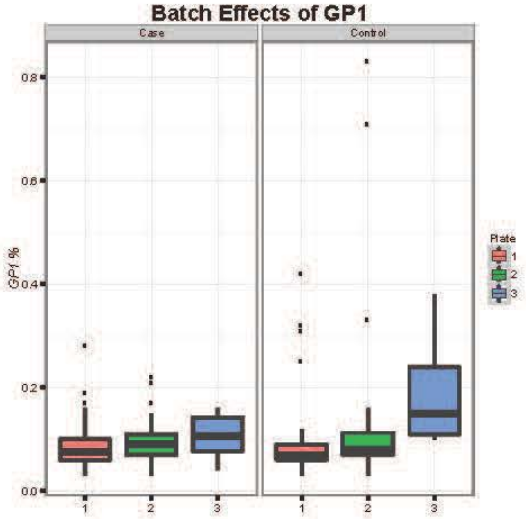

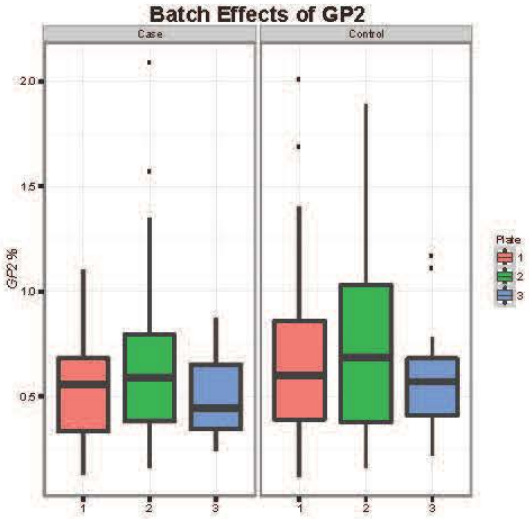

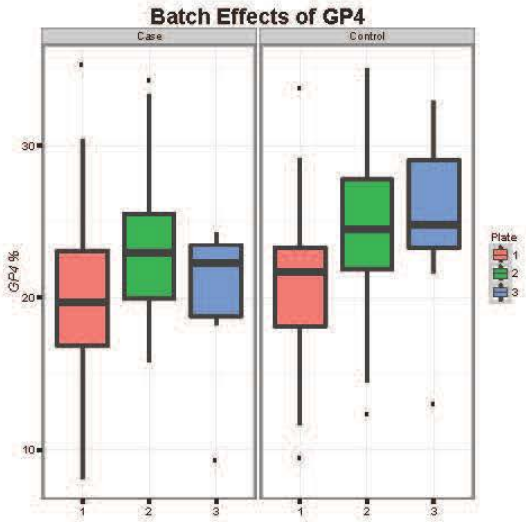

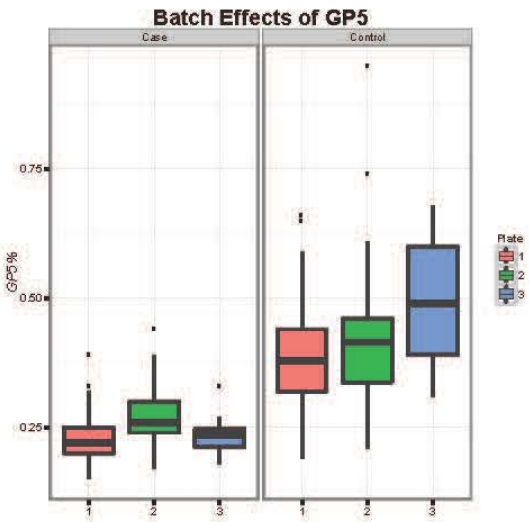

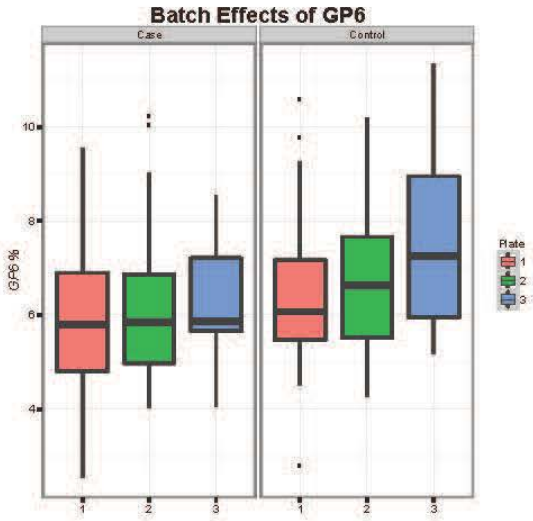

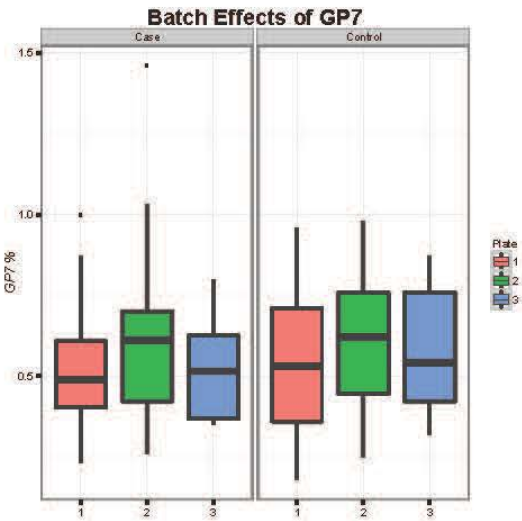

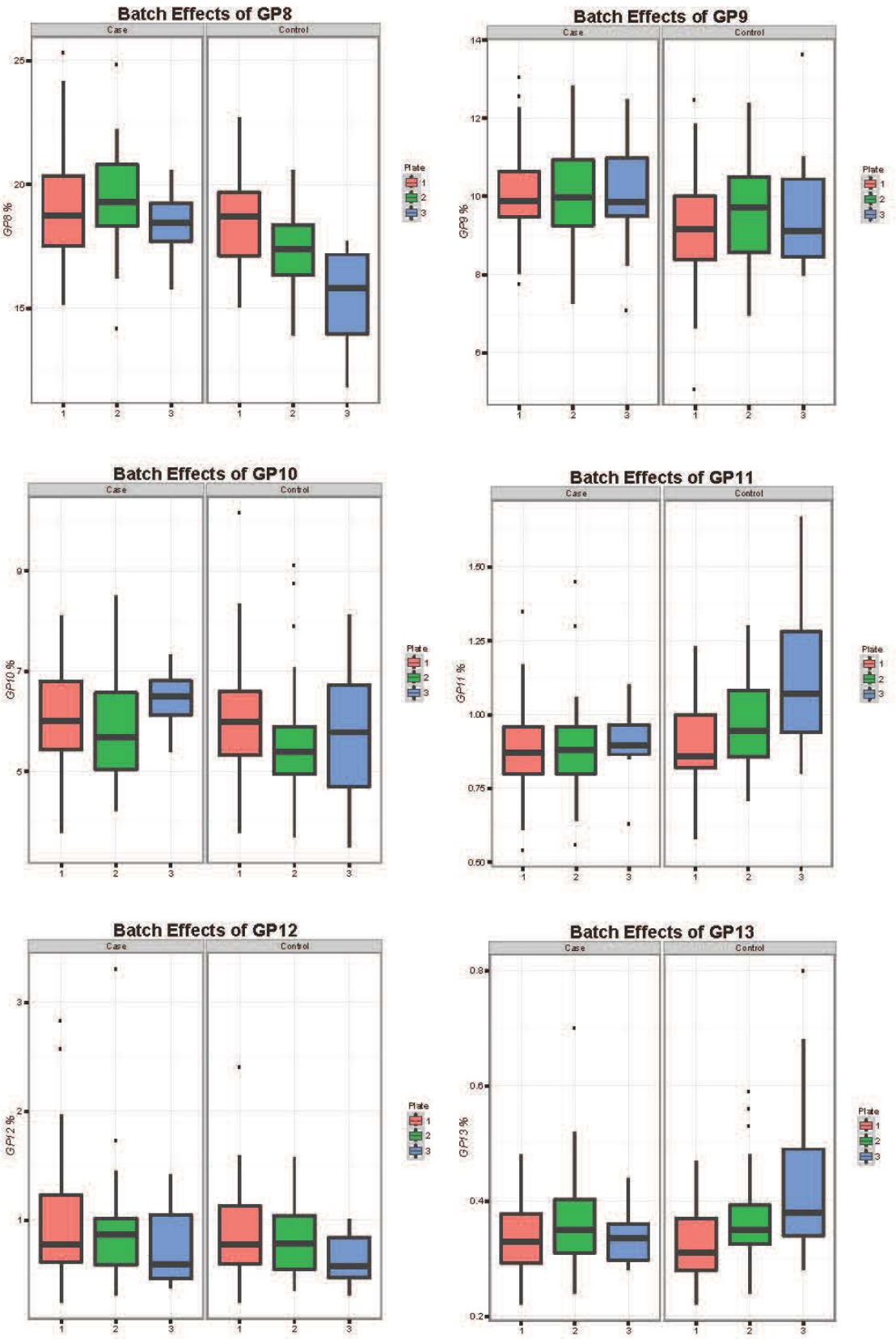
Batch Effects of GP8
Case
Control
GP8 %
Plate
1
2
3
Batch Effects of GP9
GP9 %
Batch Effects of GP10
GP10 %
Batch Effects of GP11
GP11 %
Batch Effects of GP12
GP12 %
Batch Effects of GP13
GP13 %

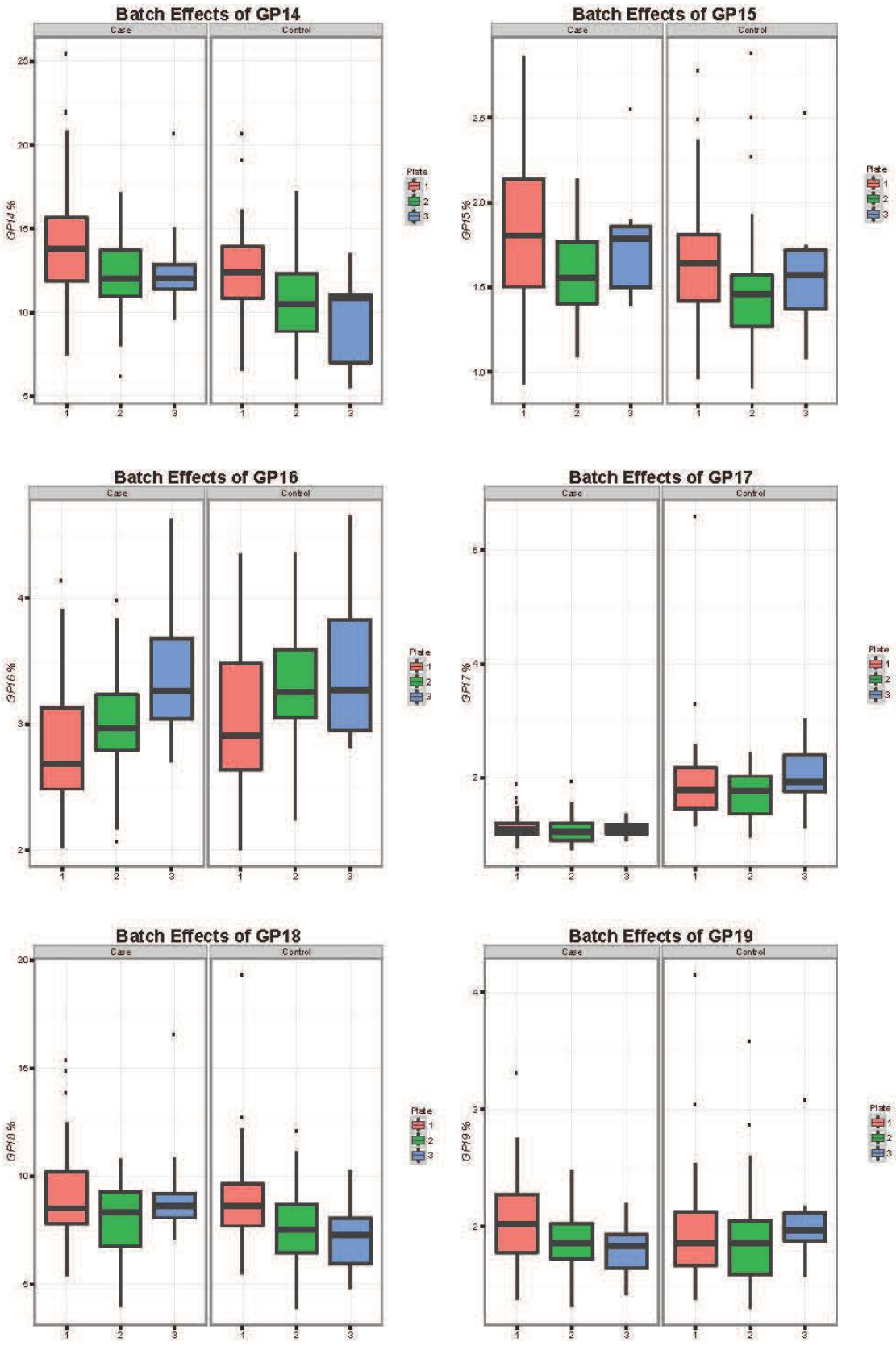
Batch Effects of GP14
Case
Control
GP14 %
Plate
1
2
3
Batch Effects of GP15
GP15 %
Batch Effects of GP16
GP16 %
Batch Effects of GP17
GP17 %
Batch Effects of GP18
GP18 %
Batch Effects of GP19
GP19 %

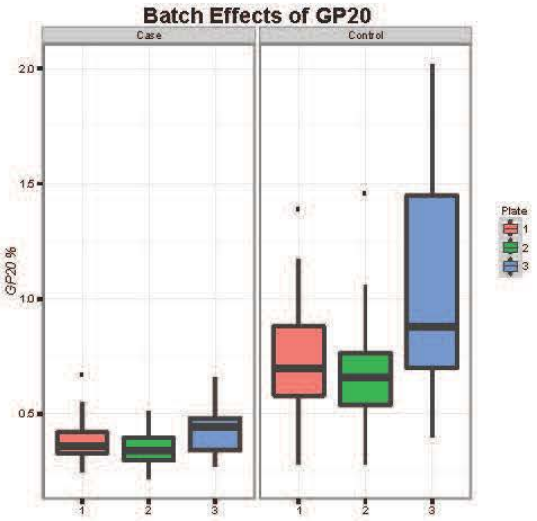
Batch Effects of GP20
Case
Control
GP20 %
Plate
1
2
3

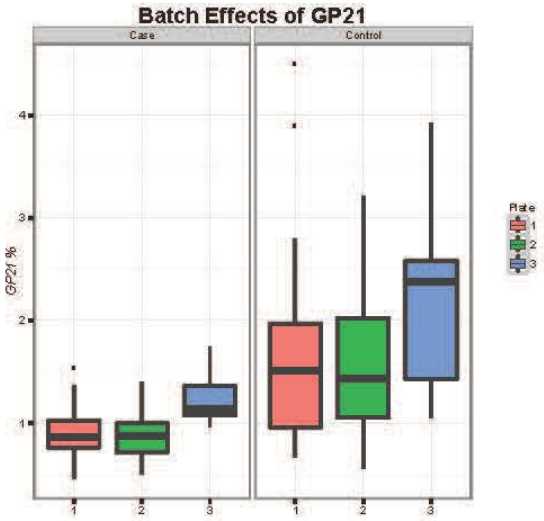
Batch Effects of GP21
Case
Control
GP21 %
Plate
1
2
3

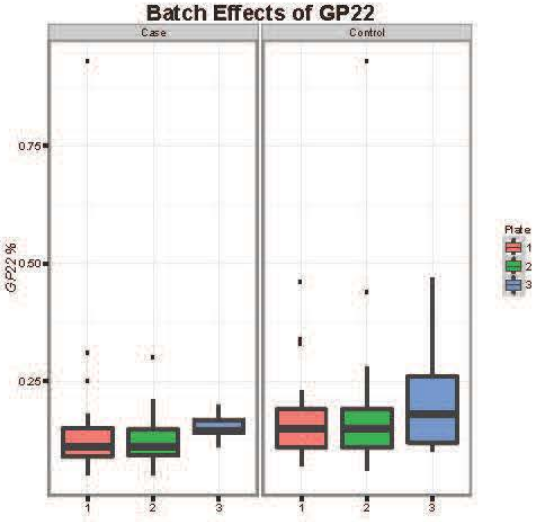
Batch Effects of GP22
Case
Control
GP22 %
Plate
1
2
3

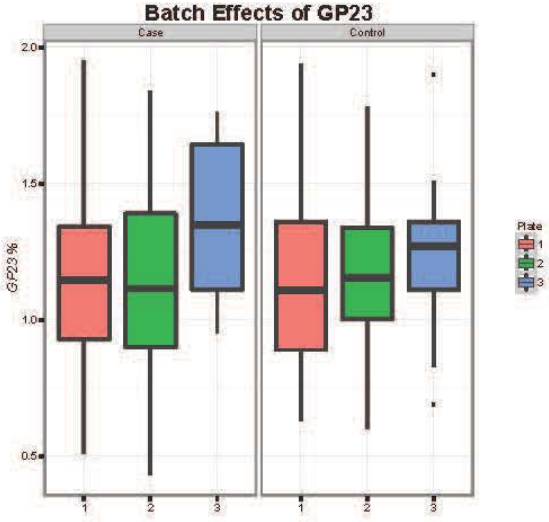
Batch Effects of GP23
Case
Control
GP23 %
Plate
1
2
3

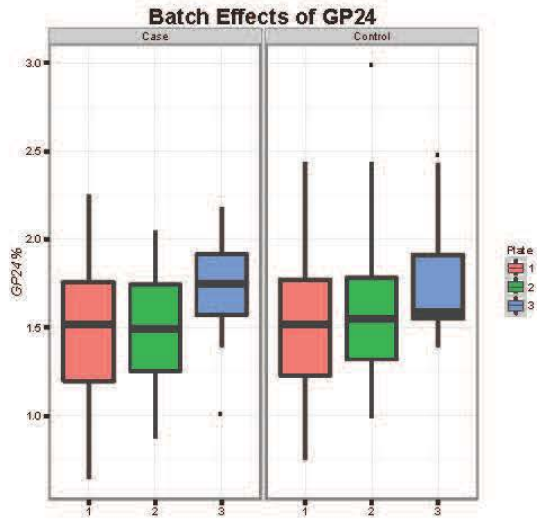
Batch Effects of GP24
Case
Control
GP24 %
Plate
1
2
3

Appendix 5 – Q-Q Plot for Visual Inspection of Normality

Below are the Q-Q plot for the PD cases and controls at each variable before transformation. Transformation details can be found in **Appendix 6.**

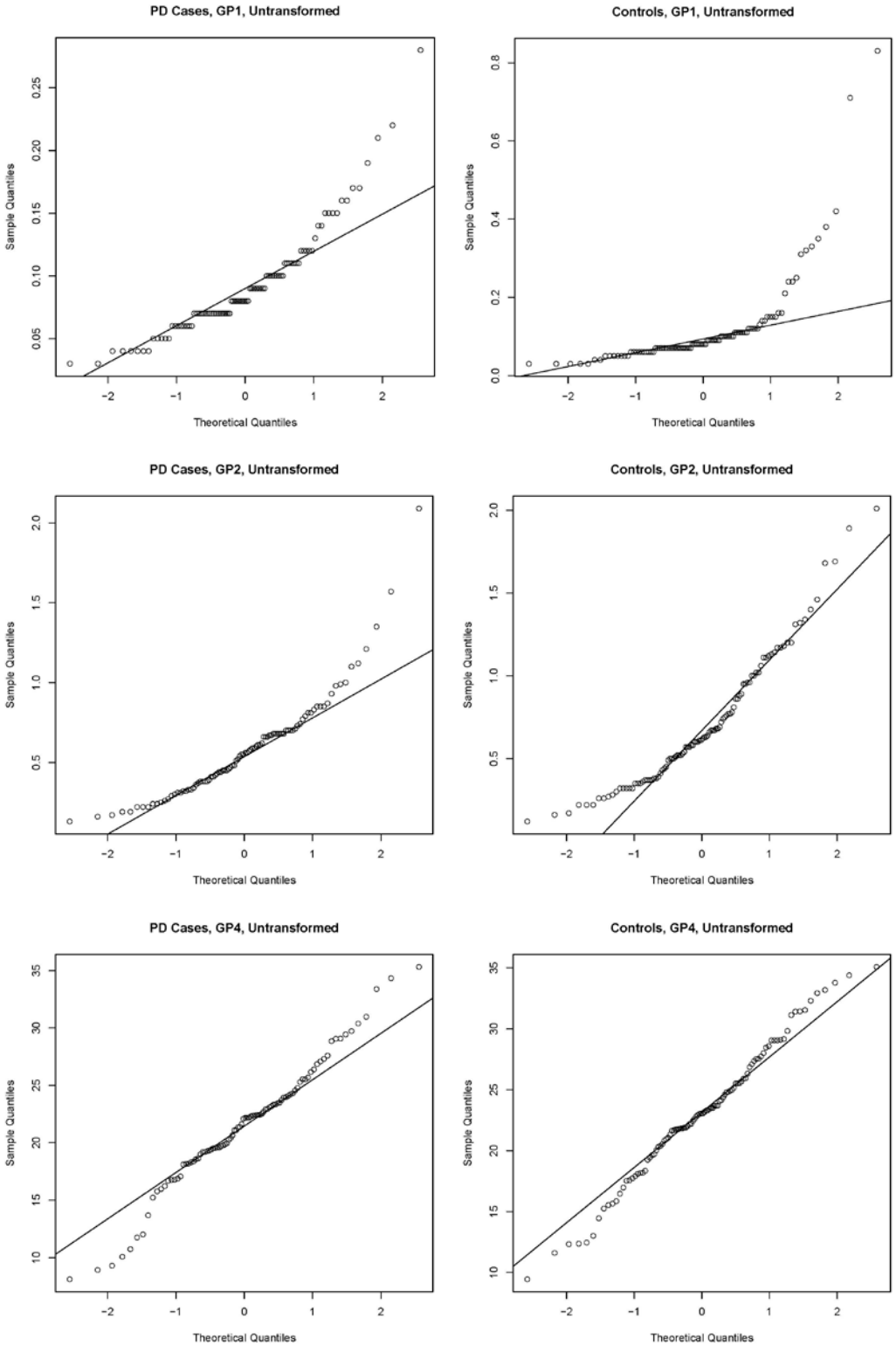

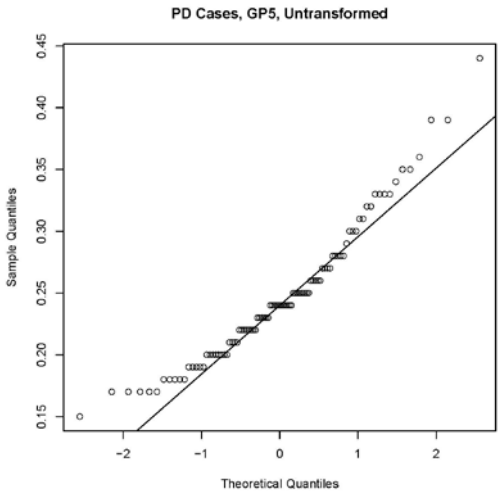
PD Cases, GP5, Untransformed
Sample Quantiles
Theoretical Quantiles

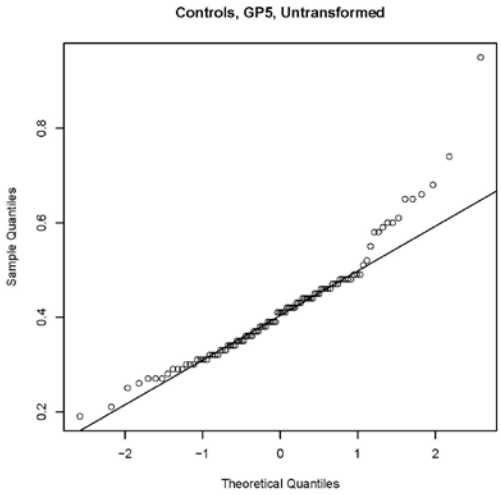
Controls, GP5, Untransformed
Sample Quantiles
Theoretical Quantiles

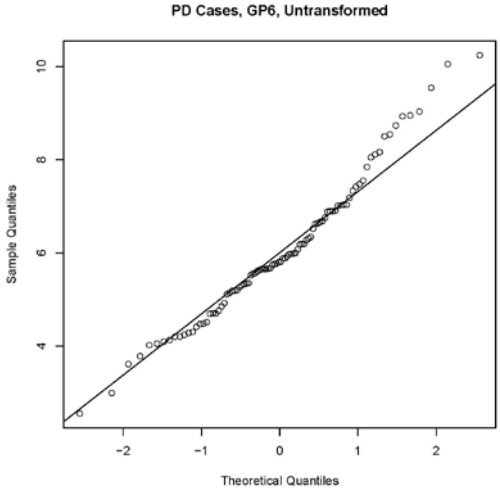
PD Cases, GP6, Untransformed
Sample Quantiles
Theoretical Quantiles

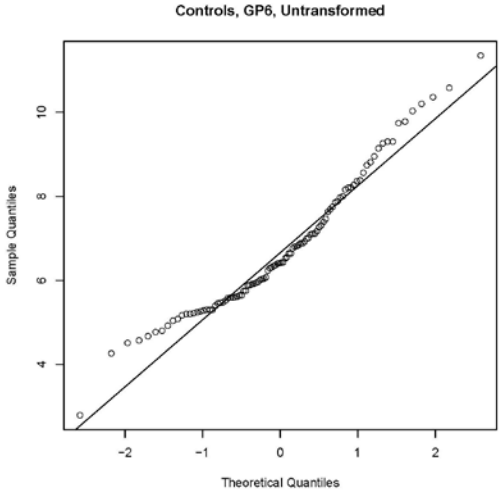
Controls, GP6, Untransformed
Sample Quantiles
Theoretical Quantiles

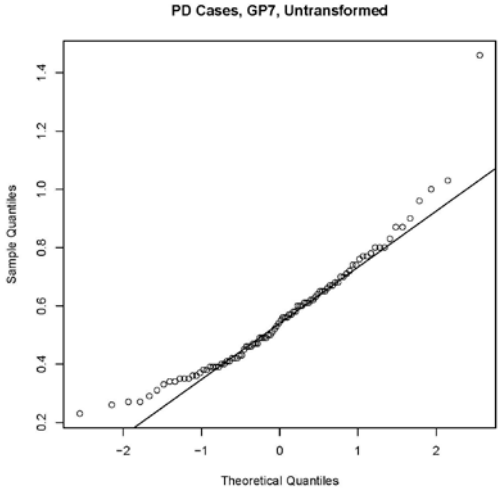
PD Cases, GP7, Untransformed
Sample Quantiles
Theoretical Quantiles

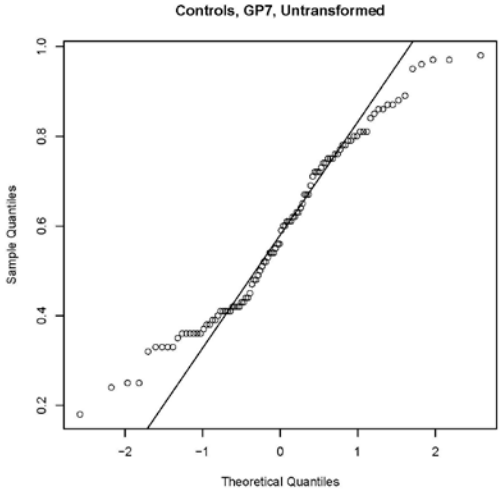
Controls, GP7, Untransformed
Sample Quantiles
Theoretical Quantiles

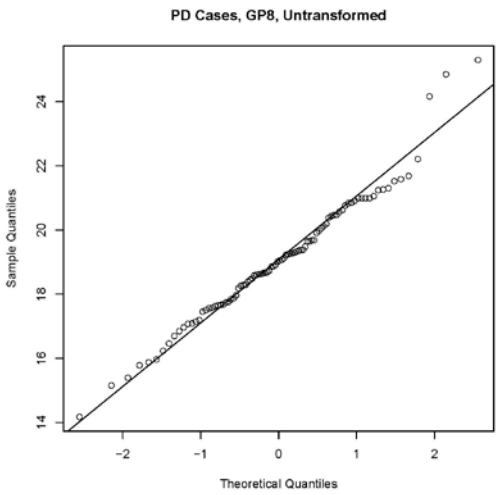
PD Cases, GP8, Untransformed
Sample Quantiles
Theoretical Quantiles

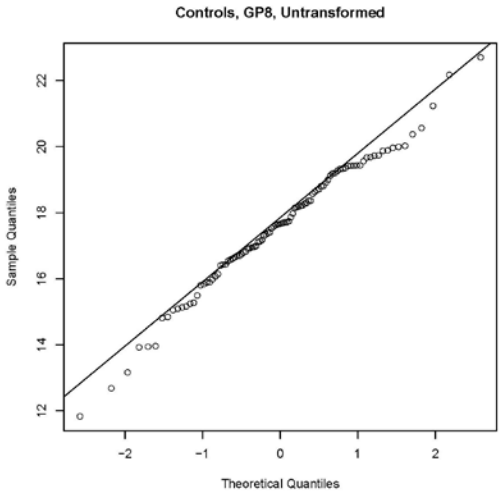
Controls, GP8, Untransformed
Sample Quantiles
Theoretical Quantiles

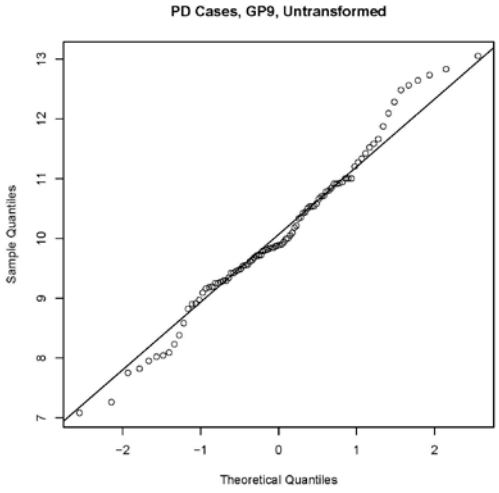
PD Cases, GP9, Untransformed
Sample Quantiles
Theoretical Quantiles

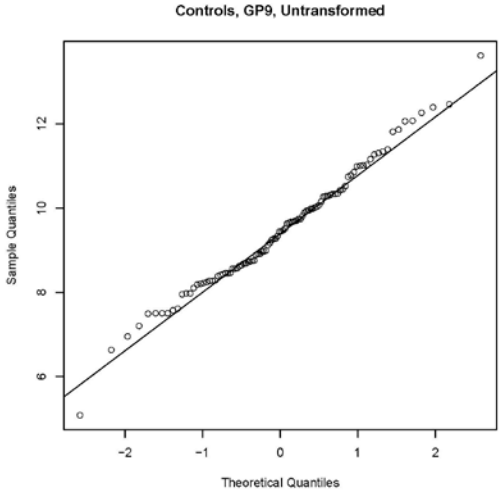
Controls, GP9, Untransformed
Sample Quantiles
Theoretical Quantiles

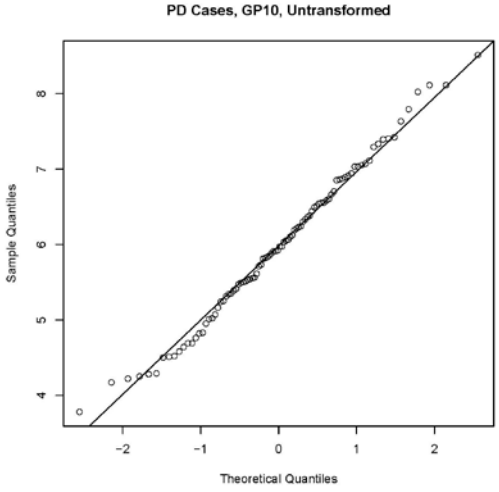
PD Cases, GP10, Untransformed
Sample Quantiles
Theoretical Quantiles

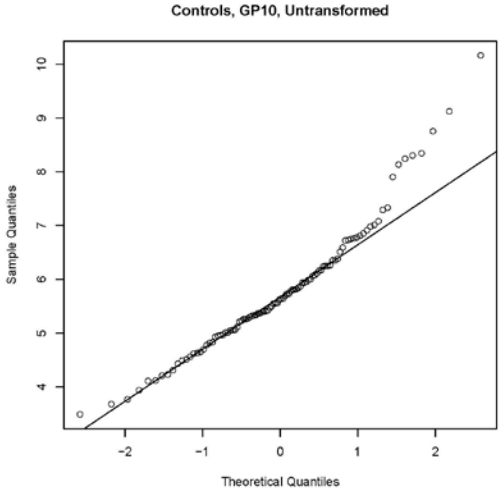
Controls, GP10, Untransformed
Sample Quantiles
Theoretical Quantiles

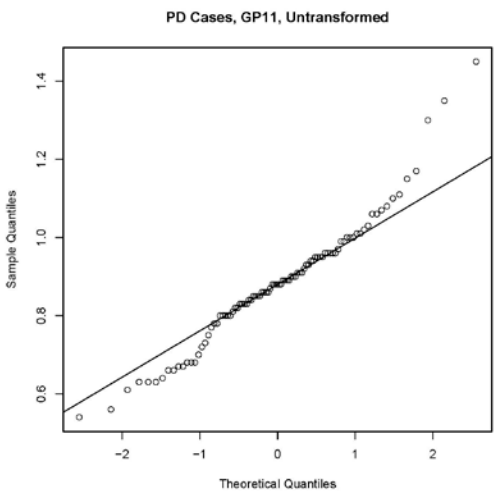
PD Cases, GP11, Untransformed
Sample Quantiles
Theoretical Quantiles

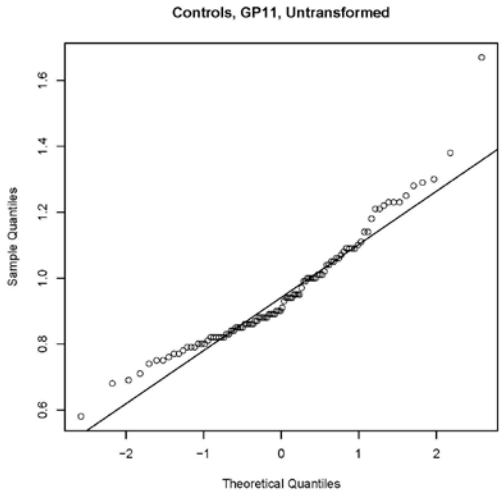
Controls, GP11, Untransformed
Sample Quantiles
Theoretical Quantiles

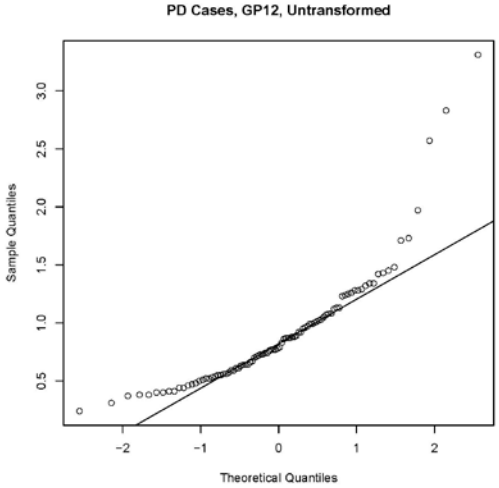
PD Cases, GP12, Untransformed
Sample Quantiles
Theoretical Quantiles

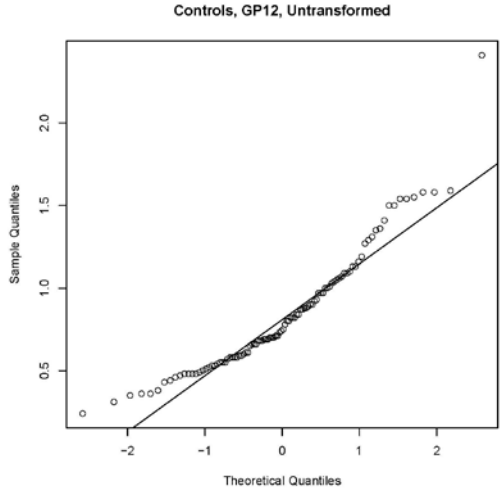
Controls, GP12, Untransformed
Sample Quantiles
Theoretical Quantiles

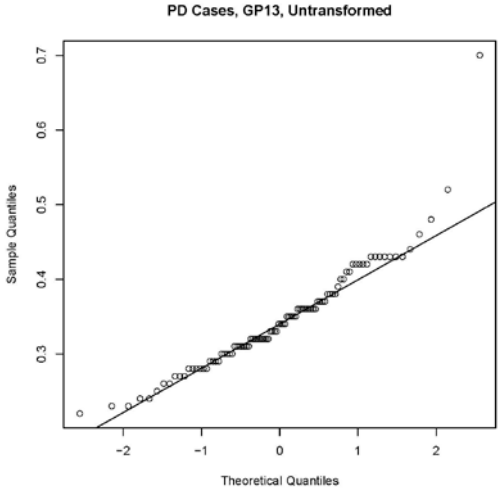
PD Cases, GP13, Untransformed
Sample Quantiles
Theoretical Quantiles

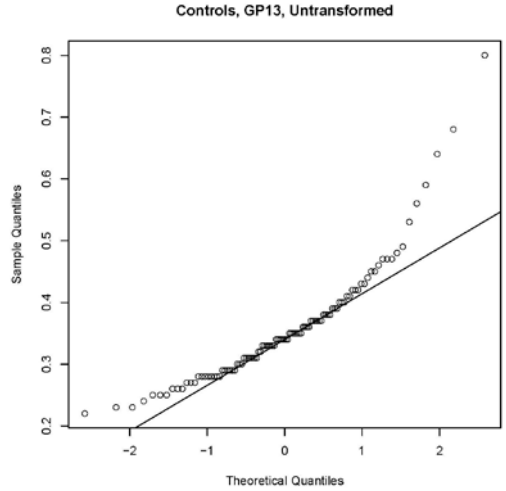
Controls, GP13, Untransformed
Sample Quantiles
Theoretical Quantiles

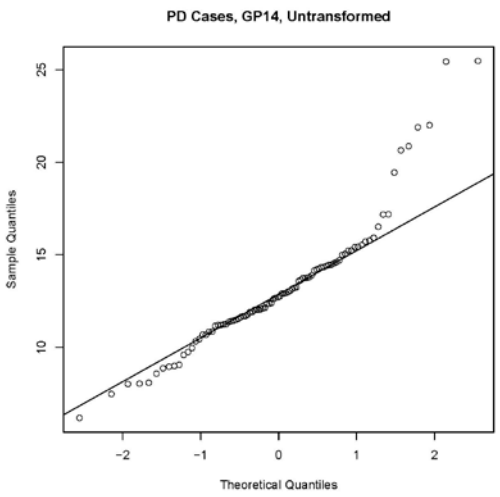
PD Cases, GP14, Untransformed
Sample Quantiles
Theoretical Quantiles

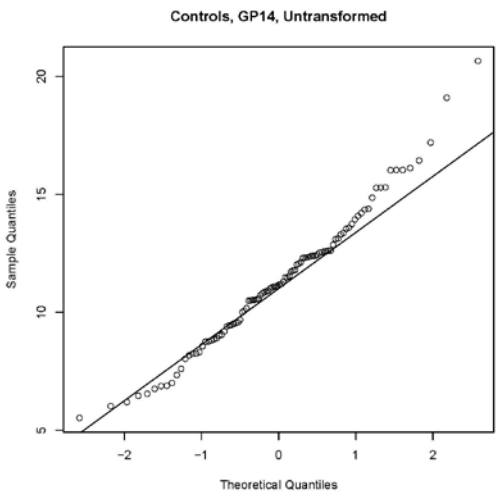
Controls, GP14, Untransformed
Sample Quantiles
Theoretical Quantiles

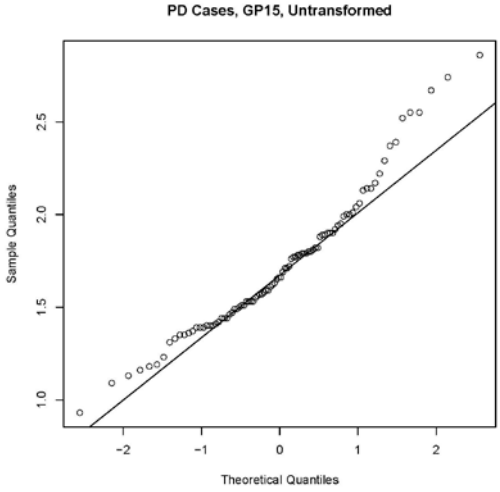
PD Cases, GP15, Untransformed
Sample Quantiles
Theoretical Quantiles

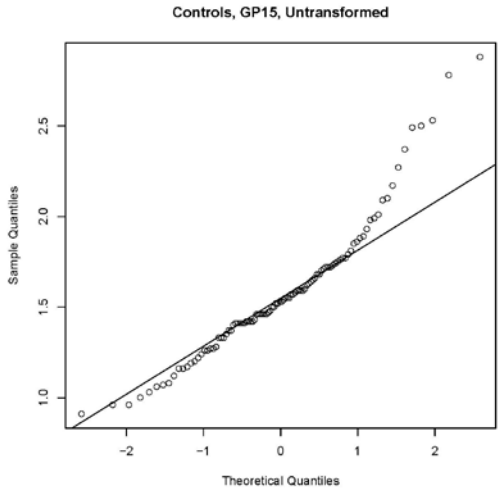
Controls, GP15, Untransformed
Sample Quantiles
Theoretical Quantiles

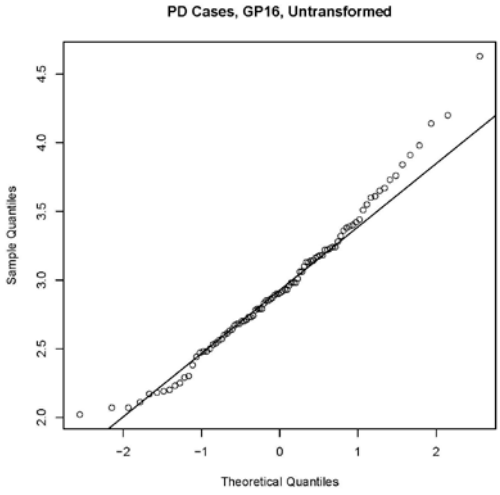
PD Cases, GP16, Untransformed
Sample Quantiles
Theoretical Quantiles

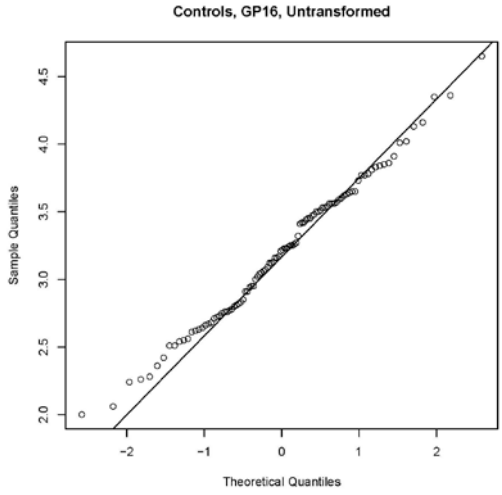
Controls, GP16, Untransformed
Sample Quantiles
Theoretical Quantiles

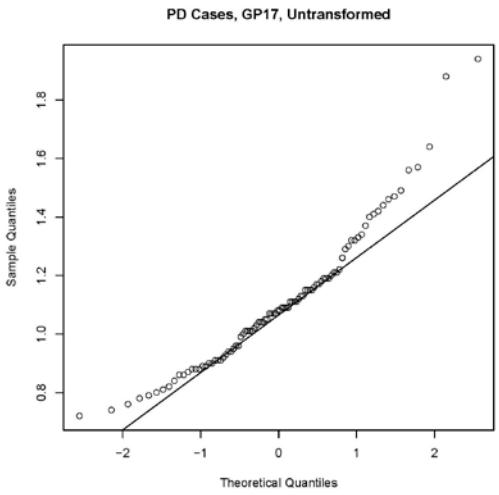
PD Cases, GP17, Untransformed
Sample Quantiles
Theoretical Quantiles

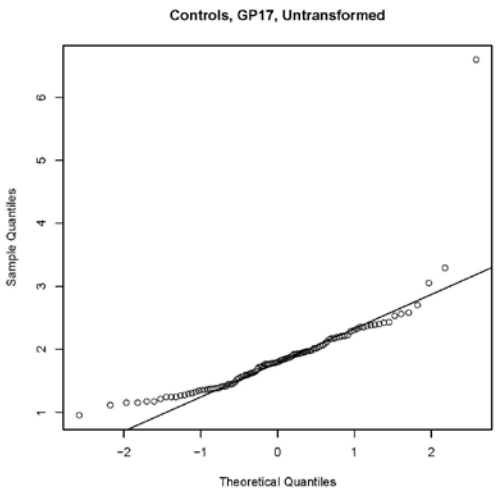
Controls, GP17, Untransformed
Sample Quantiles
Theoretical Quantiles

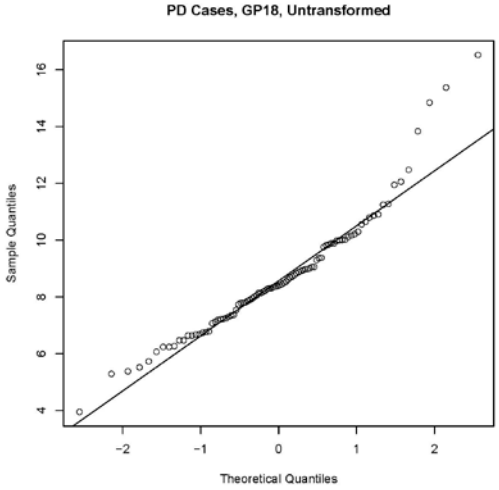
PD Cases, GP18, Untransformed
Sample Quantiles
Theoretical Quantiles

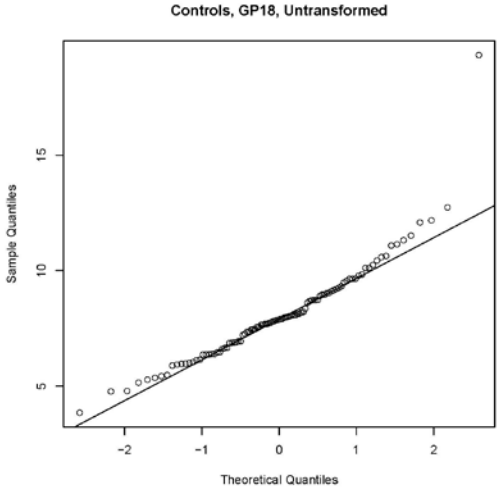
Controls, GP18, Untransformed
Sample Quantiles
Theoretical Quantiles

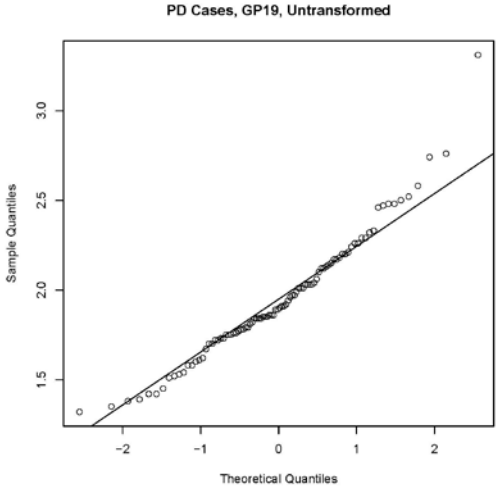
PD Cases, GP19, Untransformed
Sample Quantiles
Theoretical Quantiles

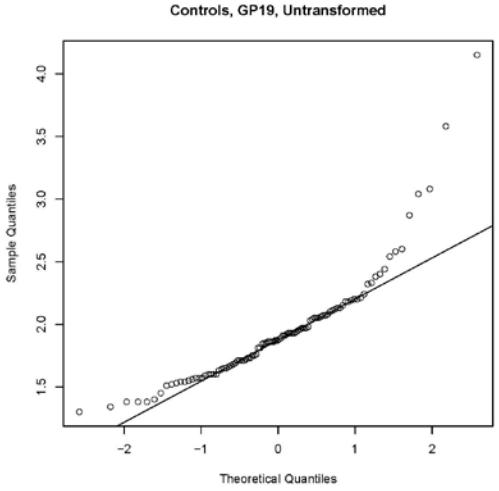
Controls, GP19, Untransformed
Sample Quantiles
Theoretical Quantiles

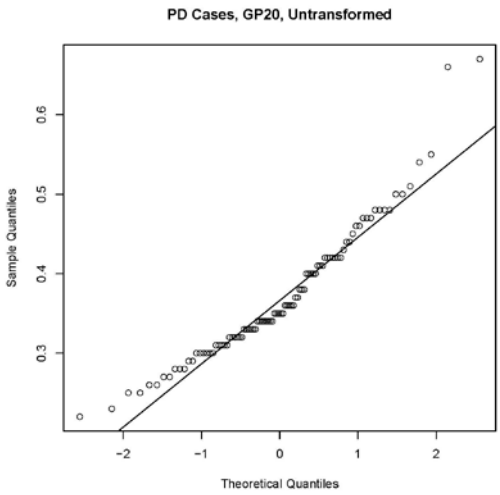
PD Cases, GP20, Untransformed
Sample Quantiles
Theoretical Quantiles

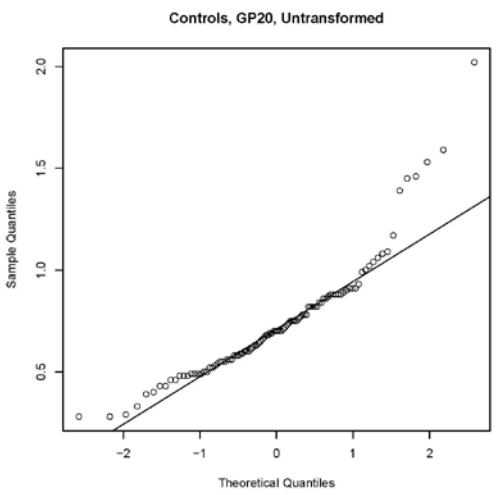
Controls, GP20, Untransformed
Sample Quantiles
Theoretical Quantiles

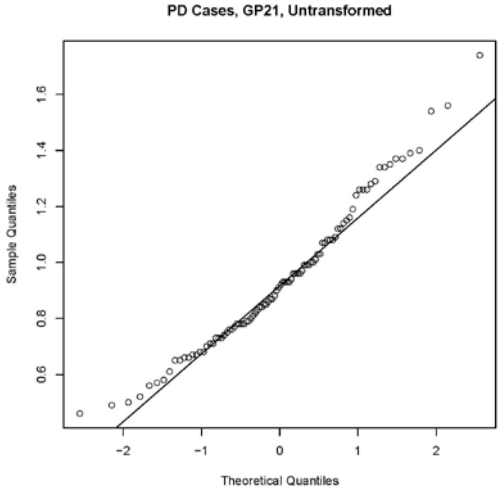
PD Cases, GP21, Untransformed
Sample Quantiles
Theoretical Quantiles

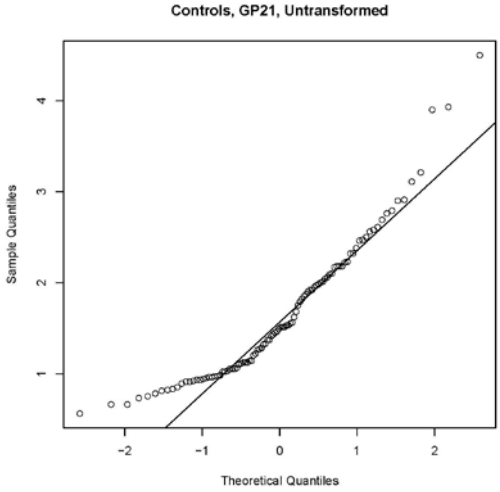
Controls, GP21, Untransformed
Sample Quantiles
Theoretical Quantiles

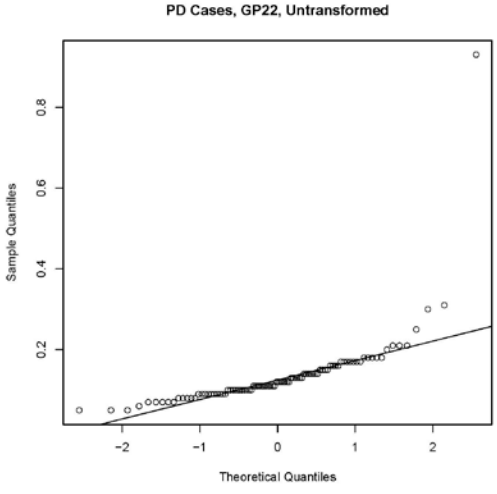
PD Cases, GP22, Untransformed
Sample Quantiles
Theoretical Quantiles

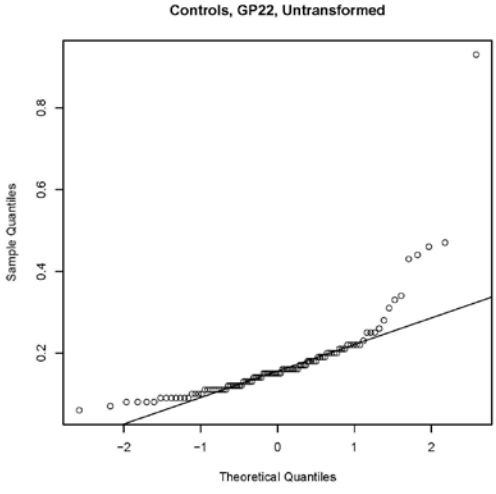
Controls, GP22, Untransformed
Sample Quantiles
Theoretical Quantiles

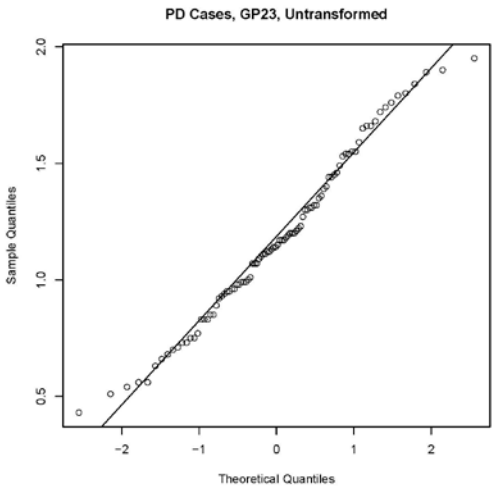
PD Cases, GP23, Untransformed
Sample Quantiles
Theoretical Quantiles

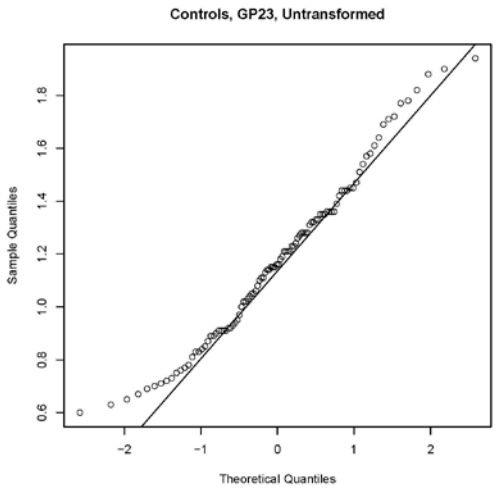
Controls, GP23, Untransformed
Sample Quantiles
Theoretical Quantiles

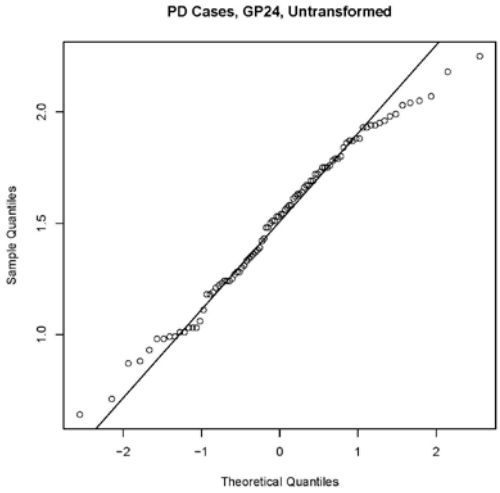
PD Cases, GP24, Untransformed
Sample Quantiles
Theoretical Quantiles

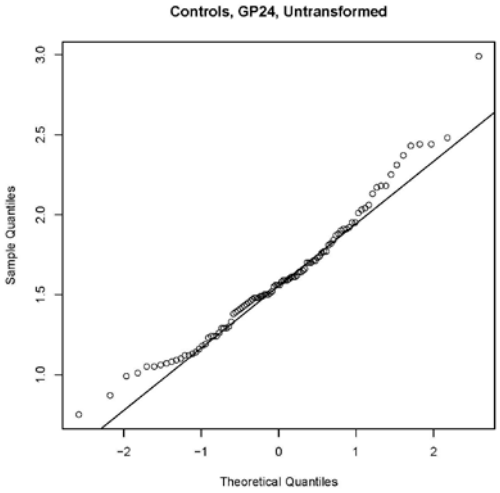
Controls, GP24, Untransformed
Sample Quantiles
Theoretical Quantiles

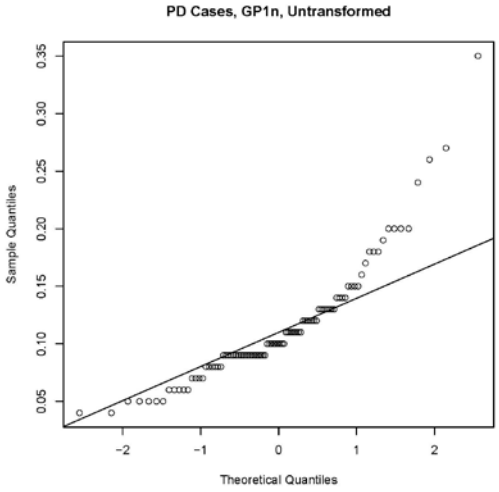
PD Cases, GP1n, Untransformed
Sample Quantiles
Theoretical Quantiles

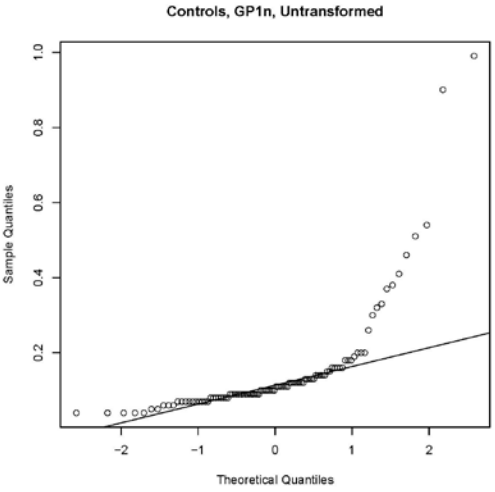
Controls, GP1n, Untransformed
Sample Quantiles
Theoretical Quantiles

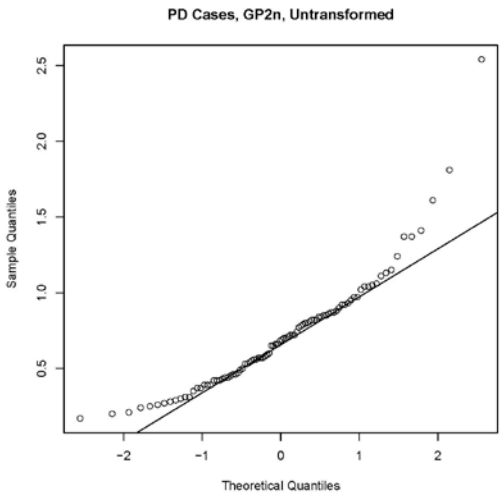
PD Cases, GP2n, Untransformed
Sample Quantiles
Theoretical Quantiles

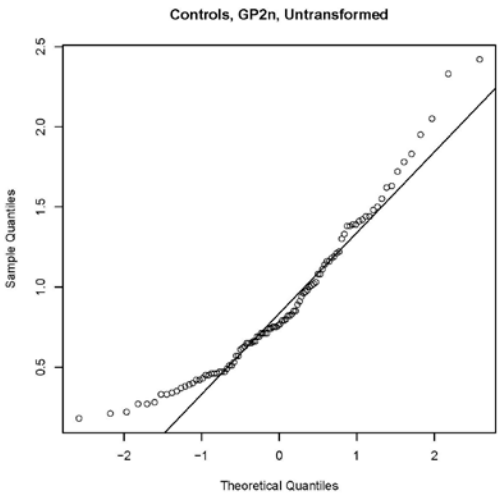
Controls, GP2n, Untransformed
Sample Quantiles
Theoretical Quantiles

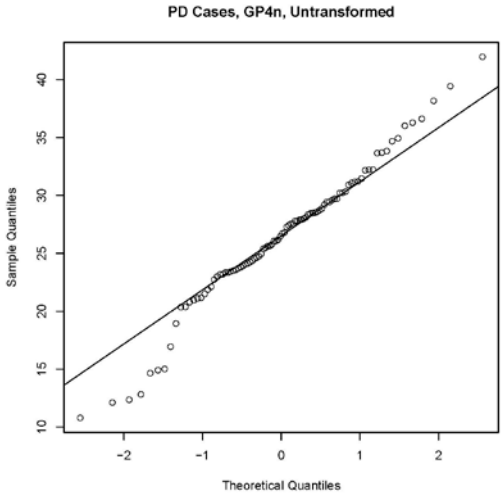
PD Cases, GP4n, Untransformed
Sample Quantiles
Theoretical Quantiles

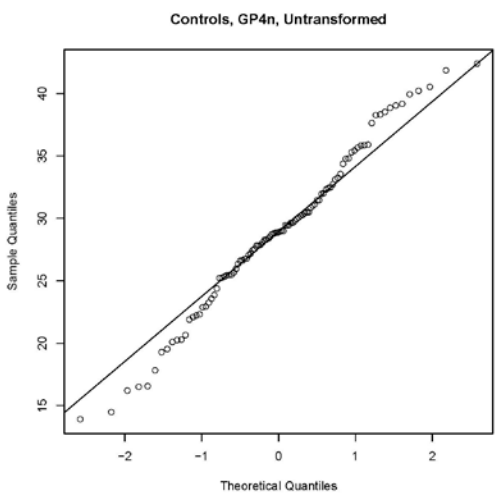
Controls, GP4n, Untransformed
Sample Quantiles
Theoretical Quantiles

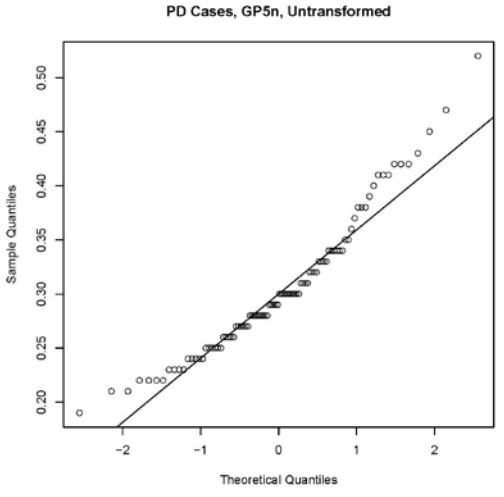
PD Cases, GP5n, Untransformed
Sample Quantiles
Theoretical Quantiles

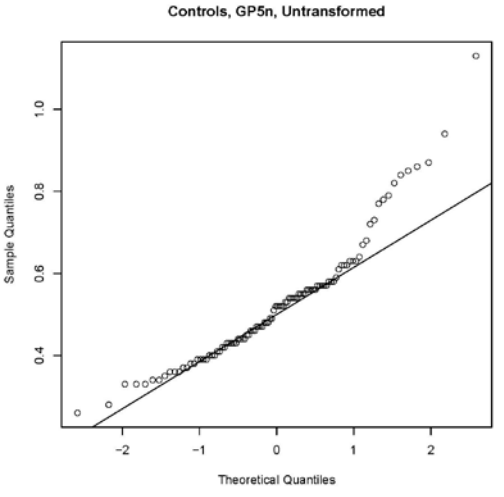
Controls, GP5n, Untransformed
Sample Quantiles
Theoretical Quantiles

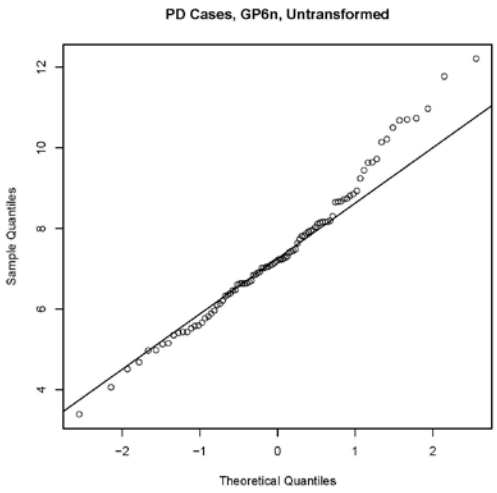
PD Cases, GP6n, Untransformed
Sample Quantiles
Theoretical Quantiles

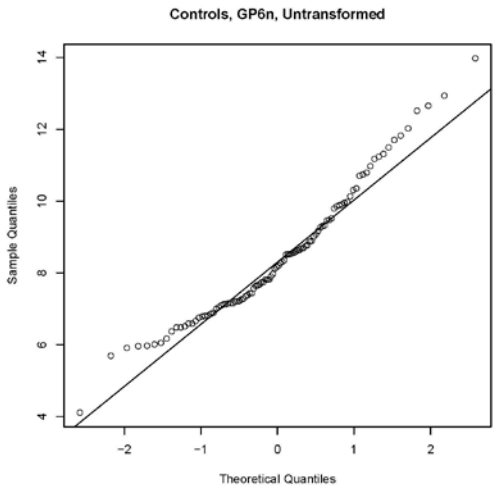
Controls, GP6n, Untransformed
Sample Quantiles
Theoretical Quantiles

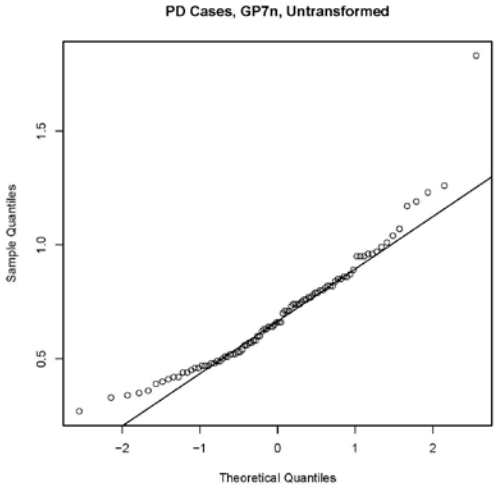
PD Cases, GP7n, Untransformed
Sample Quantiles
Theoretical Quantiles

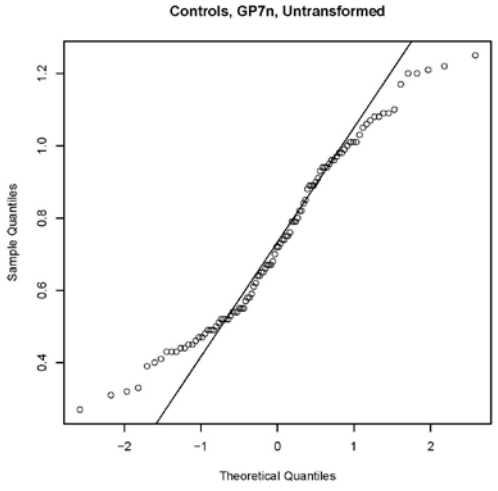
Controls, GP7n, Untransformed
Sample Quantiles
Theoretical Quantiles

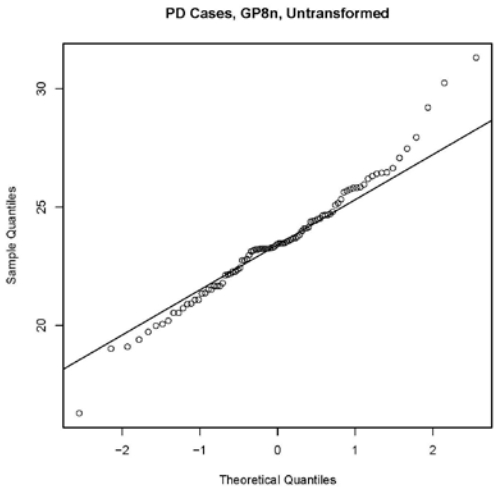
PD Cases, GP8n, Untransformed
Sample Quantiles
Theoretical Quantiles

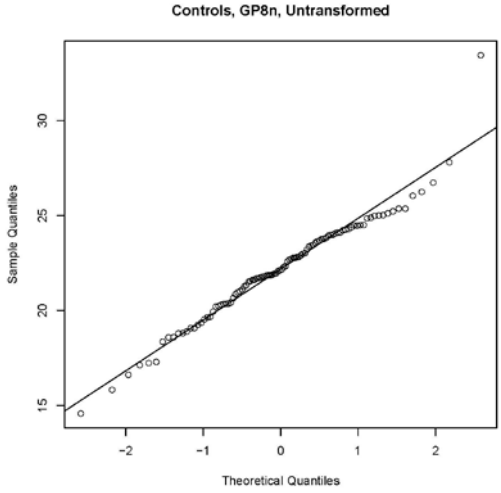
Controls, GP8n, Untransformed
Sample Quantiles
Theoretical Quantiles

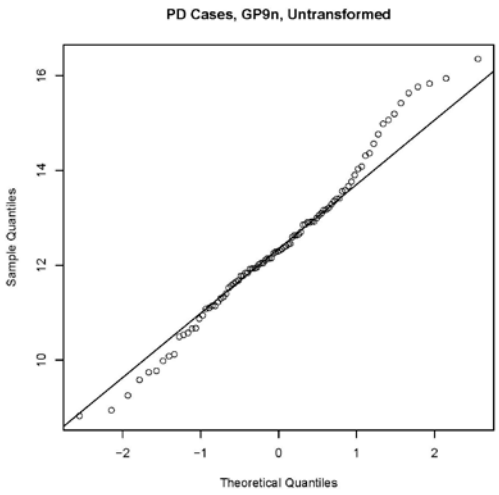
PD Cases, GP9n, Untransformed
Sample Quantiles
Theoretical Quantiles

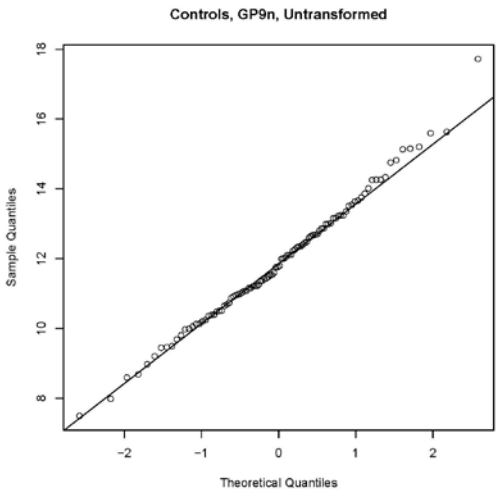
Controls, GP9n, Untransformed
Sample Quantiles
Theoretical Quantiles

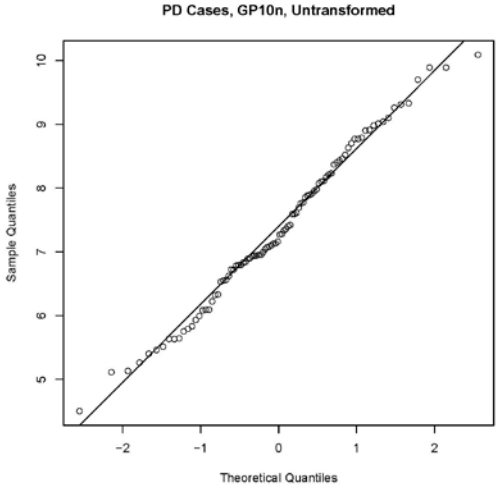
PD Cases, GP10n, Untransformed
Sample Quantiles
Theoretical Quantiles

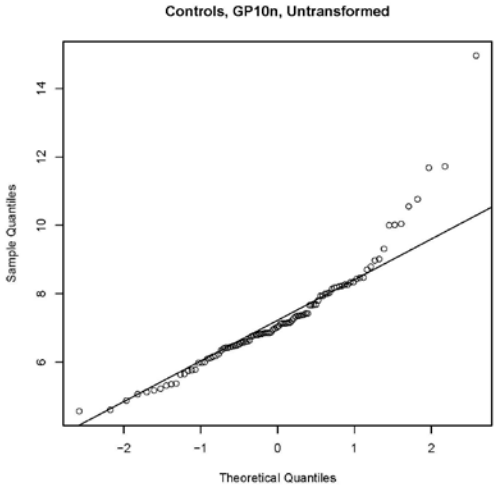
Controls, GP10n, Untransformed
Sample Quantiles
Theoretical Quantiles

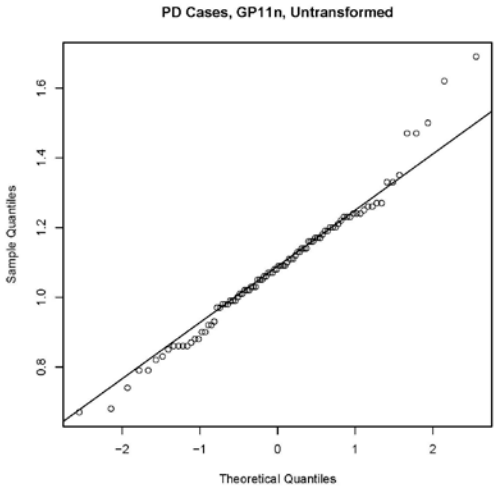
PD Cases, GP11n, Untransformed
Sample Quantiles
Theoretical Quantiles

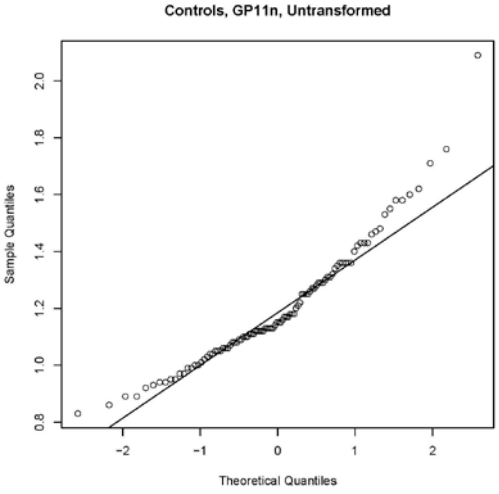
Controls, GP11n, Untransformed
Sample Quantiles
Theoretical Quantiles

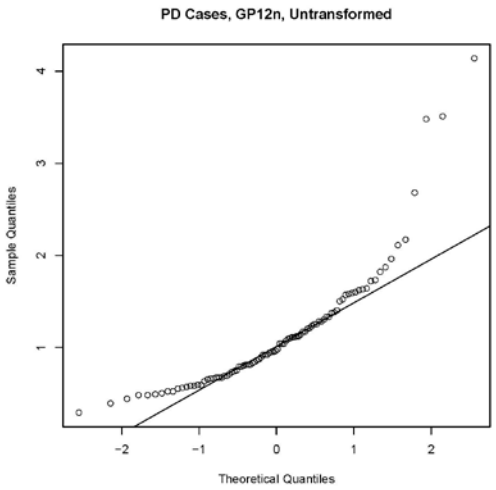
PD Cases, GP12n, Untransformed
Sample Quantiles
Theoretical Quantiles

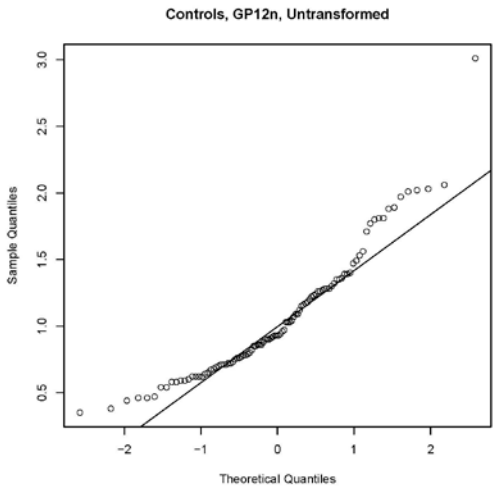
Controls, GP12n, Untransformed
Sample Quantiles
Theoretical Quantiles

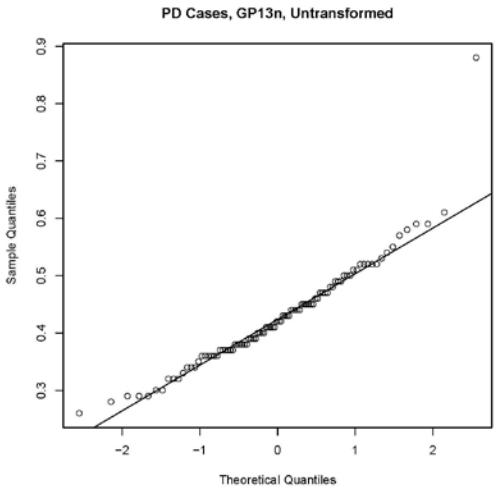
PD Cases, GP13n, Untransformed
Sample Quantiles
Theoretical Quantiles

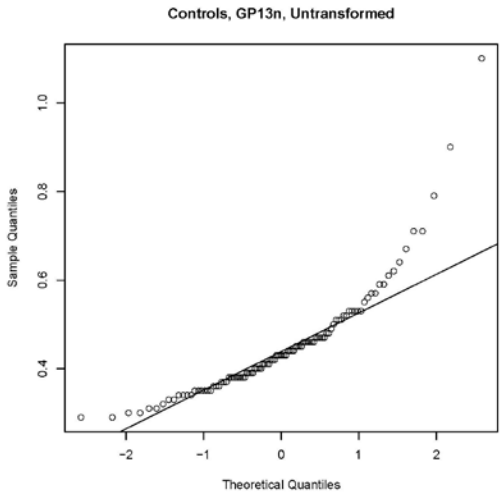
Controls, GP13n, Untransformed
Sample Quantiles
Theoretical Quantiles

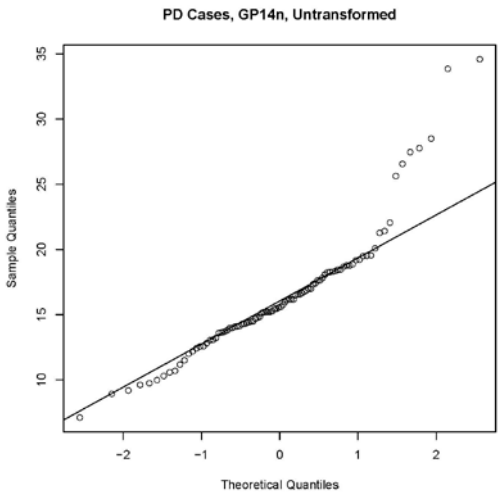
PD Cases, GP14n, Untransformed
Sample Quantiles
Theoretical Quantiles

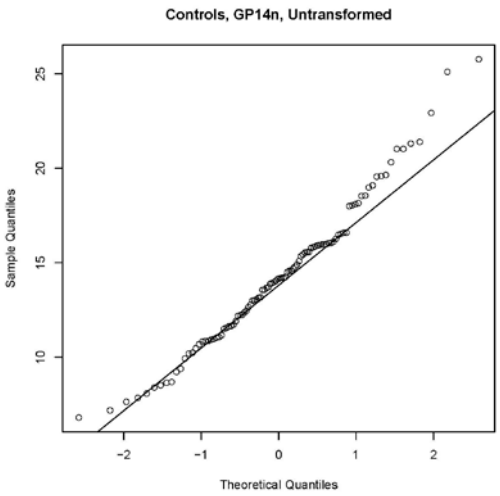
Controls, GP14n, Untransformed
Sample Quantiles
Theoretical Quantiles

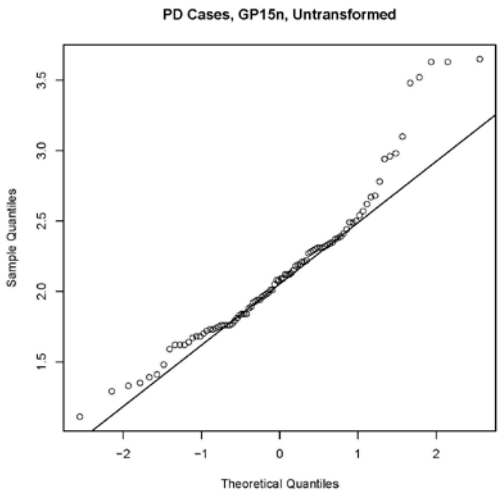
PD Cases, GP15n, Untransformed
Sample Quantiles
Theoretical Quantiles

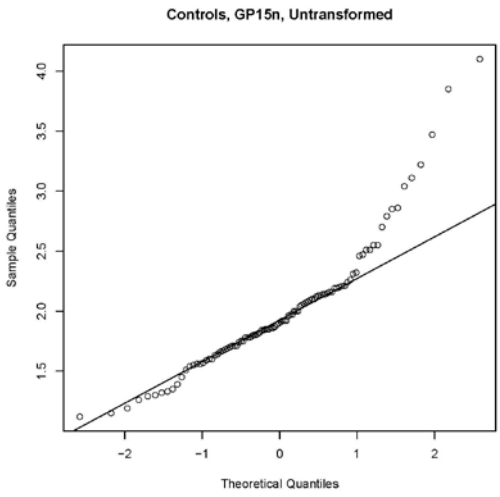
Controls, GP15n, Untransformed
Sample Quantiles
Theoretical Quantiles

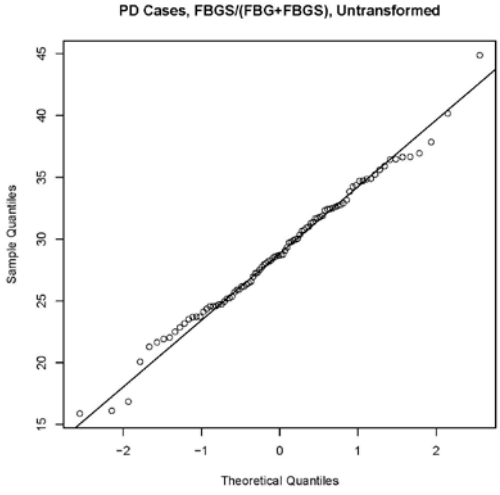
PD Cases, FBGS/(FBG+FBGS), Untransformed
Sample Quantiles
Theoretical Quantiles

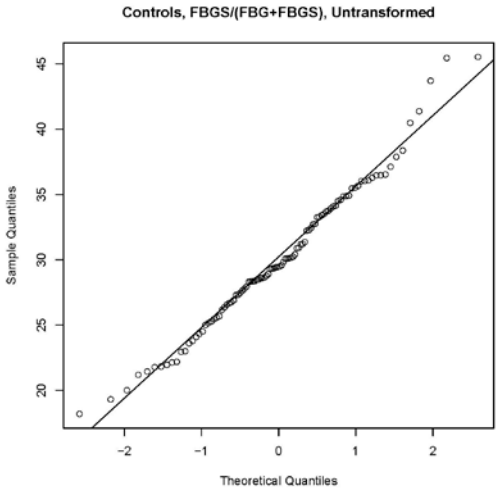
Controls, FBGS/(FBG+FBGS), Untransformed
Sample Quantiles
Theoretical Quantiles

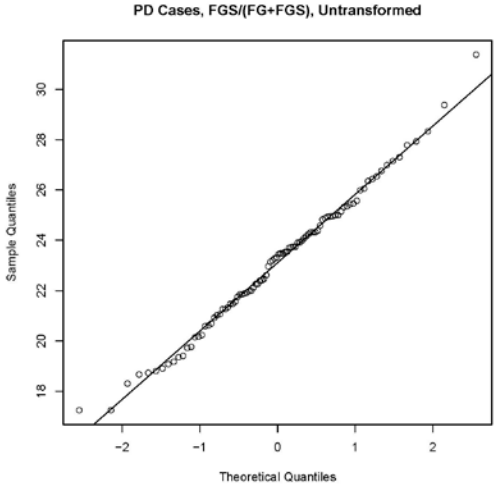
PD Cases, FGS/(FG+FGS), Untransformed
Sample Quantiles
Theoretical Quantiles

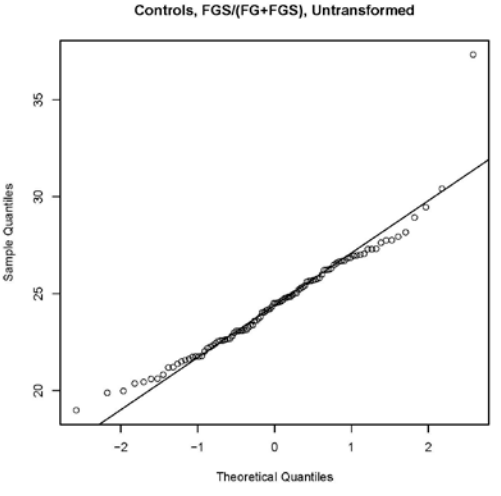
Controls, FGS/(FG+FGS), Untransformed
Sample Quantiles
Theoretical Quantiles

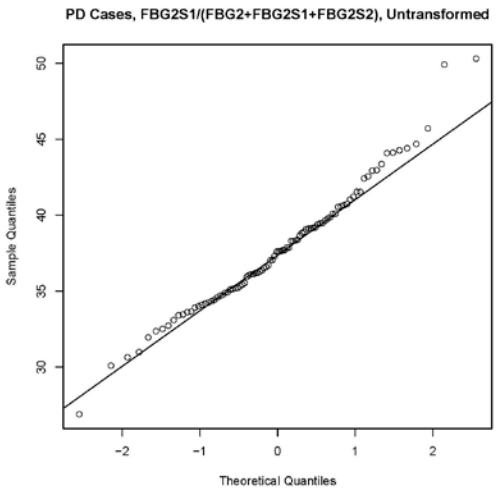
PD Cases, FBG2S1/(FBG2+FBG2S1+FBG2S2), Untransformed
Sample Quantiles
Theoretical Quantiles

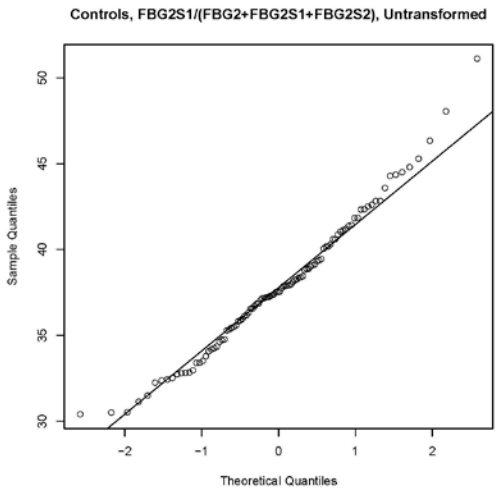
Controls, FBG2S1/(FBG2+FBG2S1+FBG2S2), Untransformed
Sample Quantiles
Theoretical Quantiles

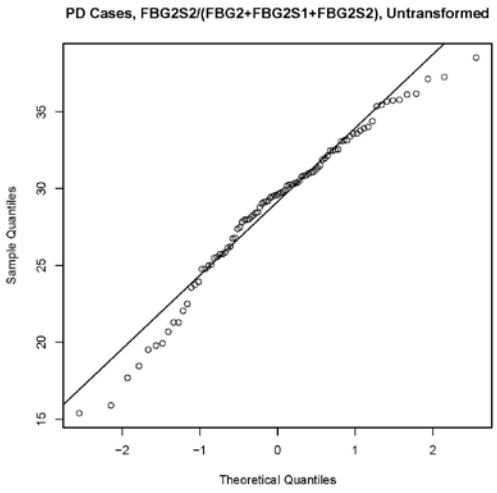
PD Cases, FBG2S2/(FBG2+FBG2S1+FBG2S2), Untransformed
Sample Quantiles
Theoretical Quantiles

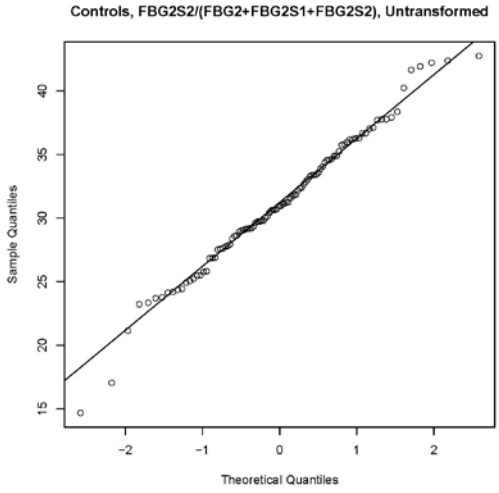
Controls, FBG2S2/(FBG2+FBG2S1+FBG2S2), Untransformed
Sample Quantiles
Theoretical Quantiles

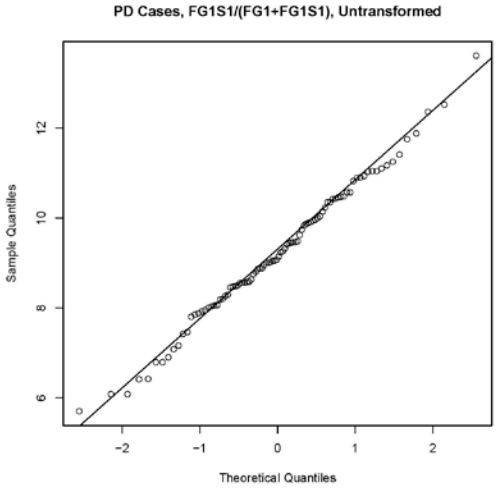
PD Cases, FG1S1/(FG1+FG1S1), Untransformed
Sample Quantiles
Theoretical Quantiles

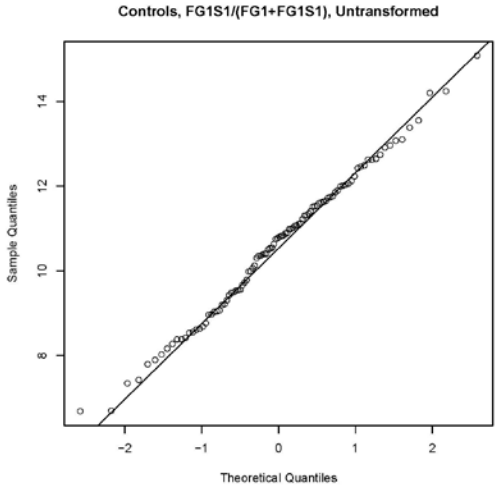
Controls, FG1S1/(FG1+FG1S1), Untransformed
Sample Quantiles
Theoretical Quantiles

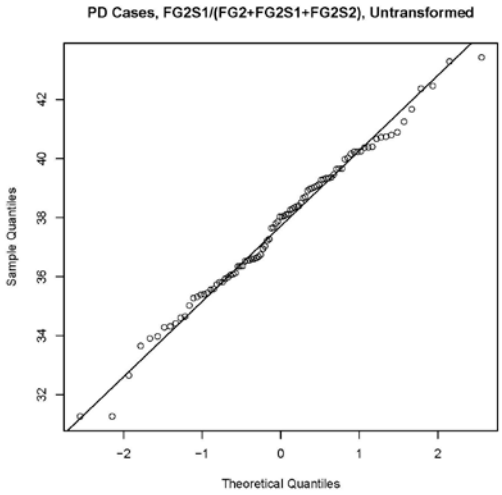
PD Cases, FG2S1/(FG2+FG2S1+FG2S2), Untransformed
Sample Quantiles
Theoretical Quantiles

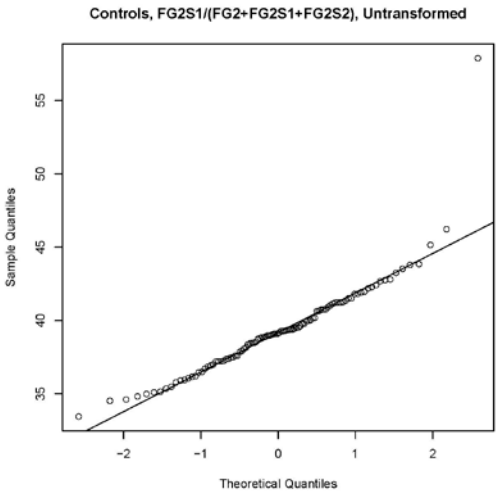
Controls, FG2S1/(FG2+FG2S1+FG2S2), Untransformed
Sample Quantiles
Theoretical Quantiles

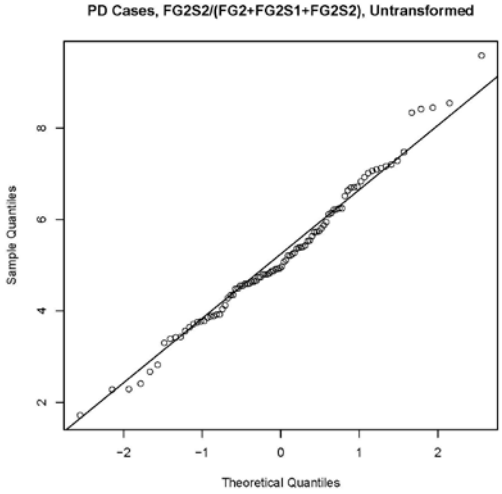
PD Cases, FG2S2/(FG2+FG2S1+FG2S2), Untransformed
Sample Quantiles
Theoretical Quantiles

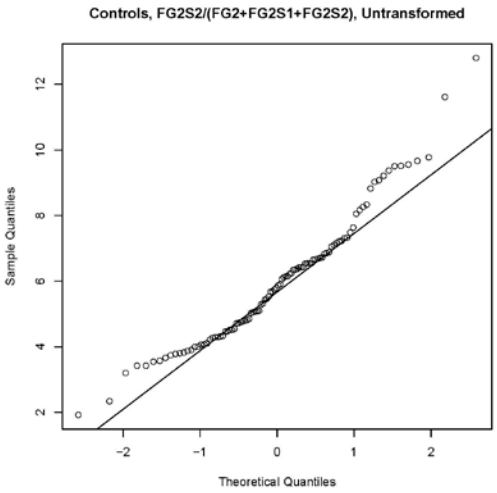
Controls, FG2S2/(FG2+FG2S1+FG2S2), Untransformed
Sample Quantiles
Theoretical Quantiles

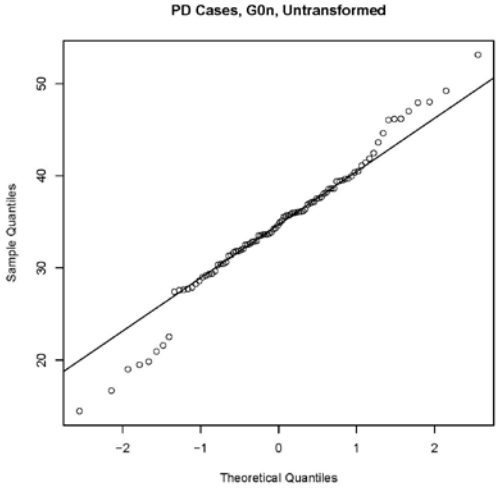
PD Cases, G0n, Untransformed
Sample Quantiles
Theoretical Quantiles

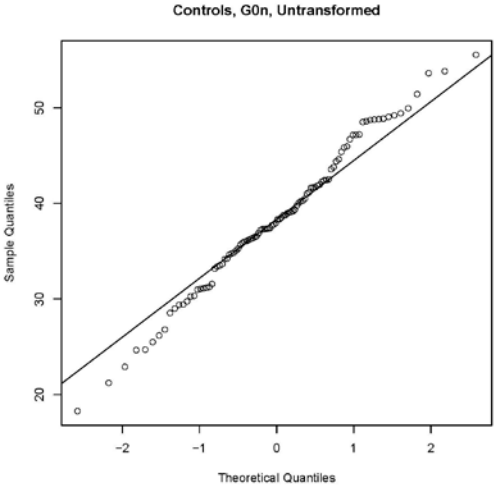
Controls, G0n, Untransformed
Sample Quantiles
Theoretical Quantiles

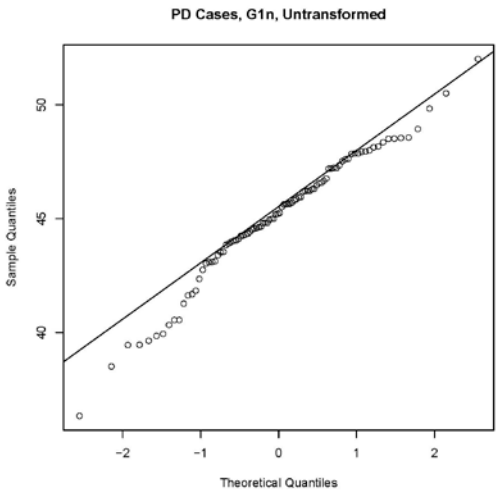
PD Cases, G1n, Untransformed
Sample Quantiles
Theoretical Quantiles


Controls, G1n, Untransformed
Sample Quantiles
Theoretical Quantiles

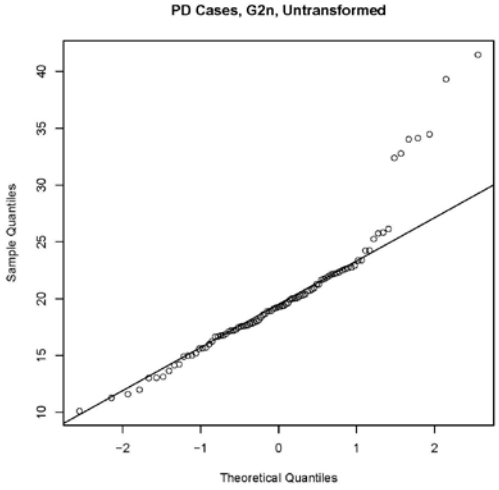
PD Cases, G2n, Untransformed
Sample Quantiles
Theoretical Quantiles

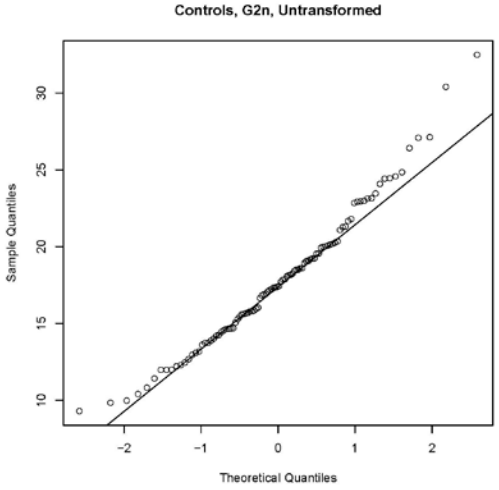
Controls, G2n, Untransformed
Sample Quantiles
Theoretical Quantiles

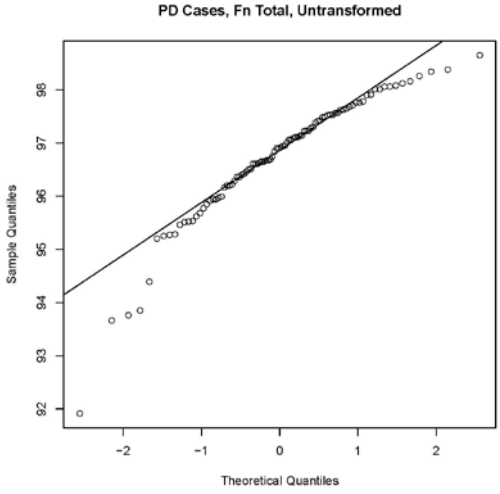
PD Cases, Fn Total, Untransformed
Sample Quantiles
Theoretical Quantiles

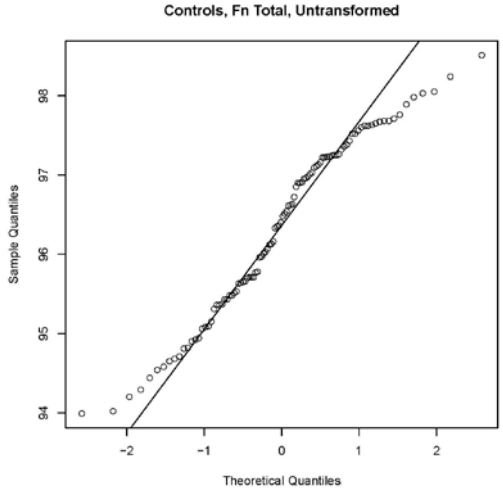
Controls, Fn Total, Untransformed
Sample Quantiles
Theoretical Quantiles

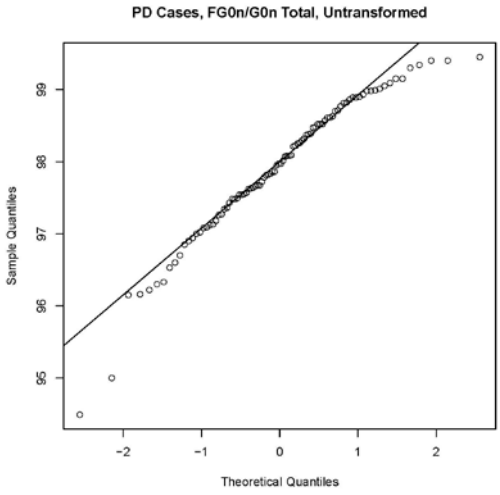
PD Cases, FG0n/G0n Total, Untransformed
Sample Quantiles
Theoretical Quantiles

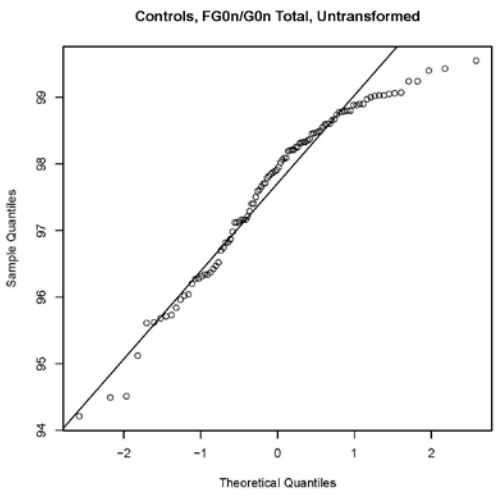
Controls, FG0n/G0n Total, Untransformed
Sample Quantiles
Theoretical Quantiles

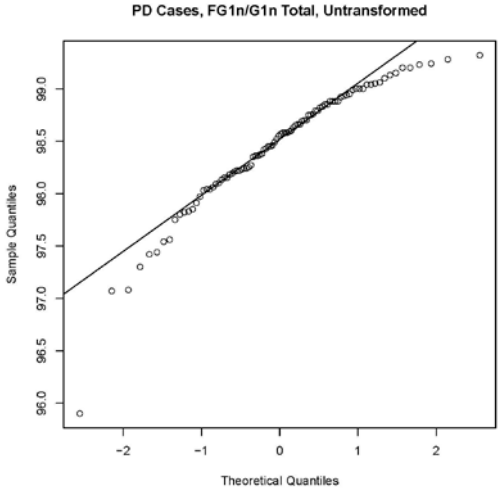
PD Cases, FG1n/G1n Total, Untransformed
Sample Quantiles
Theoretical Quantiles

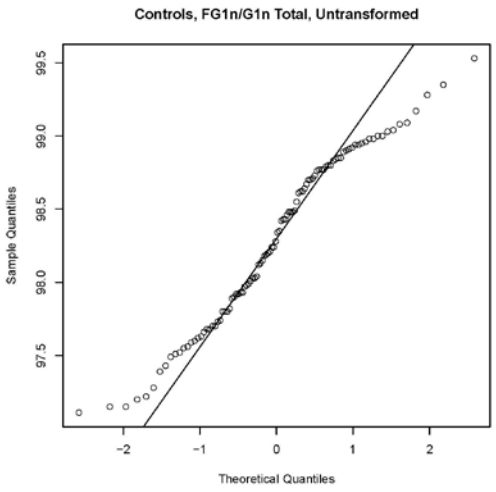
Controls, FG1n/G1n Total, Untransformed
Sample Quantiles
Theoretical Quantiles

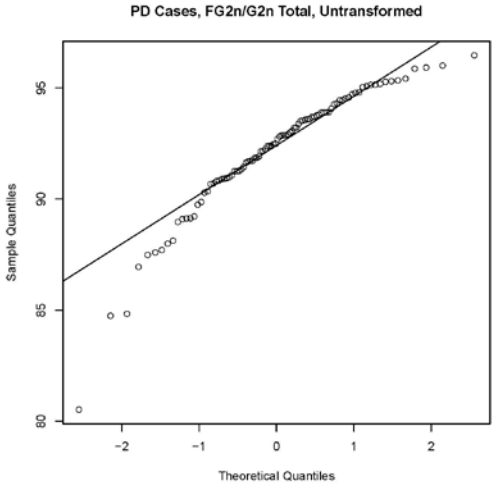
PD Cases, FG2n/G2n Total, Untransformed
Sample Quantiles
Theoretical Quantiles

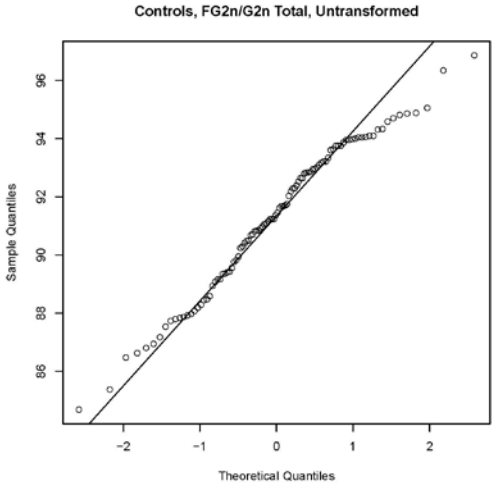
Controls, FG2n/G2n Total, Untransformed
Sample Quantiles
Theoretical Quantiles

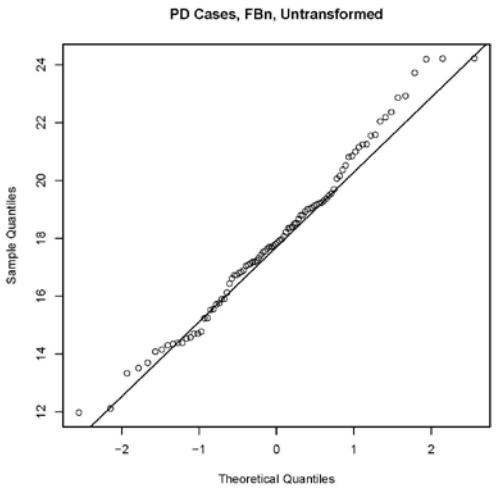
PD Cases, FBn, Untransformed
Sample Quantiles
Theoretical Quantiles

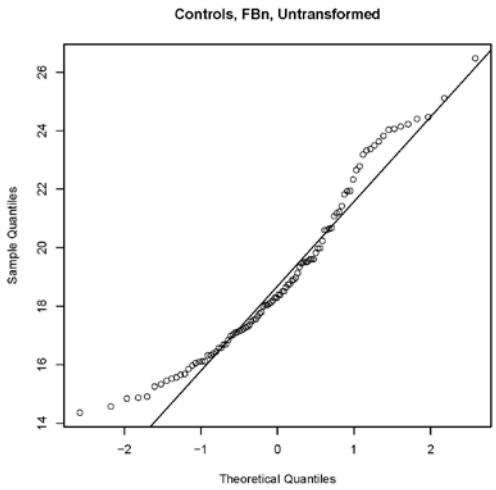
Controls, FBn, Untransformed
Sample Quantiles
Theoretical Quantiles

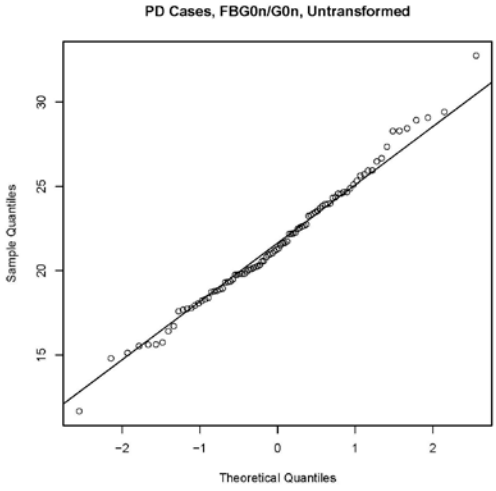
PD Cases, FBG0n/G0n, Untransformed
Sample Quantiles
Theoretical Quantiles

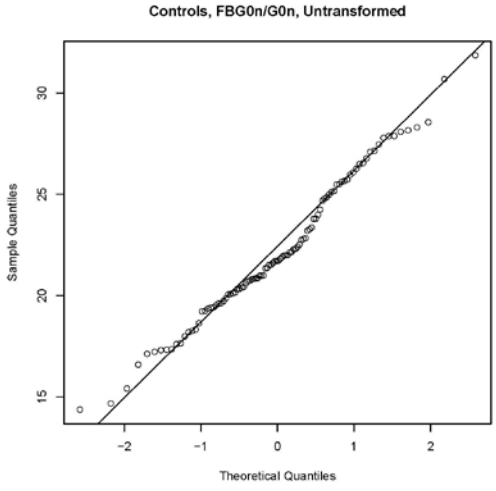
Controls, FBG0n/G0n, Untransformed
Sample Quantiles
Theoretical Quantiles

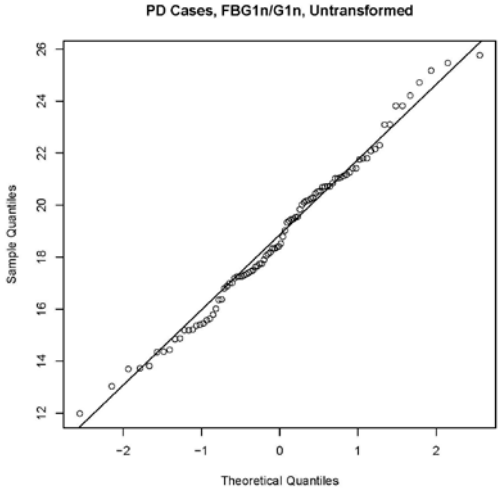
PD Cases, FBG1n/G1n, Untransformed
Sample Quantiles
Theoretical Quantiles

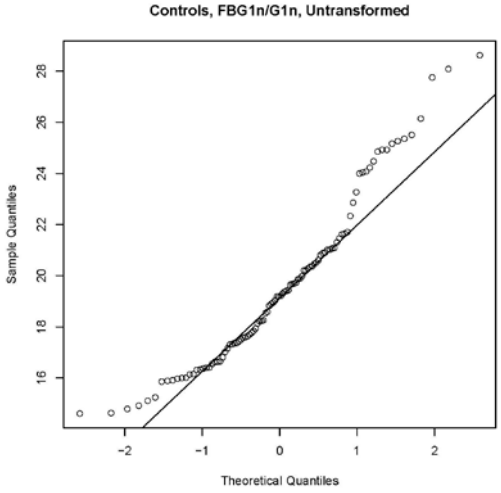
Controls, FBG1n/G1n, Untransformed
Sample Quantiles
Theoretical Quantiles

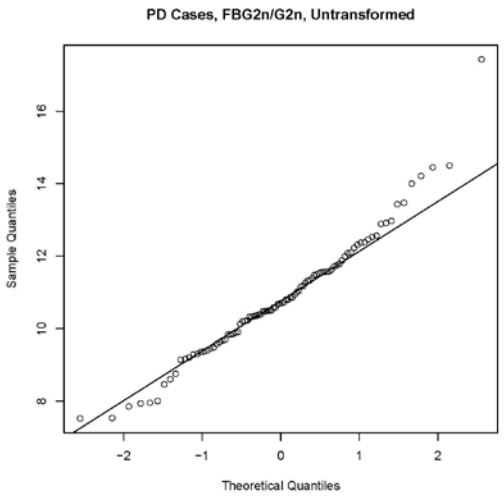
PD Cases, FBG2n/G2n, Untransformed
Sample Quantiles
Theoretical Quantiles

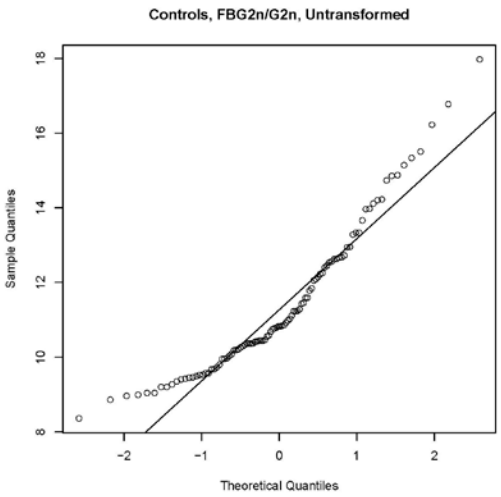
Controls, FBG2n/G2n, Untransformed
Sample Quantiles
Theoretical Quantiles

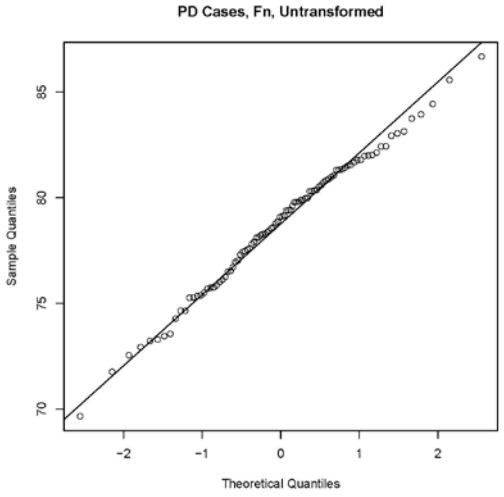
PD Cases, Fn, Untransformed
Sample Quantiles
Theoretical Quantiles

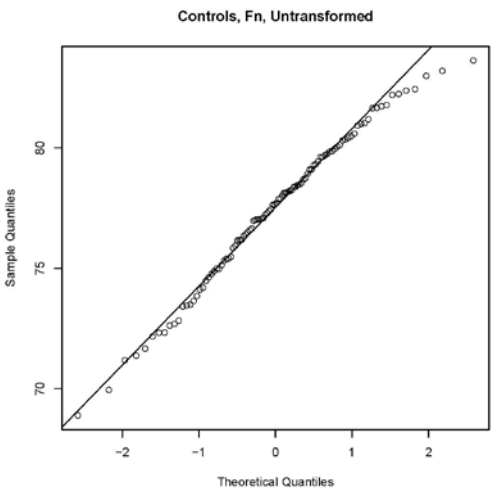
Controls, Fn, Untransformed
Sample Quantiles
Theoretical Quantiles

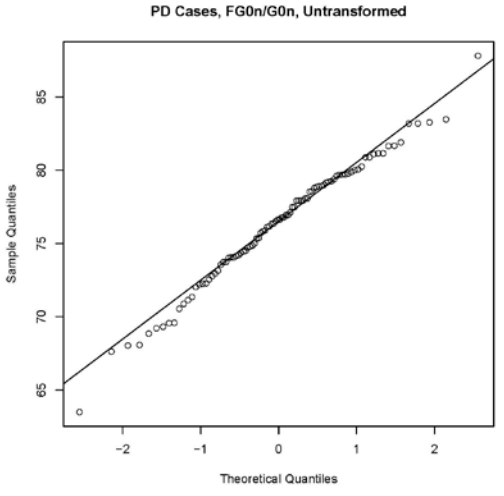
PD Cases, FG0n/G0n, Untransformed
Sample Quantiles
Theoretical Quantiles

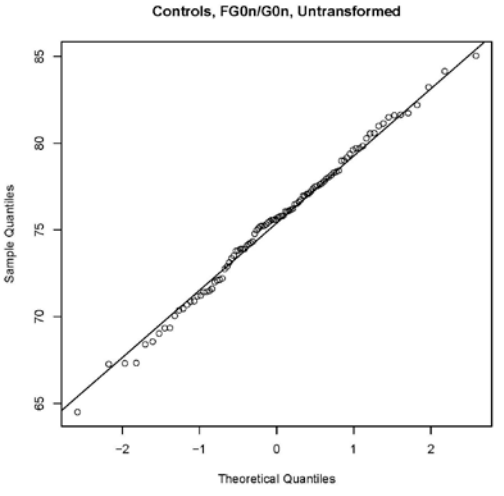
Controls, FG0n/G0n, Untransformed
Sample Quantiles
Theoretical Quantiles

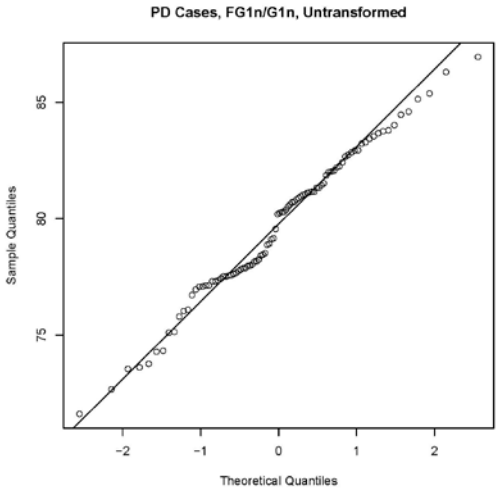
PD Cases, FG1n/G1n, Untransformed
Sample Quantiles
Theoretical Quantiles

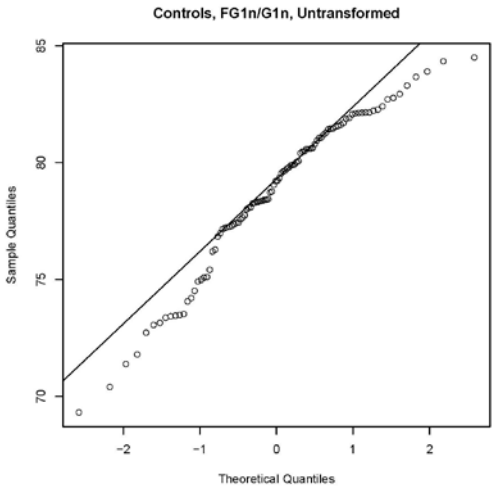
Controls, FG1n/G1n, Untransformed
Sample Quantiles
Theoretical Quantiles

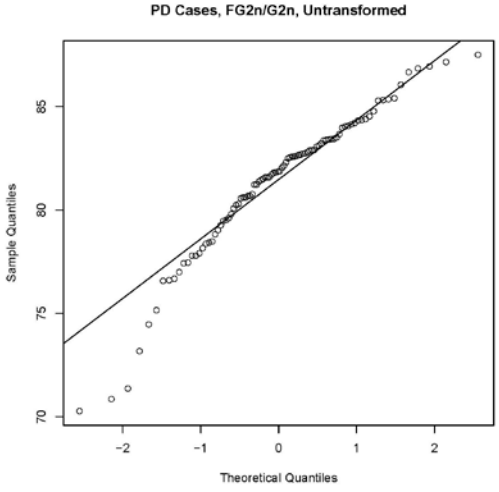
PD Cases, FG2n/G2n, Untransformed
Sample Quantiles
Theoretical Quantiles

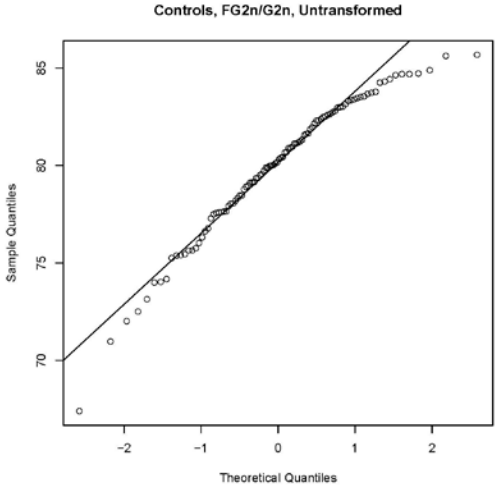
Controls, FG2n/G2n, Untransformed
Sample Quantiles
Theoretical Quantiles

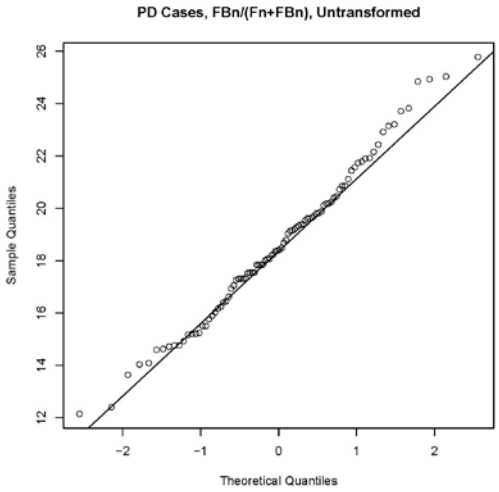
PD Cases, FBn/(Fn+FBn), Untransformed
Sample Quantiles
Theoretical Quantiles

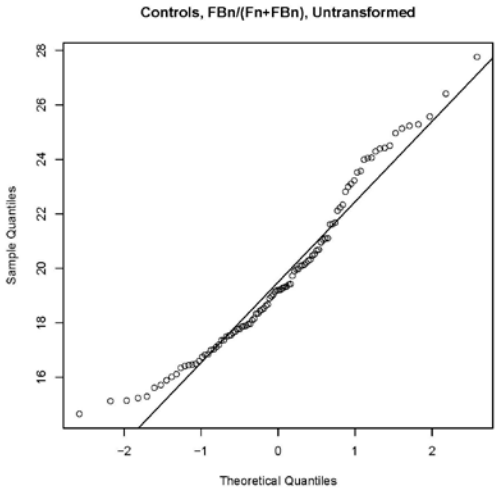
Controls, FBn/(Fn+FBn), Untransformed
Sample Quantiles
Theoretical Quantiles

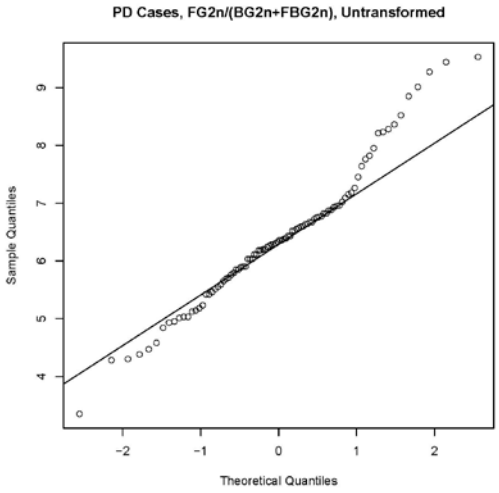
PD Cases, FG2n/(BG2n+FBG2n), Untransformed
Sample Quantiles
Theoretical Quantiles

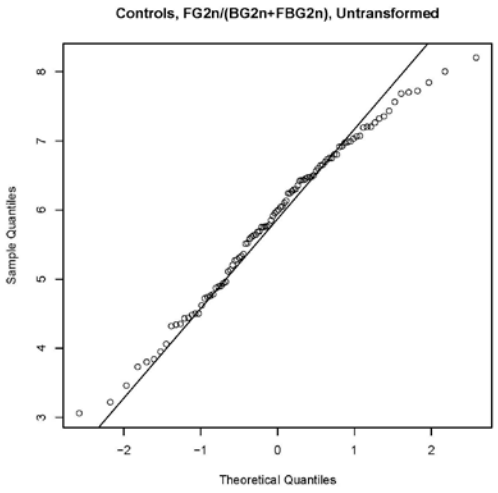
Controls, FG2n/(BG2n+FBG2n), Untransformed
Sample Quantiles
Theoretical Quantiles

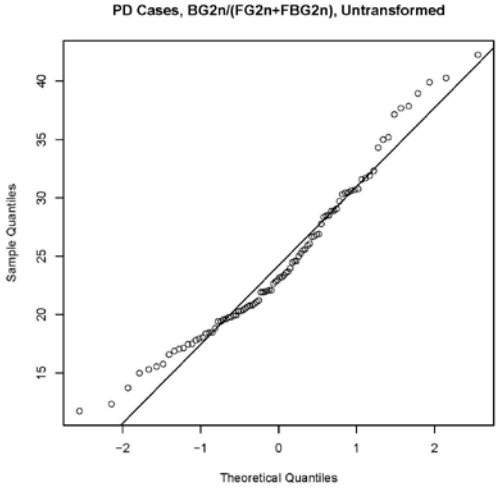
PD Cases, BG2n/(FG2n+FBG2n), Untransformed
Sample Quantiles
Theoretical Quantiles

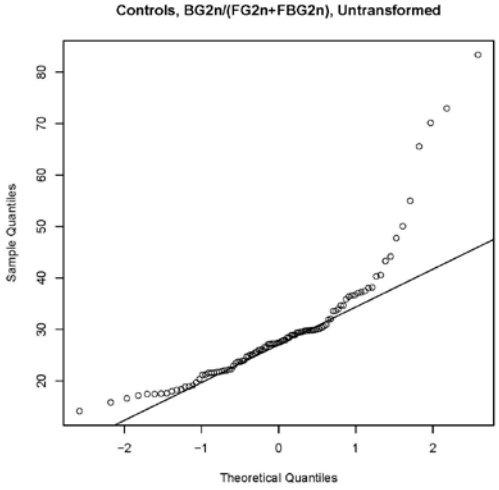
Controls, BG2n/(FG2n+FBG2n), Untransformed
Sample Quantiles
Theoretical Quantiles

Appendix 6 – Data Transformation Tables

Normality of **Study 1** data was determined using Q-Q plots. Details of transformations used are tabulated below. Transformed data was only used for the purpose of employing Student's t-test. Samples were independent of each other.

Variable	Nature	Transformation	Notes	Variable	Nature	Transformation	Notes
Case				***Control***			
GP1	pos skew		doesn't normalise	GP1	pos skew		doesn't normalise
GP2	pos skew	ln(1+x)		GP2	pos skew	ln(1+x)	
GP4	normal			GP4	normal		
GP5	pos skew	ln(1+x)		GP5	pos skew	ln(1+x)	possible outlier
GP6	pos skew	ln		GP6	pos skew	ln	
GP7	pos skew	ln(1+x)	possible outlier	GP7	slight pos skew	ln(1+x)	match transformation
GP8	pos skew	ln		GP8	slight pos skew	ln	match transformation
GP9	normal			GP9	normal		
GP10	normal	ln	match transformation	GP10	pos skew	ln	
GP11	pos skew	ln(1+x)		GP11	pos skew	ln(1+x)	
GP12	pos skew	ln(1+x)	possible outlier	GP12	pos skew	ln(1+x)	possible outlier
GP13	pos skew	ln(1+x)	possible outlier	GP13	pos skew	ln(1+x)	
GP14	pos skew	ln		GP14	pos skew	ln	
GP15	pos skew	ln(1+x)		GP15	pos skew	ln(1+x)	
GP16	pos skew	ln		GP16	normal	ln	match transformation
GP17	pos skew	ln(1+x)		GP17	pos skew	ln(1+x)	possible outlier
GP18	pos skew	ln		GP18	pos skew	ln	
GP19	pos skew	ln		GP19	pos skew	ln	
GP20	pos skew	ln(1+x)	possible outlier	GP20	pos skew	ln(1+x)	possible outlier
GP21	pos skew	ln(1+x)		GP21	pos skew	ln(1+x)	
GP22	pos skew		possible outlier	GP22	pos skew		doesn't normalise
GP23	normal			GP23	normal		
GP24	normal			GP24	normal		possible outlier

Variable	Nature	Transformation	Notes	Variable	Nature	Transformation	Notes
$GP1^n$	pos skew		doesn't normalise	$GP1^n$	pos skew		doesn't normalise
$GP2^n$	pos skew	ln(1+x)		$GP2^n$	pos skew	ln(1+x)	
$GP4^n$	normal			$GP4^n$	normal		
$GP5^n$	pos skew	ln(1+x)		$GP5^n$	pos skew	ln(1+x)	possible outlier
$GP6^n$	normal	ln	match transformation	$GP6^n$	pos skew	ln	
$GP7^n$	pos skew	ln(1+x)	possible outlier	$GP7^n$	pos skew	ln(1+x)	
$GP8^n$	normal			$GP8^n$	normal		possible outlier
$GP9^n$	normal			$GP9^n$	normal		
$GP10^n$	normal	ln	match transformation	$GP10^n$	pos skew	ln	
$GP11^n$	pos skew	ln(1+x)		$GP11^n$	pos skew	ln(1+x)	possible outlier
$GP12^n$	pos skew	ln(1+x)	possible outlier	$GP12^n$	pos skew	ln(1+x)	
$GP13^n$	pos skew		possible outlier	$GP13^n$	pos skew		doesn't normalise
$GP14^n$	pos skew	ln		$GP14^n$	pos skew	ln	
$GP15^n$	pos skew	ln		$GP15^n$	pos skew	ln	

Variable	Nature	Transformation	Notes	Variable	Nature	Transformation	Notes
			Percentage of Sialylation of Fucosylated Structures with Bisecting GlcNAc				
FBGS/(FBG+FBGS)	normal			FBGS/(FBG+FBGS)	normal		
			Percentage of Sialylation of Fucosylated Structures without Bisecting GlcNAc				
FGS/(FG+FGS)	normal	ln	match transformation	FGS/(FG+FGS)	pos skew	ln	possible outlier
			Percentage of Sialylation of Fucosylated Galactosylated Glycans with Bisecting GlcNAc				
FBG2S1/(FBG2 +FBG2S1+FBG2S2)	normal	ln	match transformation	FBG2S1/(FBG2 +FBG2S1+FBG2S2)	pos skew	ln	
FBG2S2/(FBG2 +FBG2S1+FBG2S2)	normal			FBG2S2/(FBG2 +FBG2S1+FBG2S2)	normal		
			Percentage of Sialylation of Fucosylated Galactosylated Glycans without Bisecting GlcNAc				
FG1S1/(FG1+FG1S1)	normal			FG1S1/(FG1+FG1S1 +FG2S2+FG2S2)	normal		
FG2S1/(FG2 +FG2S1+FG2S2)	normal	ln	match transformation	FG2S1/(FG1+FG1S1 +FG2S2+FG2S2)	pos skew	ln	possible outlier
FG2S2/(FG2 +FG2S1+FG2S2)	normal	ln	match transformation	FG2S2/(FG1+FG1S1 +FG2S2+FG2S2)	pos skew	ln	

Variable	Nature	Transformation	Notes	Variable	Nature	Transformation	Notes
			Percentage of Galactosylation				
G0n	normal			G0n	normal		
G1n	normal			G1n	normal		possible outlier
G2n	pos skew	ln		G2n	pos skew	ln	
			Percentage of Fucosylation (+/- Bisecting GlcNAc)				
$F^{n\ total}$	neg skew	ln(100-x)		Fn	neg skew	ln(100-x)	
$FG0^{n}/G0^{n\ total}$	neg skew	ln(101-x)		FG0n/G0n	neg skew	ln(101-x)	
$FG1^{n}/G1^{n\ total}$	neg skew	ln(101-x)		FG1n/G1n	neg skew	ln(101-x)	
$FG2^{n}/G2^{n\ total}$	neg skew	ln(98-x)		FG2n/G2n	neg skew	ln(98-x)	possible outlier
			Percentage of Fucosylation with Bisecting GlcNAc				
FB^{n}	normal	ln	match transformation	FBn	pos skew	ln	
$FBG0^{n}/G0^{n}$	normal			FBG0n/G0n	normal		
$FBG1^{n}/G1^{n}$	normal	ln	match transformation	FBG1n/G1n	pos skew	ln	
$FBG2^{n}/G2^{n}$	pos skew	ln		FBG2n/G2n	pos skew	ln	
			Percentage of Fucosylation without Bisecting GlcNAc				
F^{n}	normal			Fn	normal		
$FG0^{n}/G0^{n}$	normal			FG0n/G0n	normal		
$FG1^{n}/G1^{n}$	normal			FG1n/G1n	normal		
$FG2^{n}/G2^{n}$	neg skew	ln(90-x)		FG2n/G2n	neg skew	ln(90-x)	
			Other Traits				
$FB^{n}/(F^{n}+FB^{n})$	normal			FBn/(Fn+FBn)	normal		
$FG2^{n}/(BG2^{n}+FBG2^{n})$	normal			FG2n/(BG2n+FBG2n)	normal		
$BG2^{n}/(FG2^{n}+FBG2^{n})$	pos skew	ln		BG2n/(FG2n+FBG2n)	pos skew	ln	

Appendix 7 – Levene's Test

Levene's test [1, 194] was conducted on all normal and log-normal variables (according to the transformation tables in **Appendix 6**) to test the assumption of homogeneity of variances. For the test, $P < 0.05$ is considered to be a significant difference and thus not meet this assumption, i.e. the variable has heterogeneous variances between groups. The differences between the means of the variables with heterogeneous variances (**bolded** below) could still be performed with Welch's correction, and this is easily programed into the Student's t-test ('stats' package) R code. The degrees of freedom (df) to be used for Student's t-test for each variable are specified below.

Variable	F-statistic	*P* - value	df
GP2	3.2628	0.072	194
GP4	0.0572	0.811	194
GP5	18.5170	**2.668×10^{-5}**	**160.289**
GP6	0.2299	0.632	194
GP7	1.2590	0.263	194
GP8	1.0880	0.298	194
GP9	2.0384	0.155	194
GP10	0.4796	0.489	194
GP11	0.3763	0.540	194
GP12	1.4810	0.225	194
GP13	1.9887	0.160	194
GP14	0.6940	0.406	194
GP15	0.0877	0.768	194
GP16	0.0027	0.959	194
GP17	14.8470	**1.584×10^{-4}**	**163.601**
GP18	0.0247	0.875	194
GP19	0.6028	0.438	194
GP20	35.1200	**1.393×10^{-8}**	**134.135**
GP21	47.2640	**8.276×10^{-11}**	**149.140**
GP23	1.1053	0.294	194

Variable	F-statistic	*P* - value	df
$GP2^n$	4.2439	0.041	194
$GP4^n$	0.2462	0.620	194
$GP5^n$	25.1910	**1.171×10^{-6}**	**153.062**
$GP6^n$	0.2639	0.608	194
$GP7^n$	1.5193	0.219	194
$GP8^n$	1.2102	0.273	194
$GP9^n$	1.5239	0.219	194
$GP10^n$	0.4478	0.504	194
$GP11^n$	0.2338	0.629	194
$GP12^n$	1.4794	0.225	194
$GP14^n$	0.3655	0.546	194
$GP15^n$	0.0002	0.988	194

Variable	F-statistic	*P* - value	df
Percentage of Sialylation of Fucosylated Structures with Bisecting GlcNAc			
FBGS/(FBG+FBGS)	0.0946	0.759	194
Percentage of Sialylation of Fucosylated Structures without Bisecting GlcNAc			
FGS/(FG+FGS)	1.4582	0.229	194
Percentage of Sialylation of Fucosylated Galactosylated Glycans with Bisecting GlcNAc			
FBG2S1/(FBG2+FBG2S1+FBG2S2)	0.0482	0.826	194
FBG2S2/(FBG2+FBG2S1+FBG2S2)	0.4907	0.484	194
Percentage of Sialylation of Fucosylated Galactosylated Glycans without Bisecting GlcNAc			
FG1S1/(FG1+FG1S1)	1.5984	0.208	194
FG2S1/(FG2+FG2S1+FG2S2)	0.0001	0.991	194
FG2S2/(FG2+FG2S1+FG2S2)	1.3216	0.252	194
Percentage of Galactosylation			
$G0^n$	0.5758	0.449	194
$G1^n$	3.9443	**0.048**	**189.123**
$G2^n$	0.3070	0.580	194
Percentage of Fucosylation (+/- Bisecting GlcNAc)			
$F^{n\ total}$	0.1689	0.682	194
$FG0^n/G0^{n\ total}$	3.7264	0.055	194
$FG1^n/G1^{n\ total}$	1.7655	0.186	194
$FG2^n/G2^{n\ total}$	0.3311	0.566	194
Percentage of Fucosylation with Bisecting GlcNAc			
FB^n	0.0789	0.779	194
$FBG0^n/G0^n$	0.2858	0.594	194
$FBG1^n/G1^n$	0.1087	0.742	194
$FBG2^n/G2^n$	0.8610	0.355	194
Percentage of Fucosylation without Bisecting GlcNAc			
F^n	0.0184	0.892	194
$FG0^n/G0^n$	0.2203	0.639	194
$FG1^n/G1^n$	0.0019	0.965	194
$FG2^n/G2^n$	0.5445	0.462	194
Other Traits			
$FB^n/(F^n+FB^n)$	0.0489	0.825	194
$FG2^n/(BG2^n+FBG2^n)$	0.4573	0.500	194
$BG2^n/(FG2^n+FBG2^n)$	0.5301	0.467	194

Page intentionally left blank

Appendix 8 – Correlation Matrices

Spearman's correlation coefficients (r_s) comparing the GPs of the total IgG glycome to each other, age and BMI. Comparisons were made if at least one group produced a coefficient showing a moderate relationship ($r_s > |0.5|$). Comparisons where at least one coefficient showed a strong relationship ($r_s > |0.7|$) are boxed. Statistically significant differences between the groups are highlighted for $P < 0.05$ (red), $P < 0.01$ (yellow) and $P < 0.001$ (green).

Cases

	Age	BMI	GP1	GP2	GP4	GP5	GP6	GP7	GP8	GP9	GP10	GP11	GP12	GP13	GP14	GP15	GP16	GP17	GP18	GP19	GP20	GP21	GP22	GP23
Age																								
BMI	-0.02																							
GP1	0.32	0.09																						
GP2	0.13	0.12	0.31																					
GP4	0.37	0.27	0.62	0.24																				
GP5	0.41	0.13	0.61	0.30	0.56																			
GP6	0.36	0.12	0.52	0.44	0.53	0.52																		
GP7	0.00	-0.01	0.19	0.85	-0.07	0.22	0.24																	
GP8	-0.10	0.06	-0.28	0.02	-0.19	-0.19	-0.42	0.00																
GP9	-0.04	0.07	-0.20	-0.32	-0.05	-0.01	-0.18	-0.37	-0.07															
GP10	0.21	-0.02	0.01	0.12	-0.23	0.09	0.53	0.18	-0.06	-0.27														
GP11	0.34	0.03	0.17	0.08	0.16	0.41	0.66	-0.03	-0.40	0.25	0.59													
GP12	-0.12	-0.08	-0.06	0.54	-0.41	-0.11	-0.10	0.80	0.03	-0.40	0.15	-0.26												
GP13	0.02	-0.12	0.08	0.33	-0.31	0.19	0.07	0.54	0.03	-0.10	0.37	0.19	0.51											
GP14	-0.38	-0.24	-0.55	-0.36	-0.88	-0.57	-0.66	-0.08	0.23	0.05	-0.01	-0.35	0.32	0.12										
GP15	-0.10	-0.24	-0.36	-0.22	-0.76	-0.31	-0.08	0.06	-0.12	-0.05	0.61	0.24	0.37	0.45	0.64									
GP16	0.00	-0.08	-0.13	-0.29	-0.15	-0.04	-0.10	-0.26	-0.21	0.42	-0.03	0.25	-0.32	-0.01	-0.07	-0.02								
GP17	-0.05	-0.22	0.13	0.43	-0.19	0.03	0.00	0.58	-0.27	-0.37	-0.04	-0.16	0.73	0.40	0.08	0.17	-0.13							
GP18	-0.39	-0.27	-0.59	-0.43	-0.83	-0.60	-0.66	-0.14	0.07	-0.02	-0.04	-0.33	0.24	0.02	0.82	0.52	0.33	0.13						
GP19	-0.11	-0.08	-0.15	-0.12	-0.11	-0.07	-0.04	-0.23	-0.17	0.22	-0.20	0.14	-0.13	-0.01	0.01	0.11	0.13	0.19	0.02					
GP20	-0.08	-0.18	0.18	0.03	-0.33	0.10	-0.13	0.15	-0.16	-0.10	0.12	0.10	0.25	0.51	0.25	0.32	0.15	0.42	0.21	0.15				
GP21	-0.05	-0.07	0.19	0.08	-0.01	0.06	-0.01	0.04	-0.26	-0.13	-0.10	-0.09	0.04	0.02	-0.06	-0.09	0.30	0.40	0.11	0.09	0.41			
GP22	-0.10	-0.08	0.10	0.29	-0.23	-0.06	-0.09	0.34	-0.14	-0.17	-0.04	-0.13	0.40	0.28	0.03	0.05	0.34	0.55	0.25	0.13	0.40	0.69		
GP23	-0.24	-0.17	-0.24	-0.32	-0.23	-0.38	-0.56	-0.29	-0.02	0.15	-0.53	-0.46	-0.12	-0.20	0.21	-0.15	0.50	0.16	0.48	0.32	0.15	0.55	0.45	
GP24	0.07	-0.11	-0.17	-0.15	-0.19	-0.19	-0.14	-0.19	-0.14	0.11	-0.15	-0.03	-0.12	-0.01	-0.03	-0.01	0.63	0.20	0.28	0.56	0.17	0.54	0.57	0.75

Controls																							
	Age	**BMI**	**GP1**	**GP2**	**GP4**	**GP5**	**GP6**	**GP7**	**GP8**	**GP9**	**GP10**	**GP11**	**GP12**	**GP13**	**GP14**	**GP15**	**GP16**	**GP17**	**GP18**	**GP19**	**GP20**	**GP21**	**GP22**	**GP23**
Age																								
BMI	-0.04																							
GP1	0.26	0.04																						
GP2	0.03	-0.14	0.03																					
GP4	0.31	0.06	0.50	0.13																				
GP5	0.19	-0.03	0.55	0.19	0.36																			
GP6	0.13	0.06	0.32	0.39	0.57	0.37																		
GP7	-0.03	-0.13	-0.01	0.85	-0.08	0.07	0.20																	
GP8	-0.22	-0.06	-0.56	-0.09	-0.55	-0.56	-0.48	0.03																
GP9	0.01	-0.10	0.00	-0.32	-0.05	-0.12	-0.35	-0.18	-0.10															
GP10	-0.21	0.08	-0.21	-0.02	-0.43	-0.19	0.27	0.06	0.22	-0.27														
GP11	-0.05	0.02	0.36	-0.04	0.13	0.37	0.40	0.01	-0.51	0.29	0.40													
GP12	-0.17	-0.09	-0.28	0.67	-0.42	-0.08	-0.03	0.81	0.28	-0.23	0.17	-0.19												
GP13	-0.14	0.07	0.17	0.31	-0.19	0.07	0.08	0.52	0.07	0.02	0.31	0.42	0.36											
GP14	-0.32	0.00	-0.49	-0.29	-0.89	-0.48	-0.64	-0.07	0.60	0.16	0.31	-0.22	0.33	0.11										
GP15	-0.33	0.03	-0.29	-0.22	-0.76	-0.29	-0.20	0.01	0.27	-0.03	0.76	0.26	0.29	0.35	0.71									
GP16	0.18	-0.03	0.18	-0.33	-0.03	0.11	-0.38	-0.27	-0.30	0.47	-0.31	0.19	-0.38	0.00	-0.07	-0.13								
GP17	0.00	0.01	0.13	0.34	-0.05	0.64	0.13	0.28	-0.30	-0.21	-0.17	0.06	0.27	0.02	-0.22	-0.12	0.03							
GP18	-0.22	-0.01	-0.42	-0.35	-0.82	-0.38	-0.72	-0.16	0.45	0.09	0.14	-0.28	0.21	-0.01	0.83	0.54	0.29	-0.10						
GP19	-0.01	-0.01	0.04	-0.03	-0.07	-0.05	-0.11	-0.07	-0.04	-0.02	0.04	0.17	-0.09	0.09	0.01	0.19	0.03	0.00	-0.01					
GP20	0.01	-0.01	0.28	0.15	-0.06	0.71	0.06	0.09	-0.37	-0.08	-0.13	0.23	0.04	0.11	-0.17	-0.07	0.22	0.83	-0.03	-0.01				
GP21	0.10	0.06	0.17	0.16	0.01	0.55	0.08	0.06	-0.38	-0.15	-0.19	0.06	0.00	-0.06	-0.27	-0.18	0.21	0.81	-0.12	-0.02	0.76			
GP22	0.09	-0.02	0.15	0.44	-0.07	0.28	0.00	0.36	-0.20	-0.33	-0.12	-0.10	0.33	0.20	-0.14	-0.06	0.15	0.45	-0.03	0.18	0.42	0.54		
GP23	0.10	0.13	-0.07	-0.14	-0.06	-0.06	-0.44	-0.16	-0.05	0.02	-0.54	-0.41	-0.10	-0.26	0.01	-0.26	0.36	0.26	0.24	0.18	0.19	0.50	0.36	
GP24	0.09	0.02	0.01	-0.07	-0.04	-0.06	-0.19	-0.13	-0.12	-0.10	-0.20	-0.09	-0.14	-0.07	-0.08	-0.06	0.29	0.17	0.10	0.57	0.13	0.42	0.43	0.75

Spearman's correlation coefficients (r_s) comparing the GPs of the total IgG glycome to the derived traits. Comparisons were made if at least one group produced a coefficient showing a moderate relationship ($r_s > |0.5|$). Comparisons where at least one coefficient showed a strong relationship ($r_s > |0.7|$) are boxed. Statistically significant differences between the groups are highlighted for $P < 0.05$ (red), $P < 0.01$ (yellow) and $P < 0.001$ (green).

Cases																	
	DT1	**DT2**	**DT3**	**DT4**	**DT5**	**DT6**	**DT7**	**DT8**	**DT9**	**DT10**	**DT11**	**DT12**	**DT13**	**DT14**	**DT15**	**DT16**	**DT17**
Age	-0.17	-0.18	-0.34	-0.28	0.06	0.11	0.01	0.02	-0.05	-0.02	0.08	0.02	0.18	0.16	0.17	0.29	0.29
BMI	-0.26	-0.07	-0.27	-0.11	-0.14	-0.13	0.02	0.16	0.02	-0.06	0.02	0.04	0.17	0.17	0.17	0.11	0.10
GP1	-0.24	-0.07	-0.51	-0.27	0.02	-0.04	0.12	0.24	-0.04	-0.13	-0.08	0.11	0.31	0.31	0.31	0.21	0.22
GP2	-0.36	-0.15	-0.40	-0.31	-0.21	-0.09	-0.03	0.14	-0.05	-0.05	0.06	0.07	0.30	0.28	0.26	0.31	0.31
GP4	-0.43	0.11	-0.78	-0.18	-0.10	0.05	0.36	0.53	0.11	-0.32	-0.25	0.13	0.52	0.53	0.53	0.23	0.23
GP5	-0.35	-0.10	-0.55	-0.30	0.05	0.00	0.04	0.29	-0.07	-0.05	0.08	0.15	0.33	0.36	0.35	0.41	0.41
GP6	-0.30	-0.36	-0.53	-0.60	0.10	0.09	-0.11	0.11	-0.15	0.00	0.25	0.14	0.48	0.46	0.45	0.74	0.74
GP7	-0.20	-0.29	-0.13	-0.34	-0.14	-0.08	-0.22	-0.14	-0.15	0.15	0.22	0.04	-0.03	-0.04	-0.06	0.19	0.19
GP8	-0.38	-0.02	-0.12	0.08	-0.54	-0.26	-0.07	0.09	0.01	0.06	-0.04	0.04	-0.08	-0.05	-0.05	-0.21	-0.21
GP9	-0.01	0.26	0.05	0.29	0.20	-0.19	0.13	0.18	0.06	-0.07	-0.13	0.05	0.08	0.12	0.11	-0.10	-0.10
GP10	-0.06	-0.75	0.00	-0.70	0.09	0.10	-0.54	-0.49	-0.32	0.41	0.62	0.02	-0.04	-0.08	-0.09	0.62	0.62
GP11	-0.07	-0.34	-0.19	-0.41	0.35	0.15	-0.23	-0.02	-0.22	0.17	0.39	0.15	0.32	0.30	0.29	0.70	0.69
GP12	0.04	-0.27	0.20	-0.18	-0.17	-0.12	-0.32	-0.30	-0.22	0.24	0.22	0.04	-0.24	-0.23	-0.24	-0.06	-0.05
GP13	-0.05	-0.27	0.07	-0.19	0.04	-0.10	-0.31	-0.28	-0.17	0.21	0.27	0.01	-0.03	-0.03	-0.05	0.25	0.25
GP14	0.29	-0.08	0.65	0.19	-0.13	-0.29	-0.39	-0.39	-0.25	0.40	0.21	0.05	-0.62	-0.56	-0.56	-0.45	-0.45
GP15	0.26	-0.44	0.51	-0.21	0.09	-0.10	-0.58	-0.55	-0.41	0.48	0.51	0.10	-0.34	-0.31	-0.31	0.15	0.15
GP16	0.68	0.32	0.54	0.35	0.89	0.66	0.42	-0.29	0.60	-0.33	-0.24	-0.64	-0.12	-0.25	-0.27	0.03	0.02
GP17	0.26	0.11	0.22	0.10	0.11	0.12	0.11	-0.06	0.04	-0.15	-0.15	-0.06	0.06	0.03	0.04	-0.08	-0.08
GP18	0.72	0.07	0.93	0.33	0.30	0.23	-0.10	-0.54	0.09	0.18	0.06	-0.30	-0.69	-0.72	-0.72	-0.46	-0.46
GP19	0.18	0.64	0.13	0.64	0.14	0.04	0.32	0.50	0.15	-0.42	-0.36	0.11	0.62	0.61	0.61	0.13	0.13
GP20	0.27	0.02	0.29	0.11	0.24	-0.01	-0.03	-0.21	0.00	0.00	0.00	-0.10	-0.10	-0.12	-0.11	-0.06	-0.05
GP21	0.44	0.32	0.28	0.26	0.42	0.25	0.57	-0.24	0.60	-0.59	-0.55	-0.63	0.08	-0.08	-0.08	-0.18	-0.18
GP22	0.49	0.26	0.40	0.26	0.43	0.33	0.36	-0.29	0.51	-0.42	-0.33	-0.59	0.01	-0.15	-0.16	-0.05	-0.06
GP23	0.68	0.74	0.60	0.82	0.43	0.36	0.75	-0.08	0.73	-0.67	-0.79	-0.64	-0.09	-0.20	-0.19	-0.59	-0.59
GP24	0.64	0.67	0.50	0.69	0.61	0.51	0.66	-0.09	0.81	-0.75	-0.61	-0.72	0.30	0.10	0.10	0.03	0.03

Controls																	
	DT1	DT2	DT3	DT4	DT5	DT6	DT7	DT8	DT9	DT10	DT11	DT12	DT13	DT14	DT15	DT16	DT17
Age	0.07	0.20	-0.14	0.09	0.23	0.18	0.27	0.08	0.27	-0.21	-0.21	-0.18	0.12	0.06	0.05	-0.01	0.00
BMI	0.04	-0.03	-0.02	-0.03	0.01	-0.02	0.07	-0.04	0.03	-0.08	-0.13	-0.07	0.02	0.00	-0.02	-0.14	-0.15
GP1	0.03	0.15	-0.32	-0.06	0.35	0.17	0.31	0.24	0.10	-0.20	-0.19	0.03	0.25	0.24	0.23	0.07	0.08
GP2	-0.22	0.01	-0.29	-0.16	-0.16	-0.03	0.13	0.12	0.00	-0.13	-0.12	0.05	0.24	0.22	0.22	0.10	0.12
GP4	-0.22	0.31	-0.76	-0.08	0.19	0.18	0.55	0.48	0.29	-0.41	-0.42	0.03	0.46	0.45	0.45	-0.03	-0.01
GP5	0.11	0.08	-0.22	-0.15	0.35	0.25	0.25	0.15	0.05	-0.14	-0.15	0.04	0.18	0.17	0.18	0.03	0.04
GP6	-0.33	-0.21	-0.66	-0.55	-0.05	0.05	0.11	0.19	-0.08	-0.13	-0.03	0.17	0.42	0.41	0.42	0.38	0.39
GP7	-0.21	-0.13	-0.12	-0.19	-0.20	-0.10	-0.04	-0.05	-0.11	0.03	0.04	0.06	0.05	0.05	0.05	0.07	0.08
GP8	-0.25	-0.21	0.23	0.06	-0.61	-0.32	-0.42	-0.13	-0.19	0.28	0.26	0.07	-0.28	-0.22	-0.21	-0.07	-0.08
GP9	-0.09	0.08	0.07	0.14	0.16	-0.17	-0.10	0.06	-0.09	0.20	0.14	0.09	-0.20	-0.17	-0.17	-0.15	-0.14
GP10	-0.18	-0.71	0.07	-0.51	-0.25	-0.15	-0.62	-0.31	-0.52	0.43	0.59	0.25	-0.07	-0.04	-0.02	0.57	0.55
GP11	-0.05	-0.28	-0.18	-0.32	0.31	0.08	-0.15	0.04	-0.28	0.17	0.30	0.23	0.20	0.19	0.22	0.50	0.50
GP12	-0.14	-0.21	0.15	-0.14	-0.37	-0.22	-0.25	-0.20	-0.23	0.19	0.17	0.10	-0.16	-0.15	-0.15	-0.02	-0.02
GP13	-0.05	-0.27	0.03	-0.22	0.05	-0.09	-0.22	-0.14	-0.24	0.17	0.25	0.11	0.00	0.01	0.01	0.30	0.30
GP14	0.07	-0.32	0.63	0.05	-0.35	-0.36	-0.63	-0.39	-0.37	0.48	0.46	0.09	-0.53	-0.47	-0.47	-0.11	-0.12
GP15	0.06	-0.51	0.46	-0.16	-0.19	-0.23	-0.65	-0.39	-0.52	0.47	0.56	0.21	-0.24	-0.20	-0.19	0.35	0.33
GP16	0.70	0.26	0.50	0.36	0.87	0.59	0.20	-0.17	0.35	-0.01	-0.02	-0.40	-0.25	-0.34	-0.34	-0.10	-0.09
GP17	0.24	0.19	0.10	0.09	0.22	0.16	0.32	-0.07	0.21	-0.28	-0.31	-0.19	0.13	0.05	0.07	-0.11	-0.11
GP18	0.53	-0.15	0.92	0.21	0.06	0.14	-0.42	-0.46	-0.12	0.40	0.36	-0.14	-0.64	-0.65	-0.65	-0.22	-0.23
GP19	0.11	0.54	0.07	0.63	0.09	-0.01	0.21	0.51	0.11	-0.35	-0.22	0.15	0.68	0.70	0.70	0.44	0.44
GP20	0.30	0.10	0.17	0.03	0.36	0.21	0.22	-0.11	0.14	-0.15	-0.17	-0.16	0.06	-0.01	0.00	-0.07	-0.07
GP21	0.37	0.30	0.14	0.21	0.38	0.21	0.53	-0.23	0.50	-0.50	-0.51	-0.52	0.18	0.00	0.02	-0.17	-0.17
GP22	0.30	0.31	0.18	0.30	0.30	0.14	0.37	-0.09	0.39	-0.42	-0.37	-0.38	0.24	0.12	0.12	0.03	0.03
GP23	0.56	0.70	0.43	0.74	0.31	0.19	0.70	-0.20	0.79	-0.69	-0.77	-0.73	0.12	-0.08	-0.08	-0.51	-0.50
GP24	0.49	0.73	0.32	0.77	0.35	0.11	0.61	-0.10	0.79	-0.77	-0.64	-0.68	0.51	0.27	0.27	0.14	0.15

Spearman's correlation coefficients (r_s) comparing the GPs of the neutral IgG glycome to each other, age and BMI. Comparisons were made if at least one group produced a coefficient showing a moderate relationship (r_s > |0.5|). Comparisons where at least one coefficient showed a strong relationship (r_s > |0.7|) are boxed. Statistically significant differences between the groups are highlighted for P < 0.05 (red), P < 0.01 (yellow) and P < 0.001 (green).

Cases

	Age	BMI	GP1n	GP2n	GP4n	GP5n	GP6n	GP7n	GP8n	GP9n	GP10n	GP11n	GP12n	GP13n	GP14n
Age															
BMI	-0.02														
GP1n	0.29	0.08													
GP2n	0.11	0.10	0.27												
GP4n	0.35	0.27	0.58	0.17											
GP5n	0.38	0.09	0.56	0.23	0.47										
GP6n	0.34	0.09	0.48	0.38	0.45	0.43									
GP7n	-0.04	-0.04	0.15	0.82	-0.17	0.17	0.17								
GP8n	-0.24	-0.06	-0.48	-0.09	-0.47	-0.37	-0.64	-0.03							
GP9n	-0.13	0.00	-0.29	-0.40	-0.16	-0.09	-0.31	-0.38	-0.03						
GP10n	0.14	-0.08	-0.09	0.03	-0.41	0.00	0.44	0.15	-0.06	-0.27					
GP11n	0.29	-0.03	0.08	-0.01	0.03	0.35	0.61	-0.09	-0.48	0.22	0.57				
GP12n	-0.14	-0.10	-0.09	0.53	-0.47	-0.12	-0.13	0.82	0.12	-0.31	0.19	-0.24			
GP13n	-0.03	-0.18	0.02	0.26	-0.45	0.16	-0.01	0.52	0.09	-0.04	0.40	0.19	0.53		
GP14n	-0.39	-0.25	-0.55	-0.34	-0.89	-0.53	-0.65	-0.03	0.46	0.22	0.11	-0.25	0.34	0.20	
GP15n	-0.15	-0.26	-0.37	-0.24	-0.83	-0.28	-0.10	0.07	0.08	0.09	0.68	0.30	0.38	0.51	0.68

Controls

	Age	BMI	GP1n	GP2n	GP4n	GP5n	GP6n	GP7n	GP8n	GP9n	GP10n	GP11n	GP12n	GP13n	GP14n
Age															
BMI	-0.04														
GP1n	0.28	0.05													
GP2n	0.03	-0.14	0.00												
GP4n	0.34	0.05	0.50	0.10											
GP5n	0.19	-0.01	0.54	0.18	0.35										
GP6n	0.13	0.06	0.29	0.37	0.49	0.35									
GP7n	-0.03	-0.14	-0.04	0.84	-0.14	0.07	0.16								
GP8n	0.24	-0.06	-0.58	-0.11	-0.72	-0.46	-0.64	0.04							
GP9n	0.01	-0.09	0.00	-0.34	-0.16	-0.08	-0.48	-0.17	-0.02						
GP10n	-0.21	0.06	-0.26	-0.06	-0.56	-0.17	0.22	0.03	0.23	-0.28					
GP11n	-0.07	0.01	0.33	-0.06	0.02	0.38	0.34	0.00	-0.48	0.28	0.37				
GP12n	-0.18	-0.10	-0.30	0.67	-0.46	-0.04	-0.06	0.82	0.32	-0.18	0.18	-0.16			
GP13n	-0.15	0.07	0.12	0.26	-0.30	0.08	0.00	0.49	-0.01	0.02	0.29	0.40	0.36		
GP14n	-0.30	0.00	-0.46	-0.28	-0.92	-0.38	-0.65	-0.03	0.71	0.23	0.35	-0.17	0.35	0.18	
GP15n	-0.31	0.01	-0.28	-0.21	-0.82	-0.21	-0.23	0.04	0.38	0.05	0.75	0.29	0.32	0.40	0.74

Page intentionally left blank

Spearman's correlation coefficients (r_s) comparing the GPs of the neutral IgG glycome to the derived traits. Comparisons were made if at least one group produced a coefficient showing a moderate relationship ($r_s > |0.5|$). Comparisons where at least one coefficient showed a strong relationship ($r_s > |0.7|$) are boxed. Statistically significant differences between the groups are highlighted for $P < 0.05$ (red), $P < 0.01$ (yellow) and $P < 0.001$ (green).

Cases																							
	DT1	**DT2**	**DT3**	**DT4**	**DT5**	**DT6**	**DT7**	**DT8**	**DT9**	**DT10**	**DT11**	**DT12**	**DT13**	**DT14**	**DT15**	**DT16**	**DT17**	**DT18**	**DT19**	**DT20**	**DT21**	**DT22**	**DT23**
Age	0.38	-0.21	-0.37	0.03	0.08	-0.01	-0.13	-0.19	0.06	-0.22	-0.30	0.24	-0.06	0.26	0.40	0.23	0.22	-0.22	-0.04	0.37	0.38	-0.39	0.35
BMI	0.24	-0.08	-0.26	0.05	0.02	0.04	-0.02	0.06	0.16	0.03	-0.02	-0.03	-0.17	-0.02	0.05	-0.04	-0.04	0.05	-0.17	0.03	0.04	-0.07	0.10
GP1n	0.64	-0.62	-0.50	-0.10	0.01	-0.25	-0.28	-0.17	0.10	-0.16	-0.35	0.16	-0.12	0.13	0.27	0.17	0.16	-0.16	0.02	0.31	0.31	-0.40	0.53
GP2n	0.27	-0.25	-0.26	-0.79	-0.88	-0.84	-0.81	-0.43	-0.34	-0.26	-0.66	0.23	0.17	0.13	0.10	0.29	0.28	-0.28	0.29	0.23	0.22	-0.31	0.54
GP4n	0.96	-0.68	-0.92	0.24	0.23	0.07	-0.06	0.15	0.51	0.13	-0.16	-0.07	-0.53	-0.11	0.24	-0.08	-0.09	0.10	-0.45	0.21	0.22	-0.31	0.49
GP5n	0.53	-0.35	-0.48	-0.12	-0.02	-0.22	-0.26	-0.20	0.04	-0.20	-0.38	0.20	-0.07	0.17	0.33	0.21	0.21	-0.21	0.16	0.38	0.37	-0.46	0.62
GP6n	0.65	-0.52	-0.59	-0.10	-0.10	-0.25	-0.30	-0.72	-0.44	-0.69	-0.62	0.79	0.44	0.69	0.79	0.78	0.78	-0.77	0.00	0.81	0.81	-0.81	0.59
GP7n	-0.06	-0.12	0.08	-0.97	-0.91	-0.98	-0.89	-0.48	-0.50	-0.33	-0.67	0.21	0.34	0.17	-0.03	0.28	0.27	-0.29	0.55	0.13	0.13	-0.20	0.38
GP8n	-0.59	0.76	0.43	0.02	-0.09	0.15	0.14	0.38	0.20	0.39	0.35	-0.40	-0.23	-0.37	-0.50	-0.39	-0.40	0.39	0.09	-0.48	-0.51	0.50	-0.31
GP9n	-0.25	0.37	0.17	0.39	0.35	0.42	0.45	0.43	0.27	0.46	0.46	-0.35	-0.21	-0.41	-0.19	-0.38	-0.37	0.37	-0.06	-0.27	-0.26	0.28	-0.22
GP10n	-0.22	0.22	0.19	-0.16	-0.13	-0.12	-0.12	-0.81	-0.78	-0.88	-0.43	0.87	0.83	0.91	0.67	0.87	0.87	-0.87	0.40	0.67	0.67	-0.57	0.12
GP11n	0.18	-0.01	-0.20	0.11	0.12	0.07	0.04	-0.56	-0.45	-0.59	-0.32	0.70	0.51	0.64	0.77	0.68	0.68	-0.68	0.18	0.72	0.71	-0.66	0.35
GP12n	-0.39	0.02	0.45	-0.90	-0.77	-0.79	-0.75	-0.36	-0.51	-0.25	-0.49	0.09	0.39	0.12	-0.19	0.15	0.15	-0.16	0.56	-0.05	-0.04	0.03	0.03
GP13n	-0.35	0.22	0.31	-0.57	-0.45	-0.48	-0.50	-0.42	-0.49	-0.36	-0.47	0.26	0.45	0.27	0.13	0.31	0.31	-0.33	1.00	0.22	0.21	-0.29	0.42
GP14n	-0.94	0.55	0.98	-0.05	-0.04	0.11	0.28	0.16	-0.22	0.16	0.44	-0.22	0.25	-0.16	-0.49	-0.21	-0.21	0.20	0.20	-0.50	-0.50	0.59	-0.74
GP15n	-0.72	0.39	0.75	-0.17	-0.08	-0.02	0.06	-0.46	-0.67	-0.49	-0.09	0.43	0.73	0.49	0.21	0.43	0.44	-0.45	0.50	0.21	0.22	-0.10	-0.31

Controls																							
	DT1	DT2	DT3	DT4	DT5	DT6	DT7	DT8	DT9	DT10	DT11	DT12	DT13	DT14	DT15	DT16	DT17	DT18	DT19	DT20	DT21	DT22	DT23
Age	0.32	-0.29	-0.32	0.07	0.10	-0.04	-0.04	0.08	0.22	0.07	-0.08	-0.09	-0.24	-0.11	0.06	-0.08	-0.08	0.08	-0.14	0.08	0.08	-0.12	0.21
BMI	0.05	-0.09	0.00	0.16	0.16	0.12	0.12	-0.01	0.07	-0.08	0.06	0.09	0.02	0.10	0.07	0.07	0.08	-0.08	0.04	0.08	0.06	-0.06	0.06
GP1n	0.49	-0.49	-0.46	0.05	0.19	-0.08	-0.13	0.03	0.29	-0.02	-0.23	0.01	-0.23	0.02	0.31	0.01	0.01	-0.01	0.11	0.32	0.31	-0.38	0.50
GP2n	0.24	-0.24	-0.20	-0.90	-0.93	-0.88	-0.85	-0.44	-0.45	-0.22	-0.68	0.17	0.17	0.06	0.01	0.22	0.22	-0.23	0.30	0.15	0.16	-0.24	0.43
GP4n	0.96	-0.88	-0.94	0.15	0.23	-0.06	-0.23	0.18	0.46	0.19	-0.25	-0.15	-0.48	-0.20	0.21	-0.15	-0.16	0.16	-0.29	0.22	0.24	-0.32	0.53
GP5n	0.39	-0.38	-0.36	-0.18	-0.04	-0.16	-0.27	-0.12	0.07	-0.09	-0.34	0.09	-0.08	0.07	0.26	0.10	0.10	-0.11	0.08	0.30	0.30	-0.34	0.35
GP6n	0.68	-0.64	-0.61	-0.19	-0.12	-0.31	-0.44	-0.65	-0.43	-0.59	-0.61	0.67	0.43	0.56	0.58	0.68	0.67	-0.67	0.01	0.63	0.63	-0.63	0.53
GP7n	-0.02	0.00	0.06	-0.95	-0.87	-0.97	-0.85	-0.42	-0.48	-0.22	-0.65	0.12	0.22	0.04	-0.04	0.18	0.18	-0.20	0.53	0.10	0.11	-0.20	0.42
GP8n	-0.77	0.79	0.69	-0.04	-0.16	0.15	0.24	0.18	-0.10	0.17	0.40	-0.21	0.07	-0.17	-0.48	-0.22	-0.21	0.21	-0.01	-0.48	-0.49	0.54	-0.60
GP9n	-0.28	0.34	0.20	0.26	0.25	0.26	0.37	0.50	0.37	0.51	0.44	-0.46	-0.34	-0.46	-0.24	-0.48	-0.47	0.47	0.01	-0.31	-0.30	0.30	-0.14
GP10n	-0.41	0.43	0.39	-0.05	-0.09	0.05	0.07	-0.75	-0.76	-0.84	-0.23	0.83	0.87	0.87	0.51	0.82	0.82	-0.82	0.28	0.48	0.47	-0.36	-0.09
GP11n	0.10	-0.01	-0.14	0.02	0.10	-0.01	-0.04	-0.42	-0.25	-0.47	-0.34	0.49	0.35	0.51	0.67	0.48	0.48	-0.49	0.39	0.63	0.64	-0.61	0.41
GP12n	-0.35	0.22	0.43	-0.86	-0.82	-0.74	-0.64	-0.35	-0.54	-0.19	-0.40	0.09	0.34	0.07	-0.26	0.14	0.14	-0.15	0.40	-0.13	-0.13	0.11	0.00
GP13n	-0.23	0.20	0.26	-0.45	-0.34	-0.44	-0.40	-0.41	-0.37	-0.38	-0.46	0.29	0.34	0.31	0.29	0.31	0.32	-0.34	1.00	0.37	0.35	-0.43	0.53
GP14n	-0.96	0.80	0.99	0.02	-0.06	0.21	0.41	0.09	-0.21	0.04	0.49	-0.08	0.27	0.00	-0.40	-0.09	-0.08	0.08	0.17	-0.43	-0.45	0.53	-0.67
GP15n	-0.75	0.64	0.78	-0.04	-0.06	0.10	0.21	-0.40	-0.53	-0.48	0.03	0.45	0.65	0.53	0.22	0.44	0.45	-0.45	0.38	0.18	0.17	0.06	-0.32